Title
Integrated Traffic Regulation and Data Networking for Autonomous Transportation Systems

Author
Lin, Yu-Yu

Publication Date
2017

Peer reviewed|Thesis/dissertation

UNIVERSITY OF CALIFORNIA

Los Angeles

Integrated Traffic Regulation and Data Networking for Autonomous Transportation Systems

A dissertation submitted in partial satisfaction
of the requirements for the degree
Doctor of Philosophy in Electrical Engineering

by

Yu-Yu Lin

2017

ABSTRACT OF THE DISSERTATION

Integrated Traffic Regulation and Data Networking for Autonomous Transportation Systems

by

Yu-Yu Lin
Doctor of Philosophy in Electrical Engineering
University of California, Los Angeles, 2017
Professor Izhak Rubin, Chair

Classical transportation systems have been suffering from inefficiency in utilizing road capacity and incapability of guaranteeing safety due to inconsistent and unpredictable human based manipulations. This long standing issue is expected to be resolved through the introduction of vehicular autonomy, along with a properly configured traffic management system and an underlying communication network that supports the dissemination of safety and control messages. However, mechanisms to be used in the regulation of autonomous vehicles are yet to be developed.

For the first part of the dissertation, we propose an efficient data dissemination protocol, identified as Vehicular Backbone Network (VBN), which support high throughput and low delay message delivery across a Vehicular Ad Hoc Network (VANET). Vehicles are elected as relay nodes at properly selected nominal positions to optimize system throughput rate with guaranteed outage probability. The proposed VBN mechanism is analyzed under different Medium Access Control (MAC) protocols and various stochastic traffic flow conditions.

In the second part of the dissertation, we go beyond the statistical vehicular traffic model and present our study of a platoon-based autonomous vehicular traffic regulation system. The traffic management system, serving to configure vehicles into platoons and regulating the on-ramp access of vehicular flows into the highway, is integrated with a design of a

VANET system. The latter provides for the communications of essential message flows among highway vehicles. The fundamental tradeoffs that need to be made in designing the autonomous systems are modeled and studied. We propose an optimization framework to be used in designing the traffic control system in a manner that meet throughput and latency performance metrics across the vehicular mobility and the message communications networking dimensions of the overall system. We also study the design of a core network that employs Road Side Units (RSUs) that provide communications networking support in disseminating message flows to/from and among highway vehicles.

The dissertation of Yu-Yu Lin is approved.

Felipe Caro

Lieven Vandenberghe

Kung Yao

Izhak Rubin, Committee Chair

University of California, Los Angeles

2017

To my family

Table of Contents

List of Figures

List of Tables

Acknowledgments

I must offer my sincere appreciation to my advisor, Prof. Izhak Rubin, for helping me throughout my Ph.D. program at UCLA. Your patience and knowledgable experiences in communication networks guided me through the difficult times during the early stage of my research. Our discussions have inspired me to come up with ideas that constitute the essence of this dissertation.

I am also grateful to the committee members: Prof. Kung Yao, Prof. Lieven Vandenberghe, and Prof. Felipe Caro. Thank you for willing to serve as my thesis committee members. Your precious comments have made my dissertation more solid and sound.

I would like to thank Prof. Andrea Baiocchi, Prof. Francesca Cuomo, and Pierpaolo Salvo for your technical suggestions and help in reviewing Chapters 1-3 of this dissertation.

My labmates, Hung-Bin Chang, Cheng-An Yang, Andrew Horng, Joseph Yang, and Kai Yu, I really appreciate all your supports in research, coursework, and holiday road-trip planning. I would also like to thank all other friends accompanying me during my graduate study: Kuan-Hao Su, Webber Lee, Hua-I Chang, I-Tan Lin, I-Ping Lai, Caryn Chan, Sheng-Yuan Tu, Cheng-Han Wu, Wei-Hung Liu, Chun-Hao Liu, and Mihir Laghate. You have fulled filled my life at UCLA.

I also like to thank all my colleagues when I interned at Tarana Wireless and Qualcomm Research: Phoebus Chen, Kavin Kamaraj, Thomas Svantesson, Kamaraj Karuppiah, Goel Satashu, Kun Wang, Mostafa Khoshnevisan, Farhad Meshkati, Vinay Joseph, and Damanjit Singh. Thank you for bringing me with industrial experiences and different views to look into problems.

I want to thank my parents and sister for your support, financially and mentally, in the past 30 years. Without you, this dissertation would not exist.

Last but not least, I would like to say thank you to my wife, Sung-Yin. Thank you for always being there, listening to me, and sharing all the happiness and sorrowfulness.

Vita

2012–2017	Doctor of Philosophy Candidate, Electrical Engineering Department, University of California, Los Angeles.
2008–2010	Master of Science, Communication Engineering Department, National Taiwan University.
2004–2008	Bachelor of Science, Electrical Engineering and Computer Science Honors Program, National Chiao Tung University.

Publications

[J3] **Y.-Y. Lin**; Izhak Rubin, "Integrated networking and traffic regulation for autonomous highway systems," submitted to *IEEE Trans. on Vehicular Technology.*

[J2] I. Rubin; **Y.-Y. Lin**; D. Kofman, "Optimal relay configuration for power line communication networks," *IEEE Transactions on Communications*, 2016.

[J1] I. Rubin, **Y.-Y. Lin**; A. Baiocchi; F. Cuomo; P. Salvo, "Rapid dissemination of public safety message flows in vehicular networks," in *Journal of Communications*, 2014.

[C5] **Y.-Y. Lin**; I. Rubin, "Infrastructure aided networking and traffic management for autonomous transportation," in *Information Theory and Applications Workshop*, 2017.

[C4] **Y.-Y. Lin**; I. Rubin, "Vehicular and messaging throughput tradeoffs in autonomous highway systems," in *Proc. IEEE Global Communications Conference*, 2015.

[C3] **Y.-Y. Lin**; I. Rubin, "Throughput maximization under guaranteed dissemination coverage for VANET systems," in *Information Theory and Applications Workshop*, 2015.

[C2] I. Rubin; **Y.-Y. Lin**; D. Kofman, "Relay-aided networking for power line communications," in *Information Theory and Applications Workshop*, 2014.

[C1] I. Rubin; **Y.-Y. Lin**; A. Baiocchi; F. Cuomo; P. Salvo, "Vehicular backbone networking protocol for highway broadcasting using directional antennas," in *Proc. IEEE Global Communications Conference*, 2013.

CHAPTER 1

Introduction

Intelligent Transportation Systems (ITS) are being developed as promising solutions to traffic problems. They are designed to improve road safety conditions by taking advantage of the development and use of autonomous vehicles. Through its equipped sensors and radio-access technologies, an autonomous vehicle is able to detect accidents or traffic congestion and forward relevant information to neighboring vehicles or infrastructure devices. Upon receiving these messages, vehicles may adjust speeds and spacings accordingly or take detours to prevent severe traffic jams through the aids of the equipped Adaptive Cruise Control [1, 2] system. In addition, it is essential to implement distributed control systems that allow individual vehicles to rapidly adjust their mobility plan in reacting to system state fluctuations. For this purpose, it is critical that vehicles are able to effectively disseminate and receive status messages to/from other vehicles. In considering mechanisms for vehicle-to-vehicle (V2V) communications, a multitude of networking protocols have been studied extensively, in the context of designing vehicular ad hoc networks (VANETs) [3–5].

The first part of the dissertation, including Chapters 2 ,3, and 4, presents protocols developed for VANET networking across a linear highway to support multi-hop message dissemination. To guarantee a successful delivery of messages to vehicles beyond the coverage of the infrastructure, or Road Side Units (RSUs), selecting intermediate vehicles as Relay Nodes (RN) is required. In turn, we propose a Vehicular Backbone Network (VBN) based networking mechanism. The VBN system relies on the Global Positioning System (GPS)

and a distributed election algorithm so that vehicles positioned close to prescribed nominal positions elect themselves to act as relay nodes. Optimal relay positions and the corresponding communication protocols are presented and the throughput rate performances of the system are analyzed.

In Chapter 2, we propose a directional antenna aided version of VBN protocol, noted as DVBN, for the distribution of messages generated by a RSU located at a position along a linear highway to vehicles that travel along this highway. The aim of this chapter is two-fold: a. We examine the utility of using varying inter-RN nominal position ranges in contributing to the enhancement of the system's broadcast throughput rate. We show that when minimum inter-vehicular spacing requirements are imposed, it is effective to select equal inter-RN distance levels. b. We demonstrate the superior performance offered by this DVBN protocol when compared with a corresponding (VBN) protocol that employs omni-directional antennas. We illustrate scenarios under which broadcast throughput capacity rate gains as high as ten fold are achieved by the DVBN scheme. This chapter is a version of [I. Rubin, Y.-Y. Lin, A. Baiocchi, F. Cuomo and P. Salvo, "Vehicular backbone networking protocol for highway broadcasting using directional antennas," *IEEE Global Communications Conference (GLOBECOM)*, Atlanta, GA, 2013, pp. 4414-4419.]

In Chapter 3, we develop an analytical model that accurately characterizes the maximum throughput rate performance achievable under a prescribed outage probability constraint for a VBN system. We consider a spatial-reuse TDMA-based VBN. A joint optimization of inter-relay distances, transmission rates, and spatial-reuse factors, which has not yet been addressed in the existing literatures, is carried out. These results are confirmed by comparison with simulation results. They also serve as essential benchmark and performance upper bounds that characterize the behavior of robust distributed VBN protocols, applicable to VANET systems that provide vehicle-to-vehicle communications among stochastically roaming highway vehicles. This chapter is a version of [Y.-Y. Lin and I. Rubin, "Throughput maximization under guaranteed dissemination coverage for VANET systems," *Information*

Theory and Applications Workshop (ITA), San Diego, CA, 2015, pp. 313-318.]

In Chapter 4, we study the optimal cross-layer design of a VBN based system, by presenting an analytical model to jointly select the operational data rate, scheduling mechanism and the inter-RN targeted distance levels. We show that a high level of coverage of highway vehicles, coupled with very low incurred queueing delays, can be achieved by employing a flow admission control mechanism at the source. We consider a high intensity vehicular traffic low regime under which vehicles that are elected to serve as RNs are generally located close to designated nominal positions, as well as lower rate stochastic traffic flow conditions. Furthermore, we demonstrate the capability of the system, when properly configured, to employ a vehicular Carrier Sense Multiple Access/ Collision Avoidance (CSMA/CA) access scheme to well emulate the operations of the system when managed by the use of spatial-reuse Time Division Multiple Access (TDMA) scheduling scheme. Our mathematical analyses and designs are well confirmed through the execution of system simulation analyses. This chapter is a version of [I. Rubin, Y.-Y. Lin, A. Baiocchi, F. Cuomo, and P. Salvo, "Rapid dissemination of public safety message flows in vehicular networks," *Journal of Communications*, vol. 9, no. 8, pp. 616-626, 2014.]

The second part of the dissertation, including Chapters 5 and 6, presents a new design paradigm that integrates the traffic regulation and data networking segments of autonomous transportation systems. Instead of applying classical mobility models to capture human driver behaviors, the use of autonomously controlled driverless vehicles brings up another design dimensionality: the regulation and shaping of vehicular flows. The induced joint impact of the vehicular flow process on the message communications networking system, on the vehicular throughput rate, and on on-ramp waiting times for highway systems, have not been addressed by existing studies.

In Chapter 5, we synthesize and study methods that are used to optimally group autonomously controlled vehicles to travel along a highway in platoons. Vehicular formations are structured to yield effective autonomous mobility operation and to realize high per-

formance multi-hop dissemination of multi-class messaging flows. We then investigate an on-ramp traffic flow control mechanism that serves to regulate the admission of vehicles into the highway. We characterize the tradeoffs available to the system's designer in attaining high message communications throughput rates, accounting for time delays experienced by on-ramp waiting vehicles, while also striving to enhance the highway's capacity for accommodating high vehicular flow rate levels. This chapter is a version of [Y.-Y. Lin and I. Rubin, "Integrated message dissemination and traffic regulation for autonomous highway systems," *IEEE Transactions on Vehicular Techonology*, under review.]

In Chapter 6, we study the design of an RSU-aided autonomous vehicular network that incorporates both data networking and traffic management dimensions. We investigate the inter-relationships that characterize the joint design of vehicular ad hoc networking control mechanisms and cost-effective RSU backbone network. We configure vehicles into platoon structures in aiming to guarantee a robust dissemination of data message flows. An efficient algorithm is developed to determine the optimal settings of platoon parameters and RSU locations across a highway. The result is used to demonstrate the fundamental design tradeoffs to be made when considering performance metrics that involve vehicular throughput rates, infrastructure deployment costs, and the reliability of wireless communications networking. This chapter is a version of [Y.-Y. Lin and I. Rubin, "Infrastructure aided networking and traffic management for autonomous transportation," *Information Theory and Applications Workshop (ITA)*, San Diego, CA, 2017.]

CHAPTER 2

Vehicular Backbone Networking Protocol for Highway Broadcasting Using Directional Antennas

I Introduction

Inter-vehicular communications and networking has been treated as a promising solution to enhance the reliability and functionality of a network system that uses the concurrent transportation system to support passengers with real time emergent information and infotainment flows, as well as the multicast distribution of public safety message flows. Vehicular Ad Hoc Network (VANET) technology and network systems that enable direct data exchange among vehicles have attracted much research attention and induced standardization processes [6].

Messages transmitted in the VANET, such as those involving public safety and infotainment applications, are of broadcasting nature. However, without the institution of appropriate coordination mechanisms among vehicles, broadcasting in such an ad hoc network may result in inducing broadcasting storm problems [7], leading to frequent packet collisions and retransmissions. To tackle this problem, a number of broadcasting protocols have been proposed, often restricting the number of vehicles employed to simultaneously transmit packets by using distance-based protocols to elect forwarding vehicles [8, 9], and to synthesize cluster-based [10, 11] forwarding layouts. However, many such protocols induce a high rate

of control messaging used for cluster formations and protocol implementation.

We adopt a GPS-based packet forwarding protocol in this chapter, coupled with the use of adaptive coding and uni-directional antenna systems. Pre-determined nominal positions along the highway are computed to identify the best locations for relay nodes that serve to achieve the network's highest broadcast throughput capacity rate. The idea of forming such a GPS-based VANET operation has been proposed in [12], identified as a Vehicular Backbone Network (VBN), where vehicles are assumed to employ omni-directional antennas. In this chapter, we assume that each vehicle has the capability to employ a directional antenna system to communicate with its neighboring vehicles, yielding a network system that exhibits superior performance behavior. While several papers have been published in evaluating VANET systems that use vehicles equipped with directional antennas [13–15], none of them have proposed a VBN like protocol; no analytical evaluations that determine the optimal parameters to be selected in the operation of such a network, or used to characterize its performance behavior, have as of now been published.

In this chapter, we provide a numerically efficient algorithm to determine the optimal values for the nominal positions that should be used by Relay Node (RN) vehicles to maximize the system's broadcast capacity under high traffic density conditions. In evaluating performance under stochastic vehicular traffic flows, we consider stochastic deviations of vehicles elected to serve as RNs from the underlying nominal RN positions and identify the optimal selection of the inter-relay distance levels. We demonstrate that by using the Directional Vehicular Backbone Network (DVBN) protocol, the broadcast throughput capacity level achieved by the omni-directional VBN system can be improved by a factor 10.

This chapter is organized as follows. Section II specifies the system model. Section III provides a constructive method to calculate the optimal (nominal) values for inter-relay distances. In Section IV, we study the broadcast capacity rate that can be attained under stochastic fluctuations in the vehicular traffic process. In Section V, we illustrate the throughput capacity gains that can be achieved under the DVBN protocol in comparison

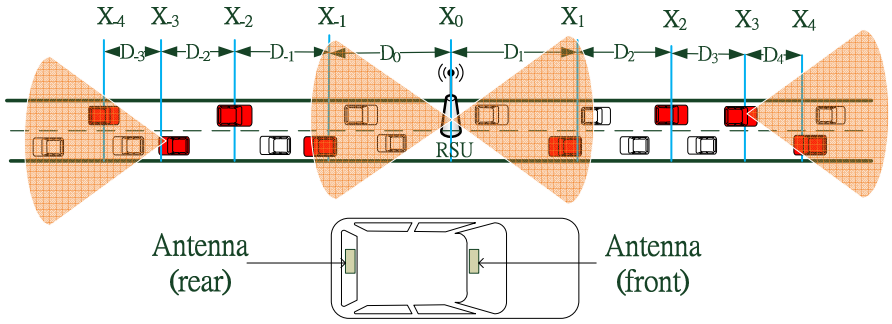

Figure 2.1: VBN on linear highway with relay elected at nominal positions (top) and antenna configuration in a vehicle (bottom)

with those achieved by a corresponding GPS-aided protocol when omni-directional antennas are employed. Conclusions are drawn in Section VI.

II System Model

We consider a linear highway model as illustrated in Fig. 2.1. A single Road Side Unit (RSU) located along the road generates downlink message traffic; such multicast messages are continuously generated aiming to reach all vehicles that travel along the highway. Since the RSU is able to broadcast its message flows across only a limited span of the highway, we introduce a network forwarding scheme under which certain vehicles are elected to act as RNs. Packets issued by the RSU are then forwarded by a RN ((i) along one side of the highway to a neighboring RN, when a directional antenna is used; (ii) both neighboring RNs, when each vehicles uses an omni-directional antenna). When a packet is transmitted from a RN to a neighboring RN, all vehicles located along the stretch of the highway that connect these two RNs are able to receive the corresponding packet. In order to alleviate the broadcast storm problem, we restrict the number of relay nodes elected to form this Vehicular Backbone Network (VBN). The set of predetermined nominal positions at which we aim elected RNs to reside is given as: $\{X_n, n \in \mathbb{Z}\}$, where X_n is the coordinate of the

n^{th} nominal position on the real line. We assume that $X_0 = 0$ is the location of RSU.

Each vehicle has the capability to employ a directional antenna system, using a transceiver operating in half-duplex mode to communicate with its neighboring vehicles, as illustrated in Fig. 2.1. Each antenna system consists of two directional antenna arrays with one installed at the front of a vehicle and the other at the rear. Consider a vehicle traveling along the highway. One of its sides (front or rear one) is facing the highway in the direction of the RSU. Its other side is facing the highway away from the RSU. Due to the high frequency ranges employed for VANET system operations, such antenna modules are rather small and easily mounted on the front and rear ends of vehicles. (Additional antenna arrays may also be used to form directional beams oriented to the sides, when considering routing packets among multiple highway systems; such configurations are however not considered here.) We note that we assume the beamwidths of the antennas to be sufficiently widely set so that for coverage of vehicles traveling along the highway under consideration, it is not necessary to align the antennas (among communicating vehicles), or to use steerable ones.

In the Fig. 2.1, the red vehicles designate elected relay nodes. The transmission power levels assumed for the RSU and each vehicle are denoted as P_{RSU} and P_{V}, respectively. We consider the pencil-beam radiation pattern of the directional antenna to have elevation and horizontal Half Power Beam Width (HPBW) values of θ_{e} and θ_{h} degrees, respectively. By assuming reciprocality of transmission and reception operational modes, the maximum transmission antenna gain $G_{\text{t}}^{\max}$ and the maximum reception antenna gain $G_{\text{r}}^{\max}$ can be approximated as [16]: $G_{\text{t}}^{\max} = G_{\text{r}}^{\max} \approx \frac{32400}{\theta_{\text{e}}\theta_{\text{h}}}$

The directional antenna gain pattern is set to be uniform, so that the same gain is achieved in all directions, considering only angles that are nested within HPBW. This is fairly reasonable approximation assumption, since the highway width is typically relatively small (10 to 20 meters) in comparison to the coverage range covered within the HPBW. In addition, to account for some gain variation that will be incurred within the effective employed beamwidth, we incorporate a deduction of channel gain from $G_{\text{t}}^{\max}$ and $G_{\text{r}}^{\max}$.

In our numerical example, we have set $\theta_{\mathrm{e}} = \theta_{\mathrm{h}} = 60$ degrees along as well as deducted 1.5 dB from the gain. The deduction results in a gain level that represents a conservative approximation of the actual channel gain. This is explained by noting that when the highway width is relatively small in comparison to the transmission range, vehicle position variations induce antenna gain changes that correspond to shifts of only 10-15 degree over the coverage span of the directional antenna. Hence, the resulting reduced antenna gain becomes equal to $G_{\mathrm{t}} = G_{\mathrm{r}} = \frac{G_{\mathrm{t}}^{\max}}{\sqrt{2}} = \frac{G_{\mathrm{r}}^{\max}}{\sqrt{2}}$.

Incorporating these gain levels, and making use of a commonly employed channel model [17], we set the channel gain function, $G(d)$, expressed as a function of the distance (d) between the transmitter and receiver through the path loss model:

$$G(d) = G_{\mathrm{t}} G_{\mathrm{r}} \Big(\frac{c}{4\pi f_{\mathrm{c}} d_0}\Big)^2 \Big(\frac{d_0}{d}\Big)^{\alpha} \tag{2.1}$$

where $c = 3 \times 10^8 m/s$ is the speed of light. $f_{\mathrm{c}} = 5.9GHz$ is the carrier frequency. d_0 is the reference distance. α is the path loss exponent. The typical value of α for inter-vehicular communication links ranges from 2 to 4, as concluded from measurement data collected in [18]. For notational simplicity, we define $g_0 = \kappa d_0^{\alpha}$, where $\kappa = G_{\mathrm{t}} G_{\mathrm{r}} \Big(\frac{c}{4\pi f_{\mathrm{c}} d_0}\Big)^2$.

III Broadcast Capacity of DVBN at High Vehicular Traffic Density

We first consider the broadcast capacity of DVBN when the members of DVBN are located at the nominal positions $\{X_n, n \in \mathbb{Z}\}$, which can be guaranteed if the density of vehicle on the high way approaches infinity. Our goal is to determine the optimal nominal positions such that the broadcast capacity is optimized. To evaluate the broadcast capacity, we first evaluate the link capacity by applying the Additive White Gaussian Noise (AWGN) channel model. Let P_{N} be the noise power and W be the bandwidth. With the aid of location

information and control channel, the vehicle that is closest to a predetermined nominal elects itself as a relay node.

The election process can be realized using a timer based mechanism [19]. The election of vehicles to serve as RNs can be performed in two different fashions (as well as in such a combined manner): a. Triggered by the reception of a data packet; b. Performed periodically even when no data packet receptions are detected. Under the former process, the operation proceeds as follows. A vehicle that receives a new packet sets the time (i.e., number of slots) that it will wait, deferring to others, prior to initiating the transmission of this packet, in accordance with the configuration of a wait counter. The state of this counter is set to be inversely proportional to the distance between the vehicle's position to the closest nominal position. Each time that an idle slot is detected, the counter's state is reduced by a unit. Upon reaching state 0, the underlying vehicle elects itself to act as a relay node, proceeding then to transmit its packet in the forward direction. Neighborhood vehicles located in the forward direction from the RN will receive the transmitted packet and will thus learn about the election of this vehicle to act as a RN.

To inform neighboring vehicles that reside along the reverse direction (from this RN) along the highway about this election, the elected vehicle can send a brief control packet across the control channel using its reverse pointing antenna beam. (Note that the system is generally configured to include a control channel and multiple data channels, using different frequency bands. A single half-duplex radio module can be used to simultaneously receive or transmit distinct control and data signals across one or both antenna elements.) Neighboring vehicles located in the reverse direction would then void their timer count-down process. Furthermore, this control packet also serves as a positive acknowledgement packet. If an Automatic Repeat Request (ARQ) mechanism is then implemented across the corresponding RN-to-RN link, the lack of reception of such an ACK packet by an RN can induce retransmission of this packet. (Such an ARQ operation is however not included in the analyses presented in subsequent sections.)

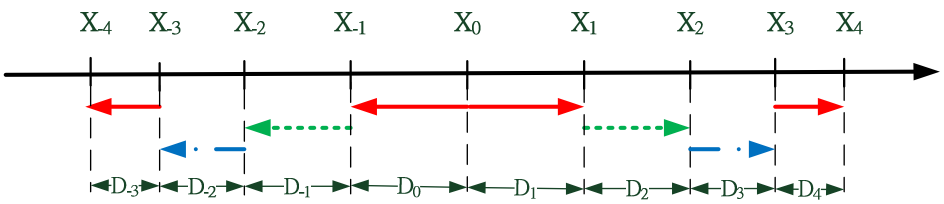

Figure 2.2: Reuse-3 scheme of RN transmissions

Under the second scheme, the election of vehicles to act as RNs is performed periodically, whether they receive or not broadcasted packets. In this case, the same count-down setting and process is used to induce the election of vehicles that are closest to the location of a nominal position. In this case, the control channel is used by a vehicle whose RN election related control packet timer has expired first to induce transmission of control packets in the forward and reverse directions to announce to neighboring vehicles that it has elected itself to act as a temporary relay node. It is noted that such an operation also resolves a potential "hidden terminal" problem, under which a vehicle located in the reverse direction of a transmitting RN may not be able to determine that the latter has elected itself to act as a relay node since it does not receive its data packet transmissions. Each vehicle that acts as a relay node (RN) is able to adjust its modulation/coding set and code rate to optimize the rate of transmission across its relay-to-relay communications link.

We assume the RN vehicles to share the communications band by employing a reuse-M scheme. Fig. 2.2 illustrate a reuse-3 scheduling of RN transmissions. Arrows with the same line pattern indicate transmissions that are taking place at the same time slot. The directions of the arrows identify the direction of packet forwarding. Of course, other Medium Access Control (MAC) schemes (including an IEEE 802.11p MAC protocol) can also be employed. Our analyses here however focus on the use of a reuse-M MAC protocol. It is noted that the implementation of such a scheduling scheme can also be greatly facilitated by the periodic exchange of synchronization packets along the control channel.

Hence, the link capacity $C_{\mathrm{L}}(X_n, X_{n-1})$ between the nominal positions X_n and X_{n-1} is

$$C_{\mathrm{L}}(X_n, X_{n-1}) =$$

$$\begin{cases} \frac{W}{M}\log_2\left(1+\frac{g_0 P_{\mathrm{RSU}} D_1^{-\alpha}}{P_{\mathrm{N}}}\right) & n=1 \\ \frac{W}{M}\log_2\left(1+\frac{g_0 P_{\mathrm{V}} D_n^{-\alpha}}{P_{\mathrm{N}}}\right) & 1<n\leq M \\ \frac{W}{M}\log_2\left(1+\frac{g_0 P_{\mathrm{V}} D_n^{-\alpha}}{P_{\mathrm{N}}+g_0 P_{\mathrm{RSU}}(L_1^{M+1})^{-\alpha}}\right) & n=M+1 \\ \frac{W}{M}\log_2\left(1+\frac{g_0 P_{\mathrm{V}} D_n^{-\alpha}}{P_{\mathrm{N}}+g_0 P_{\mathrm{RSU}}(L_1^{n})^{-\alpha}+g_0 P_{\mathrm{V}}\sum_{j=1}^{\frac{n-1}{M}-1}(L_{1+jM}^{n})^{-\alpha}}\right) & n=kM+1,\ k\geq 2 \\ \frac{W}{M}\log_2\left(1+\frac{g_0 P_{\mathrm{V}} D_n^{-\alpha}}{P_{\mathrm{N}}+g_0 P_{\mathrm{V}}\sum_{j=1}^{\frac{n}{M}-1}(L_{jM}^{n})^{-\alpha}}\right) & n=kM,\ k\geq 2 \\ \frac{W}{M}\log_2\left(1+\frac{g_0 P_{\mathrm{V}} D_n^{-\alpha}}{P_{\mathrm{N}}+g_0 P_{\mathrm{V}}\sum_{j=0}^{\lfloor\frac{n}{M}\rfloor-1}(L_{jM+\mathrm{mod}(n,M)}^{n})^{-\alpha}}\right) & o.w. \end{cases} \tag{2.2}$$

given by Eq. (2.2): where $D_n = |X_n - X_{n-1}|$ is the distance between relay X_n and X_{n-1} and $L_m^n = \sum_{j=m}^{n} D_j$, which is distance between X_{m-1} and X_n. Here, we only express the case for $n \geq 1$, the link capacity for $n < 1$ easily follows from Eq. (2.2) by symmetry. Note that there are no terms that is needed to be included in for $n \leq M$ to account for interference signals since in the first M intervals, receivers are not perturbed by interference signals, since we assume that there are no backward radiations resulting from packet transmissions performed by RNs located elsewhere along the highway. For receptions by RNs that are scheduled to transmit at the same slot assigned for RSU packet transmissions but located in distinct inter-RN intervals, we must account for interference terms that involve transmissions by the RSU as well as by other RNs, as expressed in Eq. (2.2) for the case $n = kM+1$. Receptions by RNs of transmissions that are executed during other time slots involve interference signals that are generated by other RN transmissions, as described by the last two equations in Eq. (2.2).

The broadcast capacity over a given road span from the RSU is the minimum value of

the capacities of the links involved in that road span.. Hence, to maximize the broadcast capacity by choosing D_n values, identified as a RN -layout, and simultaneously adjusting the selection of the Modulation and Coding Scheme (MCS) to realize the code rate determined by the use of Shannon's channel capacity formula, we solve the following maxi-min problem:

$$\underset{\{D_n\}}{\text{Maximize}} \quad \min_{n \in \mathbb{N}} \; C_{\mathrm{L}}(X_n, X_{n-1}) \tag{2.3}$$

A necessary condition for a RN-layout to serve as the solution of the maxi-min problem is to configure all links to operate at the same rate if feasible. For the achievability of link throughput equalization, we state the following Lemma:

Lemma 1. *Given $C_{\mathrm{L}}(X_0, X_1)$ and a prescribed D_1 level with $D_1 > 0$, there exists a sequence of D_n^* values such that $C_{\mathrm{L}}(X_0, X_1) = C_{\mathrm{L}}(X_n, X_{n-1})$ $\forall n \geq 1$.*

Proof. : From Eq. (2.2), we learn that $C_{\mathrm{L}}(X_n, X_{n-1}) \to 0$ as $D_n \to \infty$ and $C_{\mathrm{L}}(X_n, X_{n-1}) \to \infty$ as $D_n \to 0$. Since $0 < C_{\mathrm{L}}(X_0, X_1) < \infty$ given $D_1 > 0$ and $C_{\mathrm{L}}(X_n, X_{n-1})$ is continuous on D_n, by the Intermediate Value Theorem, there exists D_n^* such that $C_{\mathrm{L}}(X_0, X_1) = C_{\mathrm{L}}(X_n, X_{n-1})$ $\forall n \geq 1$. □

From Lemma 1, we learn that under the conditions stated, an optimal solution can be obtained. A numerically efficient algorithm for the calculation of the distance levels is readily obtained through the use of the following iterative procedure. Following the initial calculation of $C_{\mathrm{L}}(X_0, X_1)$, the value of D_2 is computed so that we achieve $C_{\mathrm{L}}(X_1, X_2) = C_{\mathrm{L}}(X_0, X_1)$. A simple iterative bi-section method is used for this purpose. We proceed similarly in an iterative fashion to calculate D_3, D_4,...However, the constructive method only specifies the relative quantity of inter-relay distance between different links. We have not yet specified how we determine the quantity of D_1. Once D_1 is determined, the rest D_n values can be determined accordingly.

As observed from Eq. (2.2) and Lemma 1, the capacity of each link can be increased

to very high levels by setting the inter-RN distances to very low values. However, due to physical constraints, such as induced by the size of each vehicle and the requirement of maintaining safety spacing between vehicles flowing along the highway, it is not possible to select inter-relay distance levels that are arbitrarily small. Therefore, we impose a constraint $D_{\min}$ on the minimum inter-relay distance value to be set, so that the VBN is realizable.

IV Broadcast Capacity of DVBN under a Stochastic Vehicular Traffic Process

In real world scenario, it is in general not possible to find a vehicle locating exactly at the nominal positions since the vehicle density over the high way is finite. In this case, we in turn select the vehicle that is closest to a nominal position as the relay. In addition, it is possible that there may be no vehicles locating near a nominal position, degrading the link capacity accordingly. In the following, we provide an analytical model with homogeneous selection of D_n values to evaluate the broadcast capacity with relay positions deviating from the nominal positions. The adoption of homogeneous D_n ($D_n = D\ \forall n$) values is validated by its comparable throughput performance as that of heterogeneous selection of D_n values, i.e. selecting D_n values in a way that equalize the link capacity, with imposed minimum distance constraint as illustrated in the following section.

IV.1 From Heterogeneous to Homogeneous D_n Values

To illustrate how the stochastic deviation impacts the broadcast capacity, we may first refer to Fig. 2.3. The simulation parameters are set up as follows: $M = 3$, $W = 10$ (MHz), $P_{\text{RSU}} = P_{\text{V}} = 23$ (dBm), highway length= 10 (km) (5 (km) to the each side of RSU), and $D_{\min} = 25$ (m). For the directional antenna gain, we set $\theta_{\text{e}} = \theta_{\text{h}} = 60$ degrees, corresponding to a maximum antenna gain 9.54 (dB). To account for variations in the antenna gain related with beam misalignments across the RN-to-RN link, we set $G_{\text{t}} = G_{\text{r}} = 8.04$ (dB), which

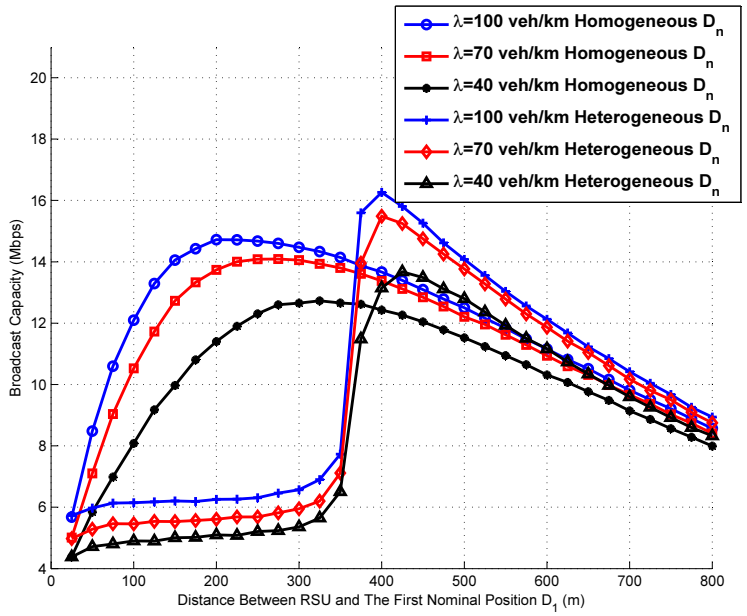

(a) $\alpha = 3$

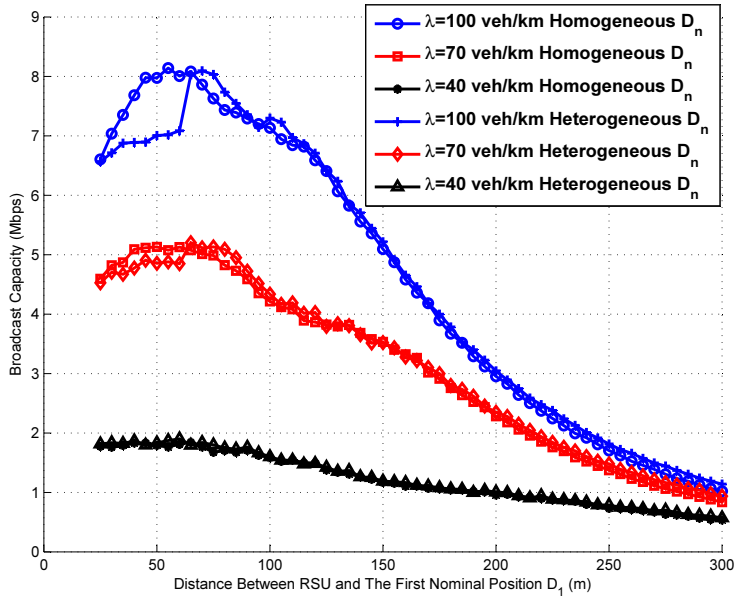

(b) $\alpha = 4$

Figure 2.3: Broadcast capacity of heterogeneous and homogeneous inter-relay distance with respect to different choices of D_1 under minimum distance constraint $D_{min} = 25$ (m).

includes 1.5 (dB) reduction from the value attained by the maximum gain. As commonly assumed, and as validated by measurement data presented in [20], we model the stochastic flow of vehicles along the highway as a Poisson process with density λ (vehicles/km).

It is of key interest to determine the magnitude of throughput improvement that can be achieved by setting the nominal positions in accordance with heterogeneous D_n values when vehicular traffic flows are modeled as stochastic processes. We study this problem by assuming the nominal positions to be pre-configured in accordance with the iterative calculation procedure presented in Section III. However, to assure the setting of realistic distances between nominal positions, we impose a minimum inter-RN nominal value ($D_{\min}$) of 25 meters. To simplify, we set the inter-RN nominal position distance to be equal to $D_n := \max\{D_n, D_{\min}\}$. Note, however, that such a setting is done for computational convenience and does not yield inter-RN nominal position distance levels that achieve the highest throughput capacity rate.

Using such settings, we show in Fig. 2.3 the behavior of the broadcast throughput capacity rate as a function of the set D_1 value. We note that, under a heterogeneous setting, for $\alpha = 3$, if the value of D_1 is lower than a certain threshold level (350 (m) in this case), the throughput rate becomes very low since the subsequent inter-RN distances must then also be selected to be low to assure high SINR levels at the receiving relay nodes. In this case, many inter-RN nominal distance levels are set equal to 25 (m), resulting in sub-optimal behavior. Under such occasions, homogeneous distance settings yield much higher throughput capacity rate levels. For $\alpha = 4$, inter-RN links tend to operate in noise dominated regime for link distances that are longer than about 75 (m), so that the impact of the exact settings used for subsequent inter-RN distances is much lower. Consequently, we note from Fig. 2.3 that for this case the use of an homogeneous setting for the inter-RN nominal distances yields a throughput capacity rate performance behaviour that follows closely that obtained under an heterogeneous setting layout.

We observe that the upper envelope of the corresponding (homogeneous and heteroge-

neous configuration setting) curves forms a curve that is a lower bound on the optimal throughput capacity level attained by solving a constrained optimization problem that imposes the minimum spacing limitation of 25 (m). The solution of such an optimization problem is not presented herein. Yet, by examining the results obtained when the optimal settings do not require the latter spacing truncation (involving the more desirable initial range value that is longer than 350 (m)) , we deduce the following conclusion. We surprisingly find that the broadcast capacity realized under the use of homogeneous inter-relay distance values shows negligible degradation in comparison to that attained under heterogeneous inter-relay distance levels, for all examined vehicular traffic density λ levels.

We also observe that under homogeneous setting, for higher vehicular traffic rate value, represented by λ, a higher broadcast capacity rate level is achievable, since it is then more likely that vehicles that are elected as relay nodes would be situated at positions that are closer to nominal positions. For lower α values, such as for the illustrated $\alpha = 3$ level, elected RN receivers will monitor higher interference levels; consequently, to achieve optimal broadcast capacity, a higher D (up to 400 (m)) level will be configured.

Based on the results presented in Fig. 2.3, we may anticipate that the adoption of homogeneous inter-relay distance is a promising solution when directional antenna is used. Furthermore, the use of homogeneous inter-relay distance may greatly simplify our analysis of the impact of stochastic deviations on broadcast capacity. In the following, we provide mathematical analysis of the broadcast capacity considering stochastic deviations.

IV.2 Modeling Stochastic Deviation

First, we consider the location deviation within a nominal position given that there is at least one candidate for relay associated with the nominal position. Candidates for relay associated with a nominal position X_n are defined as the vehicles locating in the region $[X_n - \frac{D}{2}, X_n + \frac{D}{2}]$. We first evaluate the Probability Density Function (PDF) of Δ , the location deviation of candidates from the a nominal position, which is stated in the following

lemma.

Lemma 2. *The PDF of* Δ *is evaluated as*

$$f_{\Delta}(\delta) = \begin{cases} \dfrac{\lambda e^{-2\lambda|\delta|}}{1-e^{-\lambda D}} & -\dfrac{D}{2} \leq \delta \leq \dfrac{D}{2} \\ 0 & o.w. \end{cases} \tag{2.4}$$

With Lemma 2 , we may evaluate the PDF of inter-relay distance between the n^{th} and the $(n-1)^{\text{th}}$ relay nodes ($n \geq 2$) with the random variable $W_n = R_n + Z_n$. R_n is a geometric random variable with $\Pr(R_n = kD) = (e^{-\lambda D})^{k-1}(1-e^{-\lambda D})$ for $k \geq 1$ and $Z_n = \Delta_n^{(1)} - \Delta_n^{(2)}$, with $\Delta_n^{(1)}$ and $\Delta_n^{(2)}$ being the i.i.d. random variables taking the same distribution Δ. Hence, we may evaluate the the PDF $f_Z(z)$ of Z_n through convolution of the PDF of Δ and hence derive the Cumulative Distribution Function (CDF) of Z_n.

To evaluate the broadcast capacity, we first make the following assumptions to approximate the link capacity. Firstly, we assume that $P_{\text{RSU}} = P_{\text{V}}$. The analytical deviation can be easily generalized to $P_{\text{RSU}} \geq P_{\text{V}}$. Secondly, we only consider the interference from the closest transmitter. Thirdly, we approximate the random variable W_n with $W_n = \mu + Z_n$, i.e. the geometric random variable R_n is replaced by its mean $\mu = D(1-e^{-\lambda D})^{-1}$.

Since $C_{\text{L}}(X_n, X_{n-1})$ is a decreasing function of Z_n,

$$\min_{1\leq n\leq M} C_{\text{L}}(X_n, X_{n-1}) \approx \frac{W}{M}\log_2\left(1 + \frac{g_0 P_{\text{V}}\left(\mu + \max\limits_{1\leq n\leq M} Z_n\right)^{-\alpha}}{P_{\text{N}}}\right) \tag{2.5}$$

$$\min_{M<n\leq \lfloor \frac{L}{\mu} \rfloor} C_{\text{L}}(X_n, X_{n-1}) \approx \frac{W}{M}\log_2\left(1 + \frac{g_0 P_{\text{V}}\left(\mu + \max\limits_{M<n\leq \lfloor \frac{L}{\mu} \rfloor} Z_n\right)^{-\alpha}}{P_{\text{N}} + g_0 P_{\text{V}}\left((M+1)\mu + \max\limits_{M<n\leq \lfloor \frac{L}{\mu} \rfloor} Z_n\right)^{-\alpha}}\right) \tag{2.6}$$

where L is the highway length and hence $\lfloor \frac{L}{\mu} \rfloor$ denotes the average number of relay nodes

elected. The term $(M+1)\mu$ in Eq. (2.6) represents the mean distance between the closest interferer and the receiver when reuse-M is adopted. Let $\hat{Z} = \max_{1\le n\le M} Z_n$ and $\tilde{Z} = \max_{M<n\le\lfloor\frac{L}{\mu}\rfloor} Z_n$. Let $F_{\hat{Z}}(\hat{z})(f_{\hat{Z}}(\hat{z}))$ and $F_{\tilde{Z}}(\tilde{z})(f_{\tilde{Z}}(\tilde{z}))$ be the CDF (PDF) of $\hat{Z}$ and $\tilde{Z}$, respectively. In addition, define $\gamma : \tilde{z} \to \hat{z}$ such that

$$\frac{g_0 P_{\mathrm{V}}(\mu+\gamma(\tilde{z}))^{-\alpha}}{P_{\mathrm{N}}} = \frac{g_0 P_{\mathrm{V}}(\mu+\tilde{z})^{-\alpha}}{P_{\mathrm{N}} + g_0 P_{\mathrm{V}}((M+1)\mu+\tilde{z})^{-\alpha}} \tag{2.7}$$

That is,

$$\frac{g_0 P_{\mathrm{V}}(\mu+z)^{-\alpha}}{P_{\mathrm{N}}} < \frac{g_0 P_{\mathrm{V}}(\mu+\tilde{z})^{-\alpha}}{P_{\mathrm{N}} + g_0 P_{\mathrm{V}}((M+1)\mu+\tilde{z})^{-\alpha}} \ \ \forall z > \gamma(\tilde{z}) \tag{2.8}$$

meaning that one of the link among the first M links becomes the dominant link if $z > \gamma(\tilde{z})$. Hence, we may evaluate the broadcast capacity by Eq. (2.9). The first term in Eq. (2.9) accounts for the case when some link capacity $C_{\mathrm{L}}(X_n, X_{n-1})$ with $0 \le n \le M$ becomes the dominated link; while the second term accounts for the case when some link capacity $C_{\mathrm{L}}(X_n, X_{n-1})$ with $M < n \le \lfloor\frac{L}{\mu}\rfloor$ becomes the dominated link.

$$\begin{aligned}\mathbb{E}[C_{\mathrm{B}}] = &\int_{-D}^{D} \frac{W}{M}\log_2\left(1+\frac{g_0 P_{\mathrm{V}}(\mu+\gamma(\hat{z}))^{-\alpha}}{P_{\mathrm{N}}}\right) F_{\tilde{Z}}(\gamma^{-1}(\hat{z}))f_{\hat{Z}}(\hat{z})d\hat{z} \\ &+ \int_{-D}^{D} \frac{W}{M}\log_2\left(1+\frac{g_0 P_{\mathrm{V}}(\mu+\tilde{z})^{-\alpha}}{P_{\mathrm{N}} + g_0 P_{\mathrm{V}}((M+1)\mu+\tilde{z})^{-\alpha}}\right) F_{\hat{Z}}(\gamma(\tilde{z}))f_{\tilde{Z}}(\tilde{z})d\tilde{z}\end{aligned} \tag{2.9}$$

The validity of the numerical solution, under the homogeneous inter-RN distance setting, is illustrated in Fig. 2.4 for $\alpha = 3$. Parameters are set the same as we used in Section IV.1. It can be clearly seen that despite the fact that the approximation tends to overestimate the broadcast capacity under low inter-relay distance, and underestimate the broadcast capacity under low vehicular traffic density ($\lambda = 40$ (vehicles/km)), it well captures the proper settings to be used for selecting the optimal inter-relay distances under different vehicular traffic

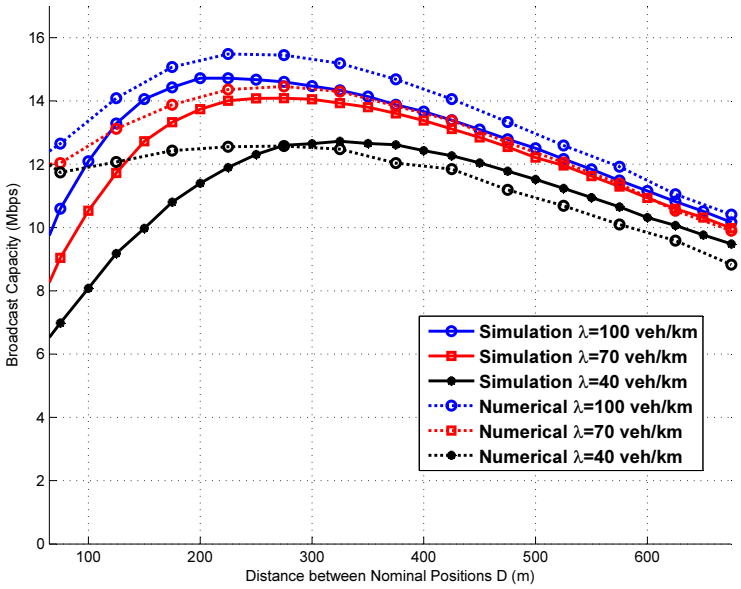

Figure 2.4: Broadcast capacity of DVBN for $\alpha = 3$ under homogeneous inter-RN distance densities.

V Illustrative Broadcast Capacity Gain Attained by Using Directional Antennas: DVBN vs. VBN

The use of directional antennas by vehicles yields higher antenna gains and results in the lowering of the aggregate interference signal power monitored at vehicular receivers. These improvements are attained by incurring higher antenna costs. It is therefore of prime importance to determine the magnitude of throughput improvement that can be achieved by using directional antenna modules in comparison with corresponding omni-directional antenna based network systems. To evaluate the antenna gain G of an employed omni-directional antenna, the following curve-fitting based formula [21] is used:

$$G = 10 \log_{10} \left[191 \sqrt{0.818 + \frac{1}{\theta_e}} - 172.4 \right] \text{ (dB)} \tag{2.10}$$

By adopting Eq. (2.10) and setting $\theta_e = 60$, we obtain an antenna gain with 3.22 (dB). For the directional antenna used in our DVBN system, we set antenna gain 8.04 dB, as derived in Section IV.1. We use the following parameters for performance evaluation: $M = 3$, $W = 10$ (MHz), $P_{RSU} = P_V = 23$ (dBm), and highway length = 10 (km) (5 (km) on each side of RSU). Our simulation based performance results, exhibiting the system's throughput capacity as a function of the distance parameter D, are shown in Fig. 2.5. To characterize the dependence of the results on the channel model, we set the attenuation exponent α to be equal to 3 and 4 in Fig. 2.5.

It can be clearly seen from Fig. 2.5 that by using a directional antenna, the broadcast throughput capacity rate is improved by a factor of 2 to 3, depending on the vehicular traffic density level. For $\alpha = 4$, we achieve even higher gains, attaining (when employing a directional antenna system) a throughput capacity improvement factor that is ranging from 6 to 10. These gains are attained due to the enhanced values of the SINR levels monitored at the RN receivers, induced by the realization of better interference rejection features and by the higher gains characterizing the use of the directional antenna systems. We further note that our use of an adaptive coding rate operations allows us to make use of such improved SINR values. We also observe that as the attenuation exponent α increases from 3 to 4, the peak throughput capacity rate value is achieved at shorter inter-RN (D) ranges. This is explained by noting that for higher α levels, the impact of interference signals is reduced, while the intended signal attenuates faster with distance, so that the inter-RN link becomes noise dominated unless the inter-RN range is sufficiently reduced.

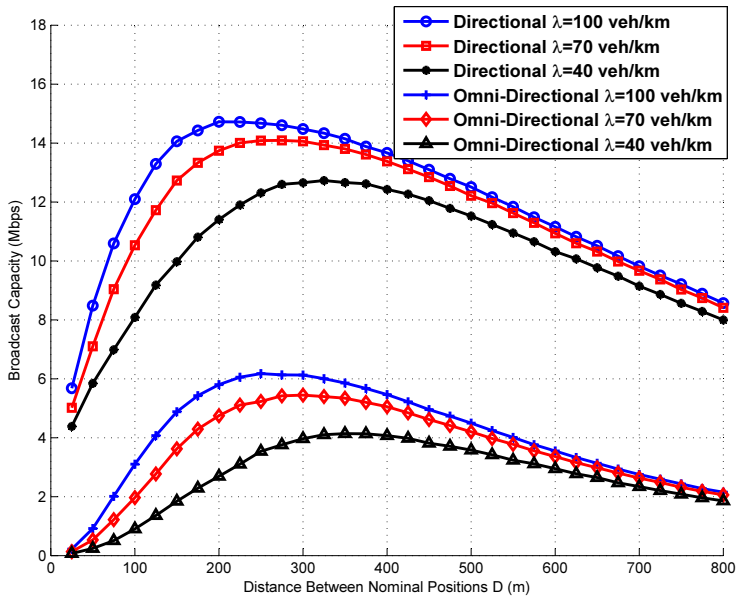

(a) $\alpha = 3$

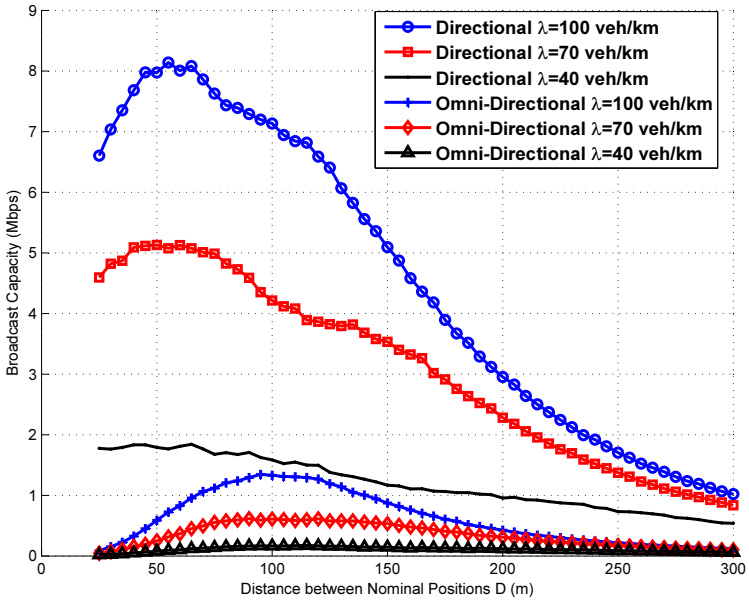

(b) $\alpha = 4$

Figure 2.5: Broadcast capacity of directional and omni-directional antennas.

VI Concluding Remarks

As a promising solution to the broadcast storm problem, the self-election mechanism proposed in this chapter, for the assignment of vehicles to act as relay nodes in a dynamic

backbone network, facilitates packet broadcasting to vehicles traveling along a highway system. GPS data is used to allow a limited number of vehicles to self-elect themselves as relay nodes (RNs), while also making use of directional antenna systems that are installed on the vehicles. Each vehicle employs an adaptive rate mechanism in adjusting the selection of a modulation/coding scheme by each vehicle that acts as a RN. We demonstrate that by targeting an homogeneous inter-relay distance pattern, we are able to achieve a throughput capacity rate performance that is virtually as high as that of a heterogeneous pattern. This observation validates the adoption of a simple homogeneous relay selection strategy even in presence of channel gain asymmetry features demonstrated by directional antenna modules. We also determine the best inter-RN range values to be set under stochastic vehicular traffic processes. We demonstrate the significant throughput capacity gains that can be achieved by using a DVBN networking mechanism, compared with a VBN scheme in which vehicles use omni-directional antennas. The presented protocol has also been shown to yield excellent performance when used in conjunction with a IEEE 802.11p based MAC, and by incorporating a distance based forwarding (DBF) mechanism in the self-election of vehicles to act as relay nodes.

CHAPTER 3

Throughput Maximization under Guaranteed Dissemination Coverage for VANET Systems

I Introduction

Messages that report real-time traffic conditions are often transmitted by the VANET system along a highway in a broadcasting manner, spanning a distance beyond the radio coverage achieved by a single vehicle-to-vehicle link. Hence, multiple vehicles must be selected to act as relay nodes (RNs), serving to forward messages along a multihop route. However, without the use of appropriate mechanisms that coordinate the spatial-reuse scheduling of such simultaneous message transmissions by multiple RNs across the highway, broadcast packets distributed in such an ad hoc network system may result in broadcasting storm problems [7].

The design of message propagating protocols in VANET systems has been studied extensively, including distance-based algorithms [8, 9] and cluster-based forwarding schemes [10, 11], aiming to alleviate broadcast storm problems by selecting only a subset of vehicles to act as relay nodes. Initially, many versions of these protocols lack rigorous methodologies to optimally set algorithmic parameters. More recently, sophisticated mechanisms have been proposed along with proofs of optimality, as in [22–25]. In [22, 23], the authors optimally select relay nodes to minimize the end-to-end delay. However, in this paper, the authors do

not study the performance impact induced the cross-layer physical and MAC layer operations, thus also ignoring the impact of the induced interference signals on the derived optimal VANET system configuration. Also, these papers do not account for the optimization of the throughput rate performance. In turn, the study performed in [24], which employs a stochastic geometry based interference model, relates to the model that we use in this chapter in the sense that both studies investigate the performance of a VANET system through the joint optimal configuration of a Time Division Multiple Access (TDMA) MAC scheme along with the optimal setting of inter-relay positions and the specification of spatial reuse factors. However, in this chapter, we take a further step by jointly optimizing the settings of relay positions, spatial reuse factors, and in addition, the link transmission rates; the joint setting of the latter parameters are not considered in [24].

We have recently developed a forwarding protocol for a VANET system that is based on a Vehicular Backbone Network (VBN) architecture [12, 26]. In a VBN, targeted nominal positions along the highway close to which it would be highly beneficial to have vehicles elect themselves to act as RNs are periodically announced. A VANET system that is synthesized in accordance with the VBN protocol has been shown to outperform other networking schemes, offering much enhanced throughput rate, packet delay, and packet delivery ratio performance behavior [19]. However, the performance of a VBN based VANET can be significantly degraded under the occurrence of high random deviations in the spacings between vehicles under low to medium vehicular traffic flow rates. In [12], we obtain the optimal spatially averaged end-to-end throughput capacity rate without considering the the outage probability of the system. Since retransmissions are generally not performed under a broadcasting service mode, such a design can result in an undesirable high packet loss rate and a low coverage scope in the broadcasting of critical message flows.

The purpose of this chapter is to stochastically characterize the attainable coverage scope of the VANET network system, and to deduce the design of the system to avoid, when feasible, low packet delivery ratio occurrences. Consequently, we present in this chapter

mathematical models that determine the best corresponding design of a VANET system, under given vehicular traffic rate conditions, based on the VBN architecture. We aim to attain a design that achieves a high message flow throughput rate while meeting a maximum prescribed outage probability, attaining a sufficiently wide coverage scope of vehicles traveling along the highway. We identify the best configuration and parameters to use for such a network system, identifying the best joint settings to use for inter-RN distances, for link transmission rates, and for the MAC layer based spatial reuse factor, under different observed vehicular traffic density levels.

This chapter is organized as follows. In Section II, we describe the system model. In Section III, we study the broadcast capacity rate that can be attained under stochastic deviations in the positions of elected RNs. In Section IV, we illustrate the throughput rate levels that can be achieved under the proposed model, when the system is optimally configured, under prescribed coverage target levels. We confirm the precision of our mathematical models via computer simulations. Conclusions are drawn in Section V.

II System Model

II.1 Vehicular Backbone Network

We consider the dissemination of messages along a linear highway. A Road Side Unit (RSU) periodically broadcasts messages to vehicles located in its vicinity. To extend the coverage of the RSU in a cost-effective way without installing additional infrastructure, vehicles on the highway can be elected as RNs to support message propagation. If nodes elect to forward received packets in a manner that is not properly coordinated, a substantial number of packets may be discarded due to the occurrence of packet collision events, leading to an operation that exhibits a low packet delivery ratio and low throughput rates.

To alleviate such performance degradation conditions, we restrict the number of activated RNs by introducing the concept of a configured backbone network (Bnet), which is formed

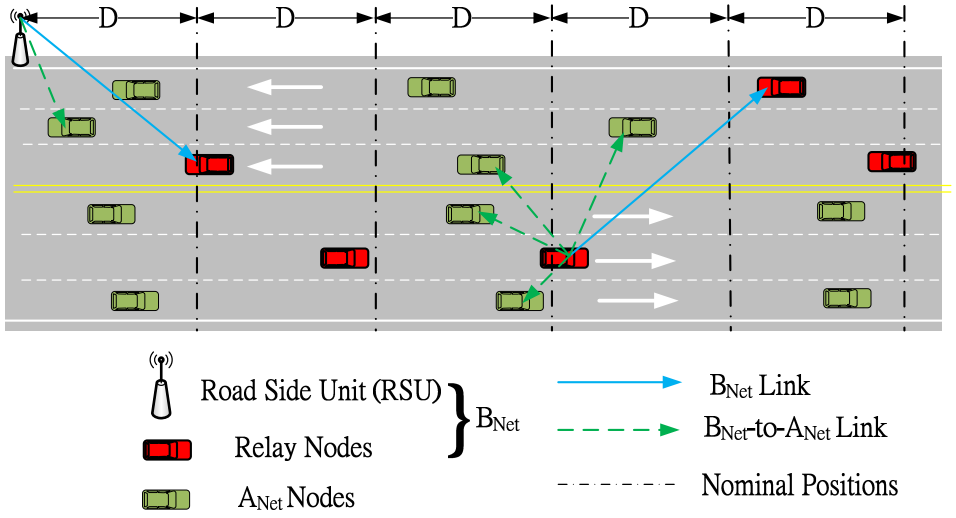

Figure 3.1: Illustration of a Vehicular Backbone Network

by selecting a subset of vehicles to act as Relay Nodes (RNs). Elected vehicles are those that are located closest to the respective predetermined nominal positions. The latter are separated by distance D, as illustrated in Fig. 3.1. Each vehicle then associates itself with an RN. An RN and its associated user stations form an Access Net (Anet). RNs form backbone links and the collection of the RNs and these links forms the Bnet. Only those nodes that are currently members of the Bnet are responsible for forwarding the messages issued by the RSU. The messages forwarded by a RN are recievd by all of its Anet clients as well as forwarded downstream to its RN neighbor. Thus, the Bnet consists of the RSU, the RNs, and the inter-RN links. Non-RN stations are Anet members.

The synthesis of the Bnet can be managed in a centralized fashion by the RSU. The RSU periodically collects control data from highway vehicles, which serve to identify the link state status of each vehicle and its attached links. Such data includes Channel Quality Indicators (CQI) that identify key parameters relating to noise and interference signal power levels experienced in communicating across each link, as well as vehicular mobility and spacing parameters. Upon receipt of a beacon from the RSU announcing the set of selected RNs across an underlying segment of the highway, each vehicle is able to identify the RN with

which it associates at the current time based on its location along the highway. A vehicle associates itself with the RN that is at the shortest distance from it along the road. For this purpose, it is assumed that vehicular geo-location attributes are kept at the stations, and announced periodically within the beacon.

II.2 Channel Model

Messages are disseminated from an RSU along a linear highway of length L. To simplify our analysis but without loss of generality, we consider the forwarding of messages on one side of an RSU. Each vehicle is equipped with an omni-directional antenna system, with transceiver operating in the half-duplex mode. All vehicles use a fixed transmission rate R, associated with a targeted Signal-to-Interference-Noise-Ratio (SINR) threshold γ_{th}. The setting the targeted SINR threshold is determined by using dynamically executed measurements that lead to the calculation of realistically attained SINR levels. Then, based on the prescribed bandwidth level allocated for the underlying broadcast service and based on the targeted bit error rate probability, the set of realizable data rate levels corresponding to employed modulaiton/coding schemes are determined [27].

A set of nominal positions, such that neighboring positions are separated by distance D level, are predetermined. Those vehicles that are located closest to these nominal positions at the relay election time are selected as RNs, aided by the use of geo-location data. This election process can be implemented in a centralized fashion through the use of election control messages sent by the RSU across a control channel [12], or through the use of a distributed election protocol [19].

We model each vehicle-to-vehicle link as an Additive White Gaussian Noise (AWGN) channel. To calculate the signal power received across a single link at a receiver that is located at a distance d away from the transmitter, we assume a simple exponential path loss model. In rural or suburban area whereby signal propagation is not generally impacted by reflected paths, such a path loss model serves well to predict the power level of signals

received across highway links. The channel gain $G(d)$ is thus expressed as

$$G(d) = G_{\mathrm{t}} G_{\mathrm{r}} \Big(\frac{c}{4\pi f_{\mathrm{c}} d_0} \Big)^2 \Big(\frac{d_0}{d} \Big)^{\alpha}, \tag{3.1}$$

where G_{t} and G_{r} are the antenna gains at the transmitter and receiver modules, respectively. In addition, $c = 3 \times 10^8$ (m/s) is the speed of light, $f_{\mathrm{c}} = 5.9$ (GHz) is the carrier frequency adopted by the IEEE 802.11p standard, d_0 is a reference distance, and α is the path loss exponent. Typical values for α range from 2 to 4, as suggested in highway measurements conducted by [18]. The received power at the intended receiver is thus expressed as

$$P_{\mathrm{r}}(d) = P_{\mathrm{t}} G(d), \tag{3.2}$$

where P_{t} is the transmit power level.

III Impact of Stochastic Deviations in RN Locations on the Performance of a TDMA reuse-M Based VBN

In this section, we obtain mathematical expressions that are used to evaluate the maximum throughput rate achievable under a prescribed outage probability constraint. Our model is based on making the following approximations:

1. Inter-relay distances are assumed to be i.i.d. random variables.
2. The number of RNs along the underlying highway segment is approximated by its mean.
3. The intended receiver experiences interference that is dominated by the signal power issued by the RN that is located closest to that receiver, at a corresponding distance

that is approximated by the mean value of the inter-relay distance.

The precision of the analysis performed using these approximations is well confirmed by the results presented in the next section through the conduct of Monte Carlo simulations.

We assume that vehicles are distributed along the linear highway according to a Poisson point process (PPP) with density λ (vehicles/km). The applicability of this model has been confirmed by measurements that show inter-vehicle distances to be accurately modeled by an exponential distribution [28] under a wide range of vehicular flow density regimes. We assume a TDMA reuse-M MAC layer operation. Such a scheduling mechanism has proven to be highly effective in best mitigating the impact of signal interferences induced by simultaneous transmissions across the highway [4].

The spatial reuse-M TDMA scheduling scheme is configured as follows. Assume that there are a total N elected RNs spanning the highway segment under consideration. These RNs are indexed in an ascending order based on their distance from the RSU. Consider a TDMA time-frame which consists of M slots. A single slot is used for the transmission of a single packet across an inter-RN link. The set of indices of RNs that are assigned to transmit their packets, if any, in the time slot i of a frame is denoted as $A^{(i)}$, where

$$A^{(i)} = \{i + kM | [k \in \{0\} \cup \mathbb{N}] \wedge [i + kM \leq N]\}. \tag{3.3}$$

We aim to maximize the throughput rate achieved by the VBN system under a prescribed outage probability constraint. The outage probability is defined as the long term fraction of time during which packets across at least a single inter-RN link cannot be delivered, when operating under the specified transmit data rate. When such an event happens, certain packets are not distributed in a complete manner over the highway segment under consideration, leading thus to reduced spatial coverage. We note that a packet will be delivered successfully across the complete span of the highway if and only if, in all time slots during which the packet has been transmitted, the received SINR levels at the corresponding RN receivers are

greater than or equal to the prescribed SINR threshold. Thus, we state an outage event to occur when the following conditions are met:

Definition 1. *Given the values of $R, L, D, \gamma_{\text{th}}$, and a realization of vehicular layout topology, an outage is declared if there exist a time slot index i and an RN index and $n \in A^{(i)}$ such that*

$$\frac{P_{\text{r}}(d(n, n+1))}{P_{\text{N}} + \sum\limits_{k \in A^{(i)} \wedge k \neq n} P_{\text{r}}(d(k, n+1))} < \gamma_{\text{th}}, \tag{3.4}$$

where $d(k, n)$ is the distance between the RN transmitter with index k and the RN receiver with index n.

To evaluate the outage probability by incorporating the stochastic behavior of the vehicular topology, we first examine the behavior of the bottleneck link. For this purpose, we derive the Probability Density Function (PDF) of the maximum distance level realized between elected RNs. Since the locations of vehicles follows a Poisson distribution, the deviation of a relay position from its nominal position is noted to be governed by a truncated-exponential variable Δ. The PDF of this variable is denoted as $f_{\Delta}(\delta)$ and its Cumulative Distribution Function (CDF) is identified as $F_{\Delta}(\delta)$. We obtain them to be expressed as:

$$f_{\Delta}(\delta) = \begin{cases} \frac{\lambda e^{-2\lambda|\delta|}}{1-e^{-\lambda D}} & -\frac{D}{2} < \delta < \frac{D}{2} \\ 0 & \text{otherwise} \end{cases} \tag{3.5}$$

$$F_{\Delta}(\delta) = \begin{cases} 0 & \delta < -\frac{D}{2} \\ \frac{1}{2(1-e^{-\lambda D})}[e^{2\lambda\delta} - e^{-\lambda D}] & -\frac{D}{2} \leq \delta < 0 \\ \frac{1}{2} + \frac{1}{2(1-e^{-\lambda D})}[1 - e^{-2\lambda\delta}] & 0 \leq \delta < \frac{D}{2} \\ 1 & \delta \geq \frac{D}{2} \end{cases} \tag{3.6}$$

In cases where the vehicular density is low, it is possible that there will be, during an election interval, no vehicle traveling in the sub-segment of the highway which covers the interval $(-\frac{D}{2}, \frac{D}{2})$ around a nominal position. In this case, there will be no vehicles that serve as elected RNs associated with this underlying nominal position. We characterize the distance between elected RNs k and $k+1$ by the random variable Z_k, whereby

$$Z_k = V_k D + \Delta_k. \tag{3.7}$$

The random variable Δ_k follows the truncated exponential distribution specified in Eq. (3.5). The random variable V_k designates the number of nominal positions spanning the distance between elected relay node k and elected relay node $k+1$. The variable V_k is characterized by following a Geometric distribution:

$$\Pr\{V_k = v\} = (e^{-\lambda D})^{v-1}(1 - e^{-\lambda D}) \quad v = 1, 2, 3..., \tag{3.8}$$

noting that $e^{-\lambda D}$ represents the probability that there is no elected relay node associated with a nominal position.

The outage probability for the system is calculated by examining the bottleneck inter-RN link, which is the longest inter-RN link for an underlying realization of the stochastic process representing RN positions. The distance between the two RNs of the bottleneck link is characterized by the random variable Y, where

$$Y = \max\{Z_k | k = 1...K\} \tag{3.9}$$

The random variables $\{Z_k | k = 1...K\}$ are independent and identically distributed. To reduce the computational complexity of the calculation, we approximate the number of links along

the highway by its mean value K, where

$$K = \frac{L}{\mathbb{E}[Z_1]} = \frac{L}{\mathbb{E}[V_1]D} = \frac{L(1-e^{-\lambda D})}{D}. \tag{3.10}$$

The first equality in Eq. (3.10) follows from the fact that $\mathbb{E}[\Delta_1] = 0$.

Given the distribution of Z_k , the outage probability for the TDMA system is then approximated as

$$P_{\text{out}} = \mathbb{P}\left\{ \frac{P_{\text{r}}(Y)}{P_{\text{N}} + P_{\text{r}}\big(\mu(M-1)\big)} < \gamma_{\text{th}} \right\}, \tag{3.11}$$

where $\mu = \mathbb{E}[Z_1] = \frac{D}{1-e^{-\lambda D}}$ and $\mu(M-1)$ represents the mean distance between the receiver and its closest interfering RN. For the simplified path loss model assumed here, the outage probability is thus written as

$$P_{\text{out}} = 1 - \left\{ F_{Z_1}\left(\left[\frac{\gamma_{\text{th}}(P_{\text{N}} + P_{\text{r}}\big(\mu(M-1)\big))}{P_{\text{t}} g_0} \right]^{\frac{-1}{\alpha}} \right) \right\}^K, \tag{3.12}$$

where $g_0 = G_{\text{t}} G_{\text{r}} \left(\frac{c}{4\pi f_{\text{c}} d_0} \right)^2 d_0^{\alpha}$.

The end-to-end throughput-rate $\eta(M)$ that is attained under the use of a reuse-M spatial TDMA operation and a link data rate R is expressed as

$$\eta = \frac{R}{M}(1 - P_{\text{out}}). \tag{3.13}$$

IV Performance Evaluation

In this section, we evaluate the performance of a VBN system that involves stochastic vehicular flows. We use our analytical models to evaluate the performance behavior of the system, in calculating the maximum attainable value for the system's throughput capacity rate. Furthermore, we identify the system configuration parameters that should be selected

Table 3.1: Maximum achievable throughput rates (in Mbps) and feasible values of D under prescribed outage constraints

100vehs/km	Outage Probability Constraint			
Transmission Rate	5%	10%	15%	20%
6Mpbs (Simulation)	1.5 (4)	1.5 (4)	1.5 (4)	1.5 (4)
Range of D (m)	80/360	70/370	70/370	70/370
6Mpbs (Analytical)	1.5 (4)	1.5 (4)	1.5 (4)	1.5 (4)
Range of D (m)	80/350	70/350	70/360	60/360
12Mbps (Simulation)	2.88 (4)	2.88 (4)	2.88 (4)	2.88 (4)
Range of D (m)	160/170	140/220	120/230	110/230
12Mpbs (Analytical)	2.88 (4)	2.88 (4)	2.88 (4)	2.88 (4)
Range of D (m)	160/190	90/210	80/230	70/230
18Mbps (Simulation)	3.59 (5)	3.59 (5)	3.59 (5)	3.59 (5)
Range of D (m)	90/220	90/220	80/230	80/230
18Mbps (Analytical)	3.6 (5)	3.6 (5)	3.6 (5)	3.6 (5)
Range of D (m)	80/190	70/210	70/220	70/220
24Mbps (Simulation)	2.62 (9)	2.73 (8)	2.73 (8)	2.73 (8)
Range of D (m)	80/120	100	80/110	80/120
24Mbps (Analytical)	2.98 (8)	3.15 (7)	3.15 (7)	3.15 (7)
Range of D (m)	80/100	70	70	70/80

40vehs/km	Outage Probability Constraint			
Transmission Rate	5%	10%	15%	20%
6Mpbs (Simulation)	1.44 (4)	1.44 (4)	1.44 (4)	1.44 (4)
Range of D (m)	210/260	180/290	160/310	150/320
6Mpbs (Analytical)	1.5 (4)	1.5 (4)	1.5 (4)	1.5 (4)
Range of D (m)	170/240	150/260	140/270	130/270
12Mbps (Simulation)	1.96 (6)	1.96 (6)	2.15 (5)	2.15 (5)
Range of D (m)	170/230	150/240	160/210	150/230
12Mpbs (Analytical)	2.37 (5)	2.37 (5)	2.37 (5)	2.37 (5)
Range of D (m)	160/190	150/200	140/200	130/210
18Mbps (Simulation)	2.45 (7)	2.45 (7)	2.63 (6)	2.63 (6)
Range of D (m)	170	160/190	150/180	140/180
18Mbps (Analytical)	2.89 (6)	2.89 (6)	3.05 (5)	3.05 (5)
Range of D (m)	170	150/180	140	140/150
24Mbps (Simulation)	0	0	0	0
Range of D (m)	X	X	X	X
24Mbps (Analytical)	0	0	0	0
Range of D (m)	X	X	X	X

to obtain the throughput capacity rate, under a prescribed value set by the system manager for the maximum allowable outage probability, when the latter is feasible. We also present performance results that are obtained by the conduct of Monte Carlo simulations, showing them to well confirm the precision of our approximate analytical models.

IV.1 Simulation Environment and Results

We use the following system parameters for the illustrative scenario under consideration. An RSU is located at the origin. Vehicles follow a Poisson Point Process along a 6 (km) highway that stretches to the right of the RSU. The transmit power of the RSU and of each vehicle is set to be equal to 200 (mW). An omni-directional antenna pattern is assumed at both transmitter and receiver nodes, with antenna gain level of 3 (dB). A simplified path loss model is applied. The pathloss exponent is set to 3. The noise power spectral density level is set equal to -174 (dBm/Hz). The channel bandwidth is equal to 10 (MHz). The

exhibited results of conducted simulations are calculated by averaging over a total number of 1000 repetitions.

The results obtained for the maximum achievable throughput rate, showing also the feasible values of inter-relay distances (D) that should be configured to attain this throughput capacity rate, under different prescribed values for the outage probability, are displayed in Table 3.1. We show lower and upper bound feasible values for the corresponding inter-nominal-position distance D. We note that any setting of a D level that lies in the respective range (between these bounds) would achieve the maximum throughput rate under the prescribed outage probability. For each desired system setting, we show the value of the spatial reuse level M that should be employed as displayed in parentheses.

IV.2 Impact of the Vehicular Traffic Density on the Optimal Spatial Reuse Level

As the density level increases, higher throughput capacity rates are attained. Furthermore, under such conditions, the performance of the system is much more robust to variations in system configuration parameters. For example, assuming a vehicular traffic density level of $\lambda = 100$ (vehicles/km), under a targeted outage-probability constraint of 5%, when the transmit rate is set to 12 (Mbps), the system achieves a throughput capacity rate of 2.88 (Mpbs), when set to employ a reuse-4 spatial-TDMA operation. In turn, assuming the same targeted outage probability level, under a lower vehicular traffic density rate of $\lambda = 40$ (vehicles/km), the attainable throughput capacity rate is reduced to 1.96 (Mbps); the latter is attainable by setting a spatial-TDMA reuse-6 operation. Clearly, a higher reuse M level is now selected to account for the higher level of incurred stochastic fluctuations in the locations of elected RNs.

IV.3 Impact of the Vehicular Traffic Density on the Choice of the Targeted Inter-relay Distance Level

It is also worthwhile to note that, under a prescribed transmit rate and an outage probability target level, when the highway is subjected to a light-traffic-density mode ($\lambda = 40$ (vehicles/km)), the range of feasible D values that can be set is more restricted. For example, under the 5% outage-probability constraint, a 6 (Mbps) transmit rate, and $\lambda = 100$ (vehicles/km), the system manager can announce inter-RN values (D) that range between 80 (m) and 360 (m), while achieving the desired maximum throughput performance behavior. In turn, under the lower vehicular density rate of $\lambda = 40$ (vehicles/km), it is essential to set inter-RN range values that lie between 210 (m) and 260 (m). This behavior is explained by noting that higher inter-RN distance deviations are incurred under the lower vehicular traffic density scenario. Then, it is necessary to set a sufficiently long D level to reduce the probability of an event under which no RN can be identified around a specified nominal position. However, under such settings, the system's communications links may operate in the noise dominant region, leading to significant throughput-rate degradations.

IV.4 Validity of the Proposed Model

In comparing the performance behavior of the system as predicted by the use of our mathematical models with the corresponding results obtained under simulations, we observe that the analytical model developed in this chapter serves as an effective tool for the conduct of system analysis and design. We note the analytically driven throughput capacity rate levels to be within 20% of those attained by simulations, under all employed transmission rates, outage probability target levels, and vehicular traffic densities. Under low transmit rates and a density of $\lambda = 100$ (vehicles/km), we find the analytical model to be even more precise, yielding performance prediction that is accurate to a level of 0.3%.

IV.5 Optimal Joint Selection of Transmission Rates, Reuse Factors, and Inter-relay Distances

For the system models and scenarios studied here, we note that the optimal rate of operation is equal to 18 (Mbps), under both heavy and light vehicular traffic densities. Under the use of such a data rate, the optimally configured VBN system achieves a throughput rate level that ranges from 2.45 (Mpbs) to 3.59 (Mbps), depending on the specified target values for the outage probability, and on the vehicular traffic density level. Under the D values around 170 (m), when employing the preferred data rate of 18 (Mbps), we show the system configuration to yield a highly robust performance behavior, achieving the maximum feasible throughput rate levels under both heavy and light traffic densities, under each one of the outage probability target levels. When using the higher transmit rate of 24 (Mbps), we note the system to not produce a higher throughput rate. This is caused by the higher sensitivity exhibited in the induced SINR levels, requiring the design to employ higher reuse M values, and thus reducing the attained throughput rate level. When subjected to a lower traffic density level, we note that the system is not capable in sustaining a link data rate of 24 (Mbps), under any prescribed outage probability level.

V Concluding Remarks

A VBN architecture facilitates packet broadcasting to vehicles traveling along a highway system, while realizing a VANET system that well regulates the occurrence of potential broadcast storm problems. Yet, it is a challenging task to configure the VBN system that achieves the high throughput rate performance while guaranteeing a prescribed outage probability level to assure the effective distribution of critical message flows that are targeted to reach a high fraction of highway vehicles. In this chapter, we develop a mathematical model that is used by the system management station to configure the parameters of the VBN system so that the highest attainable throughput rate level is achieved, while limiting

the incurred outage probability. Furthermore, we show the design to be quite robust to statistical fluctuations in the vehicular density rate. The proposed configuration of the system is capable of achieving excellent performance behavior without having to rely on rate adaptations which require the use of feedback channels for the real time reporting of experienced vehicular SINR levels.

The models and results obtained in this chapter are applicable to other system configurations. We have shown [26] that through the use of a flow admission control and pacing operation at the RSU, it is feasible to achieve a performance behavior of the system that is close to that exhibited above by using a CSMA/CA based IEEE 802.11p based protocol. We also note that the models developed in this chapter are applicable to the design of a high throughput backbone network that consists of relay stations that are located in a stationary manner along a segment of the highway, using strategic locations that can involve traffic lights, intersection entities, micro base stations and Wi-Fi access points.

CHAPTER 4

Emulating TDMA under CSMA/CA Based VBN Architecture

I Introduction

The Intelligent Transportation System (ITS) along with systems that manage the flow of automatic guided vehicles are being developed for the provision of services that enhance in-road safety. Vehicles make decisions, including whether to take detour or slow down, based on receipt of critical safety messages. To secure the successful delivery of critical messages to vehicles that may be located along the highway away from the source, an implementation of a robust vehicle-to-vehicle multi-hop networking scheme is required. The resulting Vehicular Ad Hoc Network (VANET) system must be designed to support the transport of critical message flows in a manner that assures a high Packet Delivery Ratio (PDR), guaranteeing rapid message delivery to vehicles that travel along a targeted segment of the highway.

Networking mechanisms that are based on the use of flooding oriented message forwarding approaches tend to suffer from the occurrence of broadcasting storm problems [7], caused by duplicated receptions and relaying of packets. Heuristic networking schemes that employ mechanisms such as distance based forwarding [8, 9], can incur performance degradations caused by packet losses [7]. More sophisticated mechanisms, such as those that employ cluster-based forwarding techniques described in [10,11], often lead to performance improve-

ment but can require the use of highly complex procedures for forming clusters and for electing cluster heads. More importantly, these existing forwarding protocols do not provide a systematic design guideline such that the optimal configuration of the system performances, including throughput rates, end-to-end delays, and packet delivery ratios, can be analytically determined.

In contrast, we offer to synthesize a VANET networking mechanism that is based on the dynamic location-aware formation of a Vehicular Backbone Network (VBN). The latter is a hierarchically structured network system, designed as a special case of the Mobile Backbone Network (MBN) system that we have previously studied [29]. In contrast with the algorithms used to manage an MBN, the VBN system is configured in accordance with the characteristics of vehicular movement along a linear highway system. Vehicles that reside at locations that are close to predetermined nominal positions, as determined (for example) through the use of Global Positioning System (GPS) data, are elected to act as relay nodes (RNs), serving to forward messages to their neighboring RNs. Nominal positions are calculated by using formulas that lead to an optimized operation, achieving high throughput performance and low packet discard ratios [12, 26, 30, 31].

In our recent studies of the VBN system [12, 26, 30, 31], we have generally assumed the system to employ a MAC layer scheduling protocol that operates as a spatial-reuse Time Division Multiple Access (TDMA) scheme. It employs a reuse-M operation (with the reuse level M properly set) to effectively mitigate the impact of interference signals induced by simultaneous transmissions executed by relay nodes situated across the highway. Such an operation requires the involved vehicles to acquire and maintain slot synchronization. In turn, an asynchronous distributed operation can be implemented by using a Carrier Sense Multiple Access/ Collision Avoidance (CSMA/CA) based Medium Access Control (MAC) mechanism. However, the latter MAC scheme can lead to the occurrence of frequent packet collisions and discards (noting that colliding broadcasted packets are generally not retransmitted). To assure high delivery ratios while attaining high throughput rates, we impose a

traffic pacing mechanism at the source by regulating the minimum levels of the time durations used by the RSU to transmit flow packets. In this manner, by properly configuring the pacing operation, we demonstrate here the capability of the underlying networking mechanism to significantly reduce the probability of packet collisions. In addition, we show this operation to virtually eliminate packet queueing delays that may be incurred at elected forwarding relay nodes by exploiting the tandem queueing structure [32] represented by the synthesized backbone network that covers the linear highway system. By applying this properly configured flow pacing mechanism, we also demonstrate the ability of the CSMA/CA based IEEE 802.11p [6] MAC scheduling system to achieve performance behavior that well emulates the performance attained under the use of an optimally configured spatial-reuse TDMA scheme. The precision of the analytical models that we derive in this chapter, serving to analyze and design the system, is well confirmed via simulation evaluations.

The chapter is organized as follows. Related works are summarized in Section II. In Section III, we introduce the proposed VBN scheme, as well as present the related models. In Section IV, we present mathematical models that are used to configure the system and the flow control mechanism, and to calculate the system's performance behavior, under the assumption that elected RNs are situated very close to the designated nominal positions. These analyses are extended in Section V to account for stochastic deviations of elected RNs from such nominal positions, as incurred under random vehicular flows. In Section VI, we conduct a delay analysis of the VBN system. In Section VII, we present and discuss the performance behavior of the properly configured network system, based on the conduct of analytical and simulation evaluations. The results also well confirm the precision of our analytical models. Conclusions are drawn in Section VIII.

II Related Work

Considerable recent research work has been carried out in studying the broadcasting of message flows in VANET systems. A multitude of message forwarding mechanisms have been proposed and studied for multi-hop transport of messages in such systems. TDMA and CSMA/CA MAC scheduling schemes have been considered. Most such studies have aimed to distribute vehicular safety messages, such as those originating by a vehicle and targeted to reach other vehicles that travel in its vicinity.

Preliminary forwarding mechanisms proposed in VANET system are inspired by those developed for Mobile Ad Hoc Network (MANET) systems, often focusing on mitigating the broadcast storm problem [7] induced by the occurrence of simultaneous transmissions by restricting the number of forwarding nodes. Mechanisms that employ delay based (or Distance Based Forwarding) approaches [8, 9, 13] aim to select from a group of vehicles that receive a message the vehicle that is located further away from the transmitting source of the message. Each group member will initiate a timer that will expire after a delay time that is set to be inversely proportional to the distance of the vehicle from the location of the message's source vehicle. The node whose timer expires first elects itself to act as the forwarder of the underlying message. Vehicles that hear another vehicle to forward the message, defer to the latter. Under a probabilistic based approach, vehicles elect themselves in a probabilistic manner to act as relays, with the latter probability based on their distance from the transmitter [33] or on the number of their neighbors [34, 35]. Such protocols tend to incur high packet loss rates and long distribution delays as the network size and loading levels increase.

Cluster based mechanisms [10, 11, 36, 37] have been proposed and studied as well. Vehicles that are elected to serve as cluster heads are used to coordinate message transmissions within each cluster area. Cluster-based mechanisms have generally been proven to offer enhanced and more stable performance behavior. They result in systems that can offer higher

throughput rates and packet delivery ratios, at the cost of the increased overhead required in conducting the process used to elect vehicles that serve as cluster heads. While our VBN scheme is a cluster oriented scheme, it involves a sophisticated cross-layer operation (in terms of the setting of the underlying code rate, MAC scheduling parameters and a specific targeted distance between elected RNs). Also, though proven to generally outperform distance-based and probabilistic-based mechanisms, hence-to-fore published studies of cluster-based methods have not offered mathematically tractable methods for the optimal setting of network system parameters in a manner that assures the RSU with desired performance guarantees that are essential for the distribution of public safety message flows.

Commonly studied VANET systems have been designed to employ the IEEE 802.11p CSMA/CA based MAC scheme [3, 38]. Such a mechanism supports a distributed operation while suffering from hidden terminal problems and high packet collision rates. On the other hand, a MAC scheme that is based on a TDMA protocol [39,40] offers a more reliable message distribution setup, particularly when considering the broadcasting of public safety messages, but requires synchronization and coordination in controlling the transmission schedule which can demand excess system resources. We consequently describe in this chapter a mechanism that makes use of a properly configured traffic pacing scheme, while employing a CSMA/CA MAC protocol, achieving a highly robust, high throughput and low delay performance behavior, and in this way serving to well emulate the performance behavior attained by the use of an optimally configured spatial reuse TDMA scheme.

III System Model

III.1 Vehicular Backbone Network

We consider the dissemination of message flows along a linear highway. A Road Side Unit (RSU) continuously broadcasts messages to vehicles located in its vicinity. To extend coverage, a VANET system is used to provide for vehicle-to-vehicle packet transmissions among

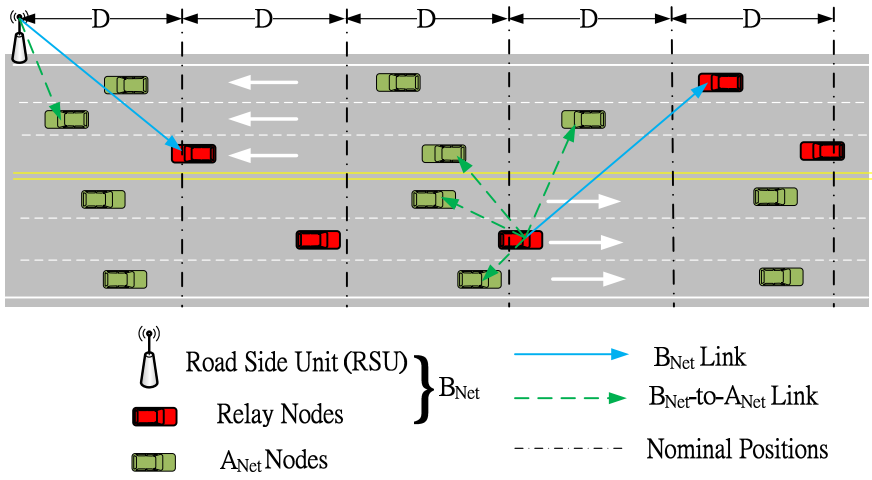

Figure 4.1: The Vehicular Backbone Network Architecture

vehicles traveling along the road. We restrict the number of vehicles that are elected to act as RNs by introducing the concept of a dynamically configured backbone network (Bnet). As illustrated in Fig. 4.1, each vehicle associates itself with an RN. An RN and its associated user stations form an Access Net (Anet). Flow packets are received by all vehicles but are forwarded only by the RN vehicles that are members of the current Bnet. We configure the VBN system in a way such strives to have RNs separated from each other by a distance D, as shown in Fig. 4.1. As we show in the following sections, the value of D is chosen, jointly with the setting of the transmission rate and the flow control pacing scheme, to maximize the throughput rate of the system and to achieve a high packet delivery ratio. We have separately studied such system in which RNs are separated by varying distance values; however, we have shown such a layout to not yield much improvement in the attained throughput rate.

A distributed algorithm for the self-election and dynamic re-election of RNs has also been developed and implemented [30]. Upon receipt of a control beacon from the RSU announcing the selected RNs, each vehicle is able to identify the RN with which it will associate. This can be done on a geo-location basis, whereby a vehicle associates itself with the closest RN.

We note that a vehicle that is elected as a relay node serves in this role for a period of time that is dictated by the maximum deviation (from the underlying nominal position) that will be permitted (to assure limited degradation in the throughput rate that will be realized if the deviation level is beyond a certain value; we have shown the attained throughput rate to be robust to such deviations provided they are within a prescribed limit). We have shown that such a time period is of the order of a second or more even when vehicles travel at high speeds [12, 30]. This is contrasted with the time it takes an RN to transmit a single packet which is of the order of a msec. Thus, a vehicle can engage in the forwarding of thousands of packets during the time that it is assigned the role of a relay node. To assure a reduced rate of RN re-elections, and thus also reduce the involved control overhead, we have described in [30] a distributed RN election protocol; this protocol also attached higher election priority to vehicles that travel at lower rates (residing in slower lanes). A version of this distributed election protocol, identified there as a Lane Based Election (LBE) protocol, makes use of the ability of vehicles to identify the lane in which they travel to implement an effective and highly timely and low overhead election algorithm.

III.2 System Models and Assumptions

Messages are issued by the RSU for broadcasting or multicasting along a linear highway of length L. To simplify our analysis, at no loss of generality, we consider here the forwarding of message across a road segment that is stretched on one side of the RSU. Each vehicle employs an omni-directional antenna, and uses a radio transceiver that operates in a half-duplex mode. The Medium Access Control (MAC) layer scheduling protocol considered here is a spatial reuse TDMA scheme, or a Carrier Sense Multiple Access/Collision Avoidance (CSMA/CA) based protocol such as the one that follows the IEEE 802.11p VANET system protocol.

A set of nominal positions separated by distance D are pre-calculated for use as the positions of vehicles that will act as RNs. Vehicles that are closest to these nominal positions

are elected to act as RNs, through the use of location data and control beacons issued by the RSU or neighboring RNs [12]. We assume that the vehicular traffic density is sufficiently high so that it is possible to elect RN vehicles that are located at (or close to) the nominal positions. We have also studied the system when elected RNs are subjected to stochastic deviations from the nominal positions.

We use a simplified path loss model to calculate the signal power detected at a receiver which is located at distance d away from the transmitter. When considering rural or suburban areas in which vehicular transmissions across the highway are not subjected to multipath effects, such a path loss model has been found to serve as a good predictor of signal attenuation, as described by the following channel gain $G(d)$ function:

$$G(d) = G_{\mathrm{t}} G_{\mathrm{r}} \Big(\frac{c}{4\pi f_{\mathrm{c}} d_0} \Big)^2 \Big(\frac{d_0}{d} \Big)^{\alpha}, \tag{4.1}$$

where G_{t} and G_{r} are the respective transmit and receive antenna gains. $c = 3 \times 10^8$ (m/s) is the speed of light, $f_{\mathrm{c}} = 5.9$ (GHz) is the carrier frequency, d_0 is the reference distance, and α is the path loss exponent. Typical values for α range from 2 to 4, as suggested by measurements conducted by [18]. The received power is thus expressed as

$$P_{\mathrm{r}}(d) = P_{\mathrm{t}} G(d), \tag{4.2}$$

where P_{t} is the transmit power level.

IV Optimal Configuration of the VBN System with Relay Nodes Residing at Ideal locations

Assume the employed Modulation/Coding Set (MCS) used at the sending module to induce a code rate of R_c (bps/Hz), the assigned bandwidth to be W (Hz), so that a transmission data rate is set to $R = R_c W$ (bps). Under a prescribed targeted Bit Error Rate (BER), the corresponding required SINR threshold is denoted as $\gamma_{\rm th}(R)$.

Consider the transmission of a packet at rate R across a single inter-RN link from an RN(k) to downstream RN($k+1$). The neighboring RNs are at distance D from each other. To allow effective time-simultaneous transmissions of packets along the highway, we configure the system so that during the time that an RN is transmitting its packet across its inter-RN link, there will be no other transmitting RNs that are located within a range that is set equal to $D_{\rm I}$ (identified as the interference range) centered around the targeted RN receiver.

Consider a reuse-M spatial-TDMA setting. Consider a time (or slot) at which RN(k) transmits a packet to its downstream neighbor RN($k+1$). At the same time, other RNs may also execute packet transmissions. The two RNs that are scheduled to transmit packets at that same time and induce the bulk of interference at the receiver of RN($k+1$), consist of the RN that is located a range of $(M-1)D$ away from the receiver on one side and the other RN that is located at $(M+1)D$ away from the receiver on the other side. We thus define the interference range $D_{\rm I} = D_{\rm I}(R)$ as the corresponding distance that satisfies the following equation:

$$\gamma_{\rm th}(R) = \frac{P_{\rm r}(D)}{P_{\rm r}(D_{\rm I}) + P_{\rm r}(D_{\rm I}+2D) + P_{\rm N}}, \tag{4.3}$$

where $P_{\rm N}$ is the noise power detected at the receivers of vehicles traveling along the highway.

Under a reuse-M TDMA operation, given the values of R and D, under the requirement that all packet transmissions are successful, and that admitted packets incur no queueing

delays, we conclude that the highest throughput level will be achieved by setting the reuse level to the lowest M value that assures such an operation. Hence, the optimal M level to be employed is given as:

$$M^* = \left\lfloor \frac{D_{\mathrm{I}}(R)}{D} \right\rfloor + 1 \tag{4.4}$$

We note that a level of 100% Packet Delivery Ratio (PDR) is achieved under such a TDMA scheme. The attained throughput level is equal to $\frac{R}{M^*}$ (bps). The latter also represents the flow admission control threshold level, assuring all packets that are admitted into the VBN to incur no in-transit queueing delays at intermediate RN queues, experiencing just frame latency and transmission time delays, as they traverse the tandem queueing system representing the elected RN-Bnet of the VBN. To achieve such excellent performance behavior under the use of a CSMA/CA MAC, we follow the following lower bound in setting the carrier-sensing threshold CS_{th}:

$$CS_{\mathrm{th}} \geq 2 \sum_{k=1}^{\left\lfloor \frac{L}{2M^*D} \right\rfloor} P_{\mathrm{r}}(kM^*D), \tag{4.5}$$

where L is the total length of the linear network. In this way, aiming the CSMA/CA system to emulate a TDMA reuse-M^* operation, we allow a node that is at sufficiently long range from a transmitting node to carry out it transmission in a time simultaneous manner. We have not specified here an upper bound level for the CS_{th} value noting that the possibility for simultaneous activity of nodes that reside in close proximity is largely eliminated by the use of the packet pacing mechanism at the source, by the linear topological layout, and by the tandem queueing structure of the relay backbone. We have found the default setting for this threshold to be generally applicable.

Based on the above setting, including the selection of $M^*(\gamma_{\mathrm{th}}(R), D)$ and CS_{th}, the end-to-end throughput rate of the flow controlled network, aiming to attain 100% PDR, under

CSMS/CA MAC, is expressed as:

$$TH^{\text{ideal}} = \frac{B}{(\frac{B}{R} + T_{\text{oh}} + \sigma\text{CW} + \text{DIFS})M^*}, \tag{4.6}$$

where B is the payload size, T_{oh} represents the time it takes to transmit the frame overhead, σ is the CSMA/CA mini-slot length, and CW is the contention window size. The denominator expression accounts for the transmission time, the CSMA/CA overhead, the backoff time (which is conservatively set equal to the maximum contention window size) and the DCF Inter-frame Space (DIFS).

Note that this throughput rate identifies the maximum level of offered load that the system can accommodate (and thus carry) in assuring performance at 100% PDR level. A different operating point, at which a higher throughput rate may be achieved, at the cost of providing a PDR level that is lower than 100% may be configured. However, our performance evaluation studies have shown (as noted in the next section) such a design to not lead to significant throughput rate improvement since the corresponding decrease in PDR is dependent in a highly non-linear manner on the resulting increase in the carried load, inducing a very rapid degradation of the PDR level as the attained throughput rate increases beyond the above calculated value.

V System Configuration and Traffic Pacing with Stochastic Deviations of RN Locations

In the previous section, we consider a system for which vehicles that are elected to serve as RNs are situated at locations that correspond to specified nominal positions. In reality, due to random variations in vehicular movements, as is also the case when the vehicular density rate is lower, vehicles that are elected to serve as RNs will deviate in a stochastic manner from those nominal positions. We study in this section the impact of such stochastic

deviations on the performance of the system and on the values of the parameters with which the system should be configured to operate in an optimal fashion.

For this purpose, we model the flow of vehicles along the highway as a stochastic Poisson point process (PPP) with density λ (vehicles/km). The applicability of this model has been confirmed by measurements that show inter-vehicle distances to be accurately modeled by an exponential distribution [28]. Given the predetermined distance between nominal positions D, the spatial deviations of elected RNs (the vehicles which are assumed at an election time to be situated closest to the nominal positions) from the nominal positions, denoted as Δ, are thus modeled to be governed by a truncated exponential distribution (as shown in [12]):

$$f_{\Delta}(\delta) = \begin{cases} \dfrac{\lambda e^{-2\lambda|\delta|}}{1 - e^{-\lambda D}} & -\dfrac{D}{2} \leq \delta \leq \dfrac{D}{2} \\ 0 & o.w. \end{cases} \tag{4.7}$$

Following the analysis approach presented in Section IV, we proceed here to evaluate the interference region D_{I}, given a transmission rate R level (and hence the associated SINR threshold γ_{th}) and given a prescribed value of D. However, due to the stochastic deviations incurred in relay positions, it is not possible now to determine an interference distance level D_{I} that assures the system with a perfect PDR level; i.e., PDR = 100%. Instead, we note that for each selected value for D_{I}, there would be a probability p that a packet will not be able to be fully distributed across the highway. This event will happen when at least one of the inter-RN links (also identified often as the bottleneck link) is sufficiently long to induce an SINR at the link's receiver that is lower than that required to sustain reception at the prescribed data rate. Consider an inter-RN link for which the transmitter and receiver are separated by a range of $D + \Delta^{(K)}$. Assume the interference at the corresponding receiver is dominated by a signal that propagates along the distance D_{I}. Then, the probability that a message transmission along this link, executed at data rate R, will fail is given by:

$$p(D_{\mathrm{I}}; D, R) = P\left\{ \frac{P_{\mathrm{r}}(D + \Delta^{(K)})}{P_{\mathrm{r}}(D_{\mathrm{I}}) + P_{\mathrm{N}}} < \gamma_{\mathrm{th}}(R) \right\}. \tag{4.8}$$

Considering the RN backbone network to be topologically characterized as a tandem queueing chain, we set the dominant deviation to be represented by the random variable $\Delta^{(K)} = \max\{\Delta_1, ..., \Delta_K\}$, where Δ_n are independent and identically distributed random variables, whose distribution is equal to that of Δ. We assume that the vehicular density is sufficiently high such that there exists an RN associated with each nominal station. In this case, we set $K = \lfloor \frac{L}{D} \rfloor$ to represent the number of elected relay stations located along a highway of length L.

For a given value of D_{I}, and assuming the use of a reuse-M MAC scheme, to assure the highest possible throughput rate, we need to select the lowest acceptable M value. Consequently, to assure the dominating interferer is an RN that is located a distance of D_{I} away, we set M to be given by:

$$M(D_{\mathrm{I}}; D) = \left\lceil \frac{D_{\mathrm{I}}}{D} \right\rceil + 1 \tag{4.9}$$

Note that instead of choosing $M = \lfloor \frac{D_{\mathrm{I}}}{D} \rfloor + 1$ as done in the case discussed in the previous section, using Eq. (4.4), we now set M to a value that is computed by using the ceiling function to account for the impact of stochastic deviations. This value of M is then used to guide the pacing operation at the source RSU, setting the minimum time intervals between the transmission of consecutive packets at the RSU to be equal to M slots.

Based on Eq. (4.8) and Eq. (4.9), under given values for R and D, using an input flow control pacing operation that is based on the calculated value for M, and assuming a reuse-M TDMA MAC scheme to be employed by the relay nodes, we calculate the value for

the maximum attainable throughput rate to be given as:

$$TH^{\text{stochastic}} = \max_{D_{\text{I}}}[1 - p(D_{\text{I}}; D, R)] \times \frac{B}{(\frac{B}{R})M(D_{\text{I}}; D)}, \tag{4.10}$$

When a CSMA/CA MAC mechanism is used, we wish to show that a low delay networking operation can be executed, effectively emulating the operation and performance induced when the above configured reuse-M TDMA procedure is used. For this purpose, we account for the overhead embedded in the CSMA/CA operation to write the following expression for the highest attainable throughput rate under a CSMA/CA scheme, given the values of R, D and enacting a pacing operation:

$$TH^{\text{stochastic}} = \max_{D_{\text{I}}}[1 - p(D_{\text{I}}; D, R)] \times \frac{B}{(\frac{B}{R} + T_{\text{oh}} + \sigma\text{CW} + \text{DIFS})M(D_{\text{I}}; D)}, \tag{4.11}$$

We use the resulting value of D_{I} that yields the highest CSMA/CA throughput rate and Eq. (4.9), to calculate the corresponding value of M to be employed by the CSMA/CA based RN backbone network. This value of M is also the one that will be used by the RSU in pacing the transmission of its packets. In this manner, we are able to assure critical packets that are distributed across the highway to experience negligible queueing delays while being transported across the backbone network. This is confirmed through the performance illustrations presented in the following section. We observe there, for the underlying illustrative scenarios,that when the operating point of the design is set in this manner, the resulting packet delivery ratio (PDR) level is generally higher than 99%.

VI Delay Analysis

The probability distribution function of the end-to-end time delay incurred by packets that are broadcasted across the relay backbone of the VBN system is calculated in the following manner, using the results presented in [32]. We assume the system to be configured in

the manner presented above, including the incorporation of the optimal pacing based flow admission control mechanism that we have described. Under such a setting, the backbone network is modeled as a tandem queueing system which is driven by the RSU source. As observed, under the application of the pacing scheme, packet queueing delays (or waiting times) incurred at relay nodes located within the network (not including the RSU node) are effectively null. Hence, the end-to-end queueing delay incurred by a packet is equal to that incurred at the RSU source.

Assuming the (application layer based) message loading rate of the source node to be lower than the throughput capacity rate calculated by us for the configured system, the queueing of packets at the source is determined by the steady-state distribution of the queueing delay (or waiting time) distribution incurred at a source node that is modeled as a G/G/1 node. For example, when messages arrive at the RSU in accordance with a Poisson process, the RSU node is modeled as a M/G/1 queueing system, whereby the effective service time of a message, $T = \mathbb{E}[S_{\text{RSU}}]$, is set equal to the time interval of the pacing process. By then using the Pollaczek-Khintchine equation (PKE), we obtain a mathematical expression for $\mathbb{E}[W]$, expressing the mean time that a message waits in the RSU system prior to the start time of its transmission. As noted above, this value also expresses that aggregate end-to-end mean waiting of a packet as it flows across the backbone queues. The end-to-end mean message delay $\mathbb{E}[D]$ of a packet, expressing the total time incurred to deliver the message across the highway, is then calculated as $\mathbb{E}[D] = \mathbb{E}[W] + \mathbb{E}[S_{\text{RSU}}] + K\mathbb{E}[S]$, where K represents the number of RNs established along the highway, and $\mathbb{E}[S]$ represents the effective transmission time of a packet frame by an RN. When a CSMA/CA MAC frame is used, we note that the effective transmission time duration accounts for the time it takes the MAC entity to complete the transmission of its MAC frame, which can be approximated as follows:

$$\mathbb{E}[S] = \frac{B}{R} + T_{\text{oh}} + \sigma E(\text{CW}) + \text{DIFS}. \tag{4.12}$$

For example, when the RSU queueing system is modeled as an M/D/1 queueing system (assuming messages to arrive in accordance with a Poisson process and packets to be of fixed length), we have

$$\mathbb{E}[W] = \frac{T}{2(1-\rho)}, \tag{4.13}$$

where $\rho = \lambda \mathbb{E}[S_{\text{RSU}}] = \lambda T < 1$ is the traffic intensity parameter, noting that T is the effective service time of a packet by the RSU transmission module. The end-to-end mean packet delay (at steady state) is then given as

$$\mathbb{E}[D] = \mathbb{E}[W] + T + K\mathbb{E}[S]. \tag{4.14}$$

VII Performance Evaluation: Numerical v.s. Simulation Results

In the following, we illustrate the system's performance behavior and the selection of the best design parameters, as well as compare our analytical results with simulation based evaluations. We have developed a C++ based simulation program for the purpose of studying the behavior of the proposed vehicular networking systems and mechanisms. We present results that exhibit the attained end-to-end throughput rate performance of a VBN system in which a single source RSU is active, multicasting an ongoing flow of packets across the highway, aiming to reach (at a high PDR) all highway vehicles distributed across a stretch of the highway that is L (m) away from the RSU.

Throughout the simulation, the CSMA/CA based 802.11p MAC layer protocol is used. The length of this highway is equal to $L = 6$ (km). The other simulation parameters are set as follows: $G_{\text{t}} = G_{\text{r}} = 3$ (dB), $f_{\text{c}} = 5.9$ (GHz), $d_0 = 1$ (m), $\alpha = 3$, and $P_{\text{N}} = -104$ (dBm). The payload size of a packet is $B = 2000$ (Bytes). The contention window size is set equal to 16 (CSMA/CA slots). The vehicular traffic density follows the statistics of a Poisson point process with parameter $\lambda = 100$ (vehicles/km).

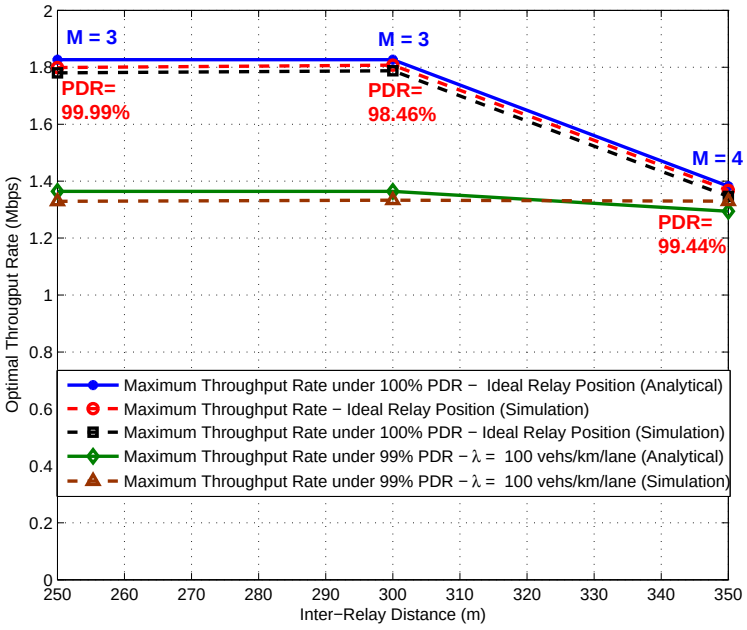

Figure 4.2: End-to-end throughput rate for $R = 6$ (Mbps)

VII.1 RNs Elected at Nominal Positions

We first consider a highway that is subjected to a high vehicular traffic flow rate so that RNs are assumed to be located at designated nominal locations. In Figs. 4.2, 4.3, 4.4, and 4.5, we display the throughput rates vs D performance behaviors for operations that use different code and data rate (R) values, when operating at the corresponding optimal (with respect to the underlying D and R values) reuse levels M^*. We show the throughput rates attained by the emulating CSMA/CA schemes as calculated by using our analytical formula (blue curves), and the results obtained by simulations. For the latter, we show in black curves the performance attained under targeted PDR = 100%; and in red curves, we exhibit the performances of systems that are configured to attain the highest throughput rates (among such MAC schemes and configurations) while yielding imperfect PDR values (which are noted in the graphs).

The following observations are drawn. The results confirm the precision of our analytical

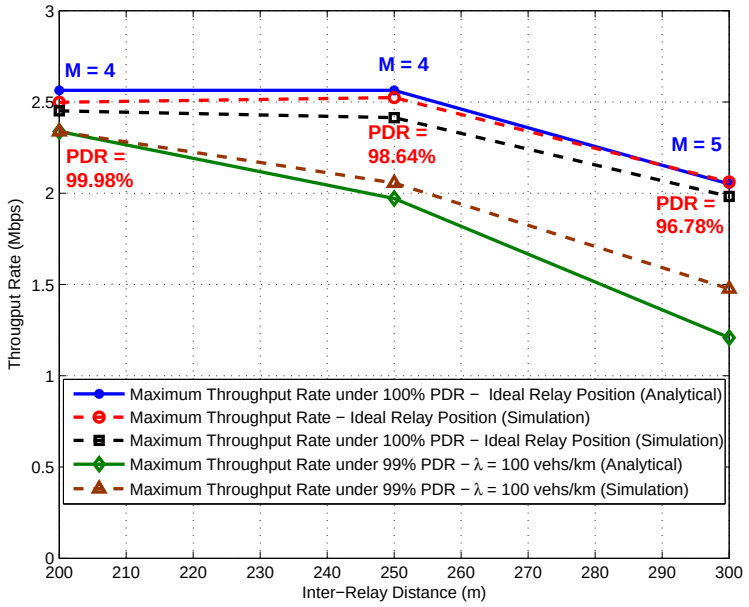

Figure 4.3: End-to-end throughput rate for $R = 12$ (Mbps)

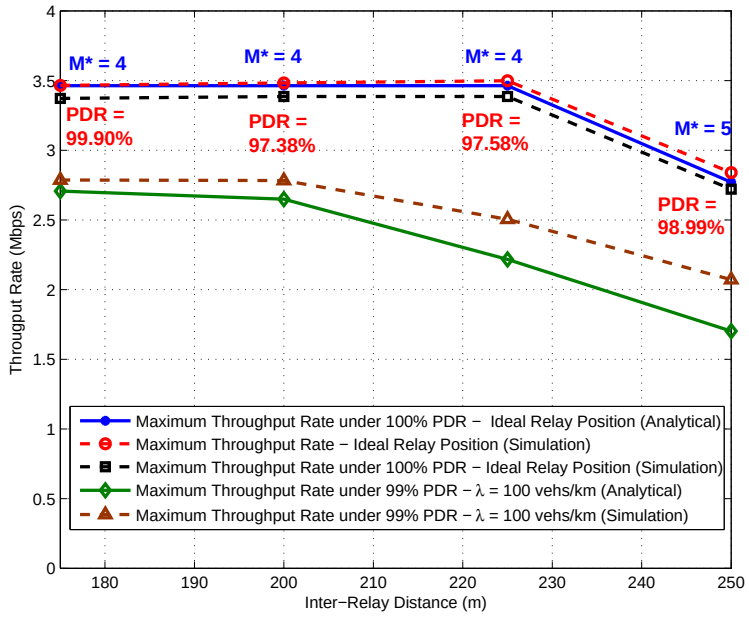

Figure 4.4: End-to-end throughput rate for $R = 18$ (Mbps)

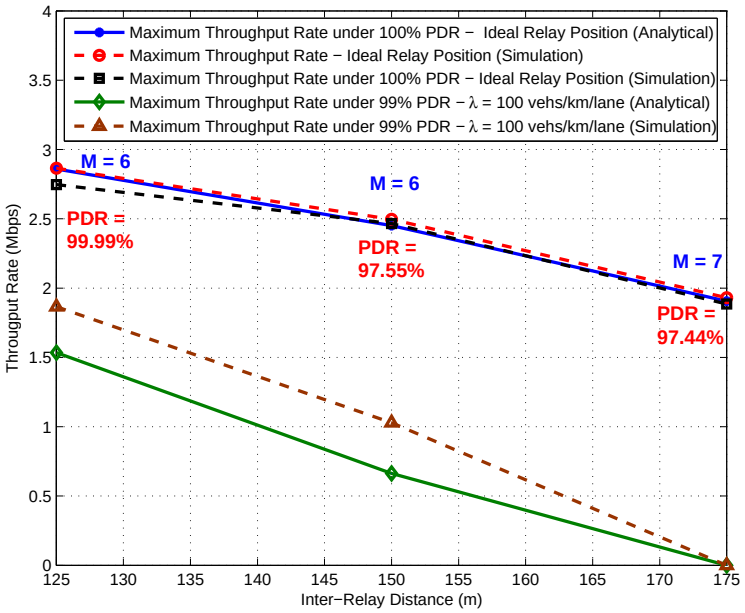

Figure 4.5: End-to-end throughput rate for $R = 24$ (Mbps)

calculations (represented by the blue lines), noting the latter to well match the performance behavior results obtained through simulations (red and black dashed lines), for all considered inter-relay distance and transmission rate values.

We note that the inter-relay distance (D) is selected such that only one receiving RN resides in the forwarding range of a transmitting RN. Since the data traffic pacing operation yields 100% PDR, we do not need to provide for potential benefits that may be attained by allowing additional relay nodes to receive the transmission of the same packet, since we have designed the system to incur a very low probability of packet collision. We also note that the latter design does not lead to an increase in the systems throughput rate while potentially inducing higher interference levels and longer multihop packet routes.

We observe that as the inter-relay (D) distance increases, the throughput rate generally decreases, since the interference range D_{I} then increases and a higher value for M^* must be set. We can also see that when we operate at a higher transmission rate, the value of M^* needs to be set higher (for example, we set $M^* = 4$ for $R = 6$ (Mbps) and $M^* = 6, 7$, or 9

for $R = 24$ (Mbps). This is induced by having to require a higher SINR threshold level as R increases, and consequently inducing a higher value for $D_{\rm I}(R)$.

Such tradeoff leads us to the joint optimal selection of (R, D) to achieve the highest throughput rate under the guarantee of 100% PDR level. The joint optimization solution leads to setting the optimal (R, D) pairs to be: $R = 18$ (Mbps) with D chosen between $180 - 225$ (m), achieving an end-to-end throughput rate of 3.4 (Mbps).

We have also examined the maximum attainable throughput rate levels when PDR levels that are lower than 100% are acceptable. We have found the corresponding operating points to achieve throughput rates that are only negligibly higher, while yielding PDR values that span the range $96\% - 99\%$, in examining all transmission rate and D settings. This is explained by noting the highly non-linear performance behavior of the PDR value as a function of the admitted load rate.

We note that in our simulations, we have set the selected values for D to be greater than half of the forwarding range; the latter is defined as the maximum transmission distance realizable under the absence of any interference sources, under a given transmission rate. In this manner, we guarantee that there is only a single RN that resides within the forwarding range of the RN transmitter, eliminating the possibility that more than one vehicle will be receiving the same packet and then transmitting it simultaneously by selecting the same value of the backoff counter, causing with probability $\frac{1}{\rm CW}$ a packet collision event. Such an occurrence is undesirable when aiming to configure the system to yield a high packet delivery ratio for the effective distribution or critical messages.

VII.2 Impact of Stochastic Deviations

In Figs. 4.2 - 4.5, we display the throughput rate performance attained under stochastic deviations incurred in the positions of elected RNs. The carrier sense threshold levels are chosen to satisfy Eq. (4.5). We note that the attained value for the throughput rate becomes more sensitive to stochastic deviations as the data rate level is increased. For instance, when

$R = 6$ (Mbps), we experience a 20% loss in the throughput rate level due to stochastic deviations; while under $R = 24$ (Mbps), the throughput degradation level reached 30% under a properly select D level. In turn, much higher degradation levels can be incurred at high data rates if the value for D is not properly configured. The best parameters to use for configuring the system are noted to be given by the use of a 18 (Mbps) data rate and a specification of an inter-RN distance of $D = 175$ (m), for both the non-stochastic and stochastic traffic cases. Under this setting, when a stochastic vehicular traffic flow model is used, we observe the optimized networking configuration to sustain a throughput rate of 2.8 (Mbps) with PDR greater than 99%. In comparison, we note that under the non stochastic setting the attained throughput capacity rate is equal to 3.5 (Mbps) with a PDR level of 100%.

Thus, impacted by the stochastic deviations in the positions of elected relay nodes, it is not feasible to guarantee a PDR level of 100%. This is induced by the possibility of an existence of an inter-RN link whose range is longer than the realizable forwarding range (at the underlying data rate). Yet, the joint operation and configuration of the system in a manner derived in this chapter, while engaging also in a flow admission control pacing oriented operation, guarantees a PDR level that can be generally as high as 99%. In fact, such a high packet delivery ratio level can be sustained when operating at any one of the examined data rates, when properly configuring the pacing based flow control operation.

Our performance evaluation results well confirm the precision of our mathematical in predicting at high precision the realized end-to-end throughput rates, under all examined values of R and D, given a high, yet reasonable, value of the vehicular density λ. The analytical values provide lower bounds on the estimated values of the throughput rates by incorporating the maximum possible value of the CSMA/CA contention window size. The calculated performance estimates are noted to be more accurate at low transmission rates, in which case the packet transmission time becomes a dominating component in the calculation of the throughput rate. A higher accuracy of the derived formula can be achieved by replacing

in Eq. (4.11) the maximum contention window size by the average contention window size, particularly when operating at higher transmission rates, in which case the impact of the value set for the backoff counter on the throughput rate level becomes more significant.

VIII Concluding Remarks

We study the reliable delivery of public safety message flows across a vehicle-to-vehicle wireless VANET. The VANET network is synthesized through the use of a Vehicular Backbone Network (VBN) approach, under which vehicles that reside closest to targeted nominal positions are elected to serve as RNs.

The analysis presented in this chapter focuses on a highway system that is subjected to relatively high vehicular traffic flow rates, so that it is generally feasible to elect vehicles that reside in close proximity of targeted nominal positions to act as relay nodes. Yet, we also demonstrate design approaches to a system that is subjected to lower vehicular traffic rates, inducing stochastic variations in the positions at which elected relay nodes are located.

We show that when employed in conjunction with the use of a reuse-M TDMA operation, with properly employed values for M, and using optimal settings for the inter-RN distance and the code rate levels, the VBN system exhibits high throughput rate and no (or minimal) in-transit packet loses and queueing delays. Furthermore, we show that when properly configured, the corresponding VBN system which employs a CSMA/CA MAC is able to effectively emulate the performance behavior achieved under the spatial TDMA MAC scheme, realizing the performance of a centralized operation under a distributed mechanism.

Furthermore, the results presented in this chapter are also of prime importance for the design and activation of a backbone network that consists of relay stations that are placed in a static (or quasi static) manner along the highway (including at highway intersection points, on traffic lights, and at other strategic locations). Consider then the use of a dedicated frequency band of such a backbone network for the multicasting of packets issued by a

RSU station across the highway. Using the results of this chapter, we proceed to configure the backbone network by selecting the corresponding optimal parameters, including the employed data rate, reuse level M, and the best distance D to use between activated static relay stations that are used to forward packets across this backbone.

CHAPTER 5

Integrated Networking and Traffic Regulation for Autonomous Vehicular Ad Hoc Networks

I Introduction

To enhance the robustness, safety and capacity of the transportation system, the introduction of autonomously navigated highway vehicles based on Adaptive Cruise Control [1,2] systems is planned [41]. For its operation, it is essential to implement distributed control systems that allow individual vehicles to rapidly adjust their mobility plan in reacting to system state fluctuations. For this purpose, it is critical that vehicles are able to effectively disseminate and receive status messages to/from other vehicles. In considering mechanisms for vehicle-to-vehicle (V2V) communications, a multitude of networking protocols have been studied extensively, in the context of designing vehicular ad hoc networks (VANETs) [3–5,31,42,43].

The performance behavior of various VANET networking protocols have been extensively studied. Most researchers studying the design of such inter-vehicular communications networks have been focusing on the development of message dissemination protocols, under assumed vehicular mobility patterns that are modeled so that they capture the behavior of human drivers. Illustrative schemes include the multitude of Poisson point process based models [44], car-following models [45], and mobility models that are calibrated by using data bases that are compiled by using real world measurements [46]. On the other hand,

as demonstrated in this chapter, the introduction of autonomous vehicles, makes it possible for the VANET system designer to regulate vehicular formations and the ensuing network's topology to enhance the performance of the underlying communication and traffic systems.

We consider an integrated autonomous highway transportation system. We aim to design a system that achieves a high vehicular and high data throughput rates, while providing vehicles with reduced on-ramp waiting times, and assuring the timely delivery of high priority safety messages. For this purpose, we propose in this chapter a scheme that is used to regulate the formations of moving vehicles so that they are aggregated into properly synthesized platoons. In general. the effectiveness of organizing mobile highway vehicles into platoon based formations has been well recognized. For example, such formations are employed by intelligent transportation system projects such as SARTRE [47] and GCDC [48]. The increase in reliability and fuel efficiency that is attained through the use of platoon formations and the use of Cooperative Adaptive Cruise Control (CACC) [49] has been well observed.

To implement a scalable distributed control mechanism, and reduce the complexity and adaptivity time of the mechanism to attain time synchronization among vehicles that move within specified ranges from each other, we configure a jointly optimized platoon-wise Spatial Time Division Multiple Access (STDMA) scheduling scheme. In this case, TDMA transmissions executed within distinct platoons are assumed to not be synchronized. We focus on two key classes of message flows: high priority event-driven flows and lower priority status message flows. The dissemination of critical event-driven message flows must meet stringent delay constraints. In turn, the transport of periodically generated status messages impose high communications throughput capacity rate requirements. The desired structuring of highway platoons is derived through the solution of a constrained optimization problem, whereby key performance metrics are incorporated. The platoon oriented solution includes the specification of platoon sizes, inter-vehicular intra-platoon spacings, and inter-platoon distances. Our performance analyses demonstrate the sensitivity of the system's performance behavior to variations in platoon oriented settings. We present the fundamental performance

tradeoffs that must be considered by the system designer when aiming to achieve enhanced performance behavior for the communications networking of both classes of message flows while also guaranteeing an acceptably high vehicular throughput rate across the highway.

Once the advantageous structures used to form platoon configurations, designed to achieve high data and vehicular throughput rates, are determined, we proceed to study ramp control mechanisms that can be used to feed vehicular traffic into the highway in a manner that is compatible with desired vehicular formation. Traffic access control mechanisms have been widely studied and employed for the purpose of regulating the loading of transportation systems [50–53], aiming to reduce vehicular congestion state across a highway. Yet, such schemes have not been designed to also guarantee, at the same time, a targeted data networking performance level. To the best of our knowledge, the study presented in this chapter is the first one to model and evaluate the impact of a basic ramp control mechanism on the ensuing delay-throughput performance function attained in the dissemination of message flows across an autonomous vehicular network that employs optimally synthesized vehicular platoons.

This chapter is organized as follows. In Section II, we summarize literatures relevant to our study. In Section III, we introduce the system model. In Section IV, we present an analytical model that is used to calculate the delay and throughput performances attained in the dissemination of message flows. In Section V, an on-ramp admission control mechanism is introduced and analyzed. In Section VI, we present performance evaluations, including results that have been obtained through simulation studies that are used to validate the derived analytical models. Conclusions are drawn in Section VII.

II Related Work

Studies of VANET systems have been generally based on statistical vehicular mobility models [44–46]. These models have been often set to capture the behavior of human drivers. In

turn, when considering an autonomous transportation system, vehicular formations can be optimally synthesized in aiming to achieve system-wide desired performance behavior, as studied in this chapter.

Similar to our joint study of data network and traffic regulation, there are studies focusing on improving the data throughput of VANETs by taking the advantage of the controllable mobility of autonomous vehicles. We note that the study in [54] investigates the positioning of vehicles along a linear highway for the purpose of enhancing the data throughput performance of the associated VANET network system. In comparison, while the design in [54] focuses on enhancing the throughput rate of the vehicular wireless network, our study uses multiple metrics in offering a design for the autonomous system, including metrics that account for the vehicular throughput rate and on-ramp waiting times.

In [55], the authors analyze the throughput rate and connectivity performance of an infrastructure-aided contention-based protocol, under a guaranteed inter-vehicular connectivity level. Vehicles that are randomly distributed along the highway form platoons. Platoon members can directly communicate with the platoon leader. In this study, the authors however do not attempt to dynamically adapt and optimize the structure of platoons, as executed in this chapter, with the aim of attaining desired and enhanced system performance behavior.

In [56], the authors investigate communications networking performance characteristics of a VANET system, evaluating the network's end-to-end throughput, packet delay, and packet delivery rate performance levels, under the employment of an IEEE 802.11p based MAC protocol, and under the setting of different values for platoon sizes and the number of highway platoons. In contrast with our study, the latter study does not attempt to derive results that identify the structures of optimal platoon configurations; it also does not evaluate the impact of the platoon structures on the attained highway's vehicular traffic throughput rate.

The authors in [57] study the relations between vehicular speeds, vehicular traffic flow

rates, and packet transmission delays incurred when communicating between two neighboring platoons. However, in this study, network connectivity is assessed on the sole basis of inter-vehicular distance levels, without considering the interdependency of communication protocols and vehicular traffic regulation parameters. Such dependencies are of paramount importance in our study.

In [58], the authors' study aims to minimize the probability of collision between neighboring vehicles in a VANET assisted system when an accident happens. The choices of inter-vehicular distances, vehicular speeds, and Carrier Sense Multiple Access/Collision Avoidance (CSMA/CA) carrier sensing thresholds are shown to impact the vehicular collision probability. In contrast to our design that accommodates multi-class message dissemination, the authors only consider single class of safety message transport.

III System Model

In this section, we first present the traffic regulation and message forwarding schemes. The ramp control mechanism is presented later in Section V. The mathematical symbols used throughout this chapter is summarized in Table 5.1.

III.1 Autonomous Highway Traffic Regulation Mechanism

Assume N autonomous vehicles[1] to be traveling at a constant speed v over a single lane highway segment of length L. In an autonomous highway system, the number of vehicles traveling in a segment of a highway can be effectively controlled through on-ramp access regulation, often identified as *Traffic Density Control* [59]. Admitted vehicles are regulated to form N_{P} platoons. For simplified analysis, we first assume each platoon to consist of an

[1]We note that our aim in this chapter is to characterize and evaluate a design of the autonomous intelligent transportation system that assumes all vehicles to be fully autonomously controlled. Prior to the full implementation of such a system, hybrid systems that involve semi-autonomous mechanisms will have to be supported, which is beyond the scope of this chapter.

Table 5.1: Summary of mathematical symbols

Symbol	Description
L	Length of the highway segment
N	Number of vehicles in the highway segement
v	Vehicular speed
N_{P}	Number of platoons
N_{V}	Number of vehicles per platoon
D_{V}	Intra-platoon vehicle spacing
D_{P}	Inter-platoon distance
s	Vehicle length
u	Deceleration level
Φ	Vehicular throughput rate
$D_{\mathrm{s}}^{(k)}$	Target span of type k message
τ	Type I delay constraint
P_{t}	Transmit power
P_{N}	Noise power
γ	SNR threshold
α	Path loss exponent
d_0	Distance between Tx and Rx
d_k	Distance between Rx and the k^{th} interferer
R	Data rate
B	Data payload
M	TDMA reuse factor
σ	TDMA slot length
N_{a}	Max. number of active vehicles per platoon
$P_{\mathrm{s}}(i)$	Success transmission prob. across link Type i
$N_{\mathrm{s}}(i)$	Number of flows sharing link Type i
P_{out}	Outage probability (Type I messages)
η	Data throughput per flow (Type II messages)
η_{T}	Aggregated data throughput (Type II messages)
T_{c}	Platoon cycle time
$N_{\max}$	Maximum number of vehicles between ramps
R_{cap}	Ramp capacity
λ	Vehicle ramp arrival rate
p	Vehicle departure probability
a_m	Prob. m arrivals at a ramp in a cycle
$\mathbb{E}[W^{(k)}]$	Average waiting time at ramp k

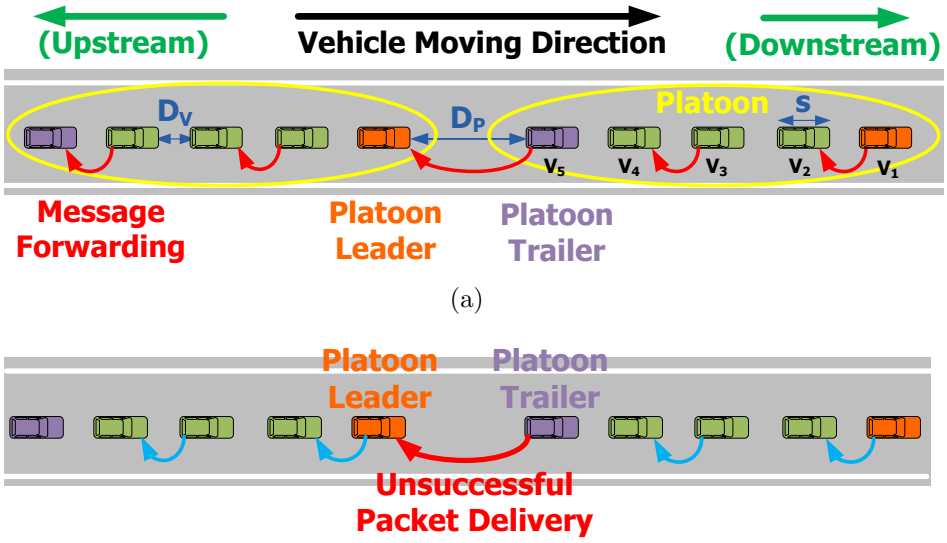

(a)

(b)

Figure 5.1: (a) Platoon structure with $N_{\mathrm{V}} = 5$ and $M = 2$ (b) An unsuccessful transmission due to uncoordinated TDMA schemes between platoons.

equal number of $N_{\mathrm{V}} = \frac{N}{N_{\mathrm{P}}}$ vehicles. We will later consider randomized platoon sizes when employing the ramp control mechanism in Section V. Assume N to be an integral multiple of N_{P}. Vehicles that belong to the same platoon are consecutively numbered as $i = 1...N_{\mathrm{V}}$, starting from the platoon leader, as shown in Fig. 5.1(a). We denote the i^{th} vehicle in each platoon by V_i. The downstream (upstream) is in the same (opposite) direction of the vehicular traffic flow.

The intra-platoon spacing D_{V} is defined as the distance between neighboring vehicles belonging to the same platoon. The value of D_{V} is regulated to be the same for all platoons. Distances between any two neighboring platoons, the inter-platoon distances, are denoted as D_{P}. They are also regulated to assume the same values for all neighboring platoons. Let s denote the length of a vehicle. An illustrative example of the platoon structure of interest is shown in Fig. 5.1(a). In this case, D_{P} is calculated as:

$$D_{\mathrm{P}} = \frac{L - Ns - N_{\mathrm{P}} D_{\mathrm{V}}(N_{\mathrm{V}} - 1)}{N_{\mathrm{P}}}. \tag{5.1}$$

We assume that $D_{\mathrm{V}} \leq D_{\mathrm{P}}$. In addition, the selection of D_{V} must satisfy a safety constraint. To account for safety spacing margins that are required for proper reaction under a sudden stop of a vehicle that it follows, we set D_{V} to a value that is longer than the stopping distance of the immediate upstream vehicle. That is,

$$\frac{v^2}{2u} \leq D_{\mathrm{V}}, \tag{5.2}$$

where u is the vehicular deceleration level. It is noted that one can extend our model to account for conditions under which different vehicles are characterized by having different deceleration levels. Yet, under a conservative design criteria, one can set the inter-vehicle distance to be based on the lowest deceleration level.

The vehicular throughput rate Φ, defined as the number of vehicles crossing a section of the highway per unit time per unit distance along the lane, is calculated as

$$\Phi = \frac{v N_{\mathrm{V}}}{N_{\mathrm{V}} s + D_{\mathrm{V}}(N_{\mathrm{V}} - 1) + D_{\mathrm{P}}}. \tag{5.3}$$

Our model is readily extended when considering the different lengths that may characterize different vehicles. For example, when the underlying distribution of vehicular length is known, one can replace in Eq. (5.3) the parameter s by its average value.

In the study conducted in this chapter, we calculate the values to be set for N_{V} and D_{V} so that the operation yields an acceptable performance in disseminating message flows (see

Table 5.2: Comparison of Type I and Type II messages

Message Type	I	II
Frequency	Event Driven	Periodic
Application	Collision Avoidance	Status Update
Priority	High	Low
Number of Sources	Single	Multiple
Performance Metrics	Delay	Throughput

Section III.2) across the highway, while also serving to maintain a high vehicular throughput rate, under given system parameter values, involving N, L, s, and u. We note that once N_{V} and D_{V} have been calculated, the values of N_{P} and the maximum possible value of v are determined.

III.2 Message Forwarding Scheme

The primary purpose of the underlying VANET system is to support safety message dissemination across a highway. We assume that each vehicle is equipped with a half-duplex radio. Safety messages are divided into two categories: (I) event driven and (II) periodic status messages. Type I messages are of higher priority than Type II messages. Often, type I messages are broadcast at a given instant of time from a single source vehicle, which is located closest to the critical event location, e.g. an accident. Type II messages are broadcast periodically by every vehicle and are used to update vehicles that are traveling in their proximity about their status.

We assume here that messages that belong to these two classes are disseminated to vehicles that travel behind the originating vehicle. Type I messages impose a strict delay requirement. Such a message must be made available to all vehicles within a specified distance span $D_{\mathrm{s}}^{(\mathrm{I})}$ behind the source vehicle within a prescribed time delay, at a prescribed probability level. Constrained by the latter delay objective, the design strives to attain a sufficiently high throughput capacity rate for the periodic distribution of Type II messages over a prescribed geographical span $D_{\mathrm{s}}^{(\mathrm{II})}$. The characteristics of these two types of messages

are summarized in Table 5.2.

Due to the dissemination criticality of these classes of messages, we assume messages to be forwarded by vehicles to other vehicles on a hop-by-hop basis. Each message is thus broadcast from its source to upstream vehicles by using intermediate vehicles to act as relay nodes. Each relay vehicle forwards the received message to its upstream neighbor along the lane, as shown in Fig. 5.1(a).

III.3 Channel Model

We consider a Rayleigh fading channel. The channel gain across a link follows an exponential distribution with mean $P_{\rm t} d_0^{-\alpha}$, where $P_{\rm t}$ is the transmit power level, d_0 is the distance between the transmitter and the receiver, and α is the path loss exponent. The noise process is assumed to be modeled as an additive white Gaussian noise process; the noise power level recorded at a receiver is equal to $P_{\rm N}$.

Corresponding to a configured transmission rate R that corresponds to an employed modulation/coding set, one determines a targeted minimum Signal-to-Interference-plus-Noise (SINR) level γ, yielding reception at a prescribed acceptable bit error rate. A message transmission across the corresponding link is declared successful if, for an ongoing transmission, the SINR level measured at the intended receiver is not lower than γ. Under a Rayleigh fading model, the probability $P_{\rm s}$ that a message transmission and reception across a link spanning a range d_0 is successfully completed is readily calculated as follows [60]:

$$P_{\rm s} = \exp\left(- \frac{\gamma P_{\rm N}}{P_{\rm t} d_0^{-\alpha}} \right) \prod_{k=1}^{n} \left(1 - \frac{\gamma}{(\frac{d_k}{d_0})^{\alpha} + \gamma} \right), \tag{5.4}$$

where n is the number of interfering nodes (i.e., those that carry out simultaneous transmissions) and d_k is the distance between the $k^{\rm th}$ interfering source and the intended receiver.

III.4 Medium Access Control Protocol

A TDMA protocol provides a robust medium sharing scheme with guaranteed delay and throughput rate performance [4,61], when compared with the IEEE 802.11p CSMA scheme. Spatial reuse can further enhance the performance of a TDMA protocol by enabling simultaneous transmissions across a highway. However, such a scheme requires a global synchronization mechanism. The spatial reuse pattern is impacted by variations in the vehicular topology.

To reduce the implementation complexity imposed by such a synchronization scheme, we limit the underlying TDMA coordinated MAC scheduling operation to involve only vehicles that are members of the same platoon. We thus employ here a platoon-based reuse-M TDMA protocol, where M is the spatial reuse factor. Given that V_i is in transmission mode, the set $\mathcal{I}(i) = \{k | k = i(\text{mod } M) \quad k = 1...N_{\text{V}}\}$ denotes the indices of vehicles in the same platoon that are activated to transmit simultaneously with V_i. For a spatial reuse factor $M = 2$, as illustrated in Fig. 5.1(a), vehicles that are set to be in transmission mode at the same time are noted to be separated by a distance of $2D_{\text{V}}$. To simplify, all platoons are assumed to employ the same value of M. Platoon leaders serve as coordinators, keeping track of the current number of vehicles residing in the platoon, as well as assigning TDMA slots to active members. Each TDMA slot is of length $\sigma = \frac{B}{R}$, where B is the size of a packet. The spatial TDMA schemes enacted in distinct platoons are not synchronized. Consequently, interference signals generated by vehicles situated at random positions within neighboring platoons can jeopardize concurrent transmissions executed by vehicles belonging to the underlying platoon. In Fig. 5.1(b), we illustrate a scenario under which an inter-platoon message delivery fails if a certain platoon leader happens to be in the transmit mode during the corresponding period.

IV Delay-Outage and Data Throughput Rate Performance Analysis

In this section, we present a mathematical model that is used to study the delay-outage performance of Type I messages and the data throughput rates attained in disseminating Type II messages. We assume channel gains to behave as statistically independent random variables over distinct TDMA slots. We also assume them to remain constant during each slot. The highway segment under consideration is assumed to be heavily loaded, and every platoon is assumed to consist of N_{V} vehicles. Such a configuration portrays a worst case scenario, in that it induces a high number of potentially simultaneously active interfering sources. Automatic Repeat Request (ARQ) schemes are employed across each link for both types of message transmissions.

IV.1 Link Success Probability

We denote the intra-platoon links with transmitter V_i and receiver V_{i+1} as L_i, where $i = 1...N_{\mathrm{V}} - 1$. We denote the inter-platoon links as $L_{N_{\mathrm{V}}}$, whereby for such a link, a platoon trailer acts as the transmitter and the closest upstream platoon leader serves as the intended receiver. Since all platoons are assumed to have identical structures, we perform our analysis by arbitrarily tagging a single (non boundary) platoon.

IV.1.1 Intra-platoon Links

Assume that in the allocated slots, the scheduled vehicles always have packets to transmit. The link success probability $P_{\mathrm{s}}(i)$ for intra-platoon links L_i, where $i = 1...N_{\mathrm{V}}-1$ is calculated as follows:

$$P_{\rm s}(i) = \mathcal{L}_{\rm N} \times \mathcal{L}_{\rm Intra}(i) \times \mathcal{L}_{\rm Inter}(i) \quad i = 1...N_{\rm V} - 1 \tag{5.5}$$

The terms $\mathcal{L}_{\rm N}$, $\mathcal{L}_{\rm Intra}(i)$, and $\mathcal{L}_{\rm Inter}(i)$ represent the components that account for the impact on the success probability imposed by the noise process, the signal interference caused by simultaneous transmissions executed within the tagged platoon, and the the signal interference caused by simultaneous transmissions executed within other platoons, respectively.

Following the same approach used for the calculation performed in Eq. (5.4), we obtain:

$$\mathcal{L}_{\rm N} = \exp\left(- \frac{\gamma P_{\rm N}}{P_{\rm t} d_0^{-\alpha}} \right); \tag{5.6}$$

$$\mathcal{L}_{\rm Intra}(i) = \prod_{k \in \mathcal{I} \setminus \{i\}} \left(1 - \frac{\gamma}{\mid k - i - 1 \mid^{\alpha} + \gamma} \right). \tag{5.7}$$

We use the following calculation to derive an approximate expression for the term $\mathcal{L}_{\rm Inter}(i)$. The result is based on using the expansion of the product term included in Eq. (5.4) and on keeping only the first order dominating terms:

$$\begin{aligned} \mathcal{L}_{\rm Inter}(i) \approx \prod_{n=1}^{N_{\rm a}} & \left[\frac{1}{1 + \gamma \left(\frac{D_{\rm d}(i) + (n-1) M D_{\rm V}}{D_{\rm V}} \right)^{-\alpha}} \times \frac{1}{1 + \gamma \left(\frac{D_{\rm u}(i) + (n-1) M D_{\rm V}}{D_{\rm V}} \right)^{-\alpha}} \right] \\ & \times \left[\frac{1}{1 + (\zeta(\alpha) - 1) \gamma \left(\frac{D_{\rm P} + (N_{\rm V} - 1) D_{\rm V}}{D_{\rm V}} \right)^{-\alpha}} \right]^2 . \end{aligned} \tag{5.8}$$

The first two terms in Eq. (5.8) characterize the impact of signal interference sources induced by transmissions executed within the two platoons that are located in closest proximity to the tagged platoon. The term $D_{\rm d}(i) = D_{\rm P} + i D_{\rm V} + \frac{D_{\rm V}(M-1)}{2}$ and the term

$D_{\rm u}(i) = D_{\rm P} + D_{\rm V}(N_{\rm V} - i - 1) + \frac{D_{\rm V}(M-1)}{2}$ represent the average distance between the receiving vehicle (with index $i+1$) and the interfering vehicles located within the closet downstream and upstream platoons, respectively. The term $N_{\rm a} = \lceil \frac{N_{\rm V}}{M} \rceil$ is the maximum number of simultaneously active vehicles in a platoon. The third term accounts for the signal interference caused by simultaneous transmissions conducted by vehicles located in other platoons, excluding the tagged platoon and the two closest platoons. Note that $\zeta(\alpha) = \sum_{i=1}^{\infty} \frac{1}{i^{\alpha}}$.

IV.1.2 Inter-platoon Links

An inter-platoon link involves a transmitting vehicle as the platoon trailer of its platoon (denoted by platoon A) and a receiving vehicle that is the platoon leader of the upstream platoon (denoted by platoon B). The link success probability for an inter-platoon link $L_{N_{\rm V}}$ is calculated as follows:

$$P_{\rm s}(N_{\rm V}) = \Big(1 - \frac{1}{M}\Big)\mathcal{L}_{\rm N} \times \mathcal{L}^{(\rm tx)}_{\rm Intra}(N_{\rm V}) \times \mathcal{L}^{(\rm rx)}_{\rm Intra}(N_{\rm V}) \times \mathcal{L}_{\rm Inter}(N_{\rm V}). \tag{5.9}$$

The term $1 - \frac{1}{M}$ is the probability that the receiver is not in the transmit mode. The term $\mathcal{L}^{(\rm tx)}_{\rm Intra}(N_{\rm V})$ accounts for the signal interference at the intended receiver due to simultaneous transmissions from vehicles belonging to platoon A. It is calculated through the following approximation:

$$\mathcal{L}^{(\rm tx)}_{\rm Intra}(N_{\rm V}) \approx \prod_{n=1}^{N_{\rm a}-1} \frac{1}{1 + \gamma\big(\frac{MnD_{\rm V}+D_{\rm P}}{D_{\rm P}}\big)^{-\alpha}}. \tag{5.10}$$

The impact of signal interference at the intended receiver caused by simultaneous transmissions from vehicles belonging to platoon B, defined as $\mathcal{L}^{(\rm rx)}_{\rm Intra}(N_{\rm V})$, is given as:

$$\mathcal{L}_{\text{Intra}}^{(\text{rx})}(N_{\text{V}}) \approx \prod_{n=1}^{N_{\text{a}}} \frac{1}{1+\gamma\left(\frac{(\frac{M}{2}+M(n-1))D_{\text{V}}}{D_{\text{P}}}\right)^{-\alpha}}. \tag{5.11}$$

The term $\mathcal{L}_{\text{Inter}}(N_{\text{V}})$ characterizes the impact of signal interference caused by transmissions executed by vehicles that are members of other platoons, excluding members of platoons A and B. It is approximated by the following expression:

$$\mathcal{L}_{\text{Inter}}(N_{\text{V}}) \approx \left[\frac{1}{1+\zeta(\alpha)\gamma\left(\frac{D_{\text{P}}+(N_{\text{V}}-1)D_{\text{V}}}{D_{\text{P}}}\right)^{-\alpha}}\right]^2. \tag{5.12}$$

It is noted that throughout Eqs. (5.10) - (5.12), we approximate the distances between the intended receiver and the interfering sources by their mean values.

IV.2 Outage Probability of Type I Messages

The outage probability characterizing the successful transport of a Type I safety message is defined as the probability that such a message is not successfully received within time τ by all upstream vehicles that reside in the targeted geographical span $D_{\text{s}}^{(\text{I})}$ originating at the source vehicle V_{i_0}. Type I packets are generated by a single source vehicle during a single activity burst duration. They are accorded highest priority. Consequently, such packets are assumed here to not incur queueing delays at the relay nodes. Upon their receipt, the latter nodes place them at the head of the transmission queue. Their experienced latency is consequently determined primarily by the number of hops that they traverse within their dissemination span $D_{\text{s}}^{(\text{I})}$, in attaining successfully dissemination over the targeted span, and the frame latency induced by the employed TDMA scheduling scheme.

Within the span $D_{\text{s}}^{(\text{I})}$ of V_{i_0} generated high priority message, the number of covered "type-i" links, representing the links that are initiated by the corresponding V_i in each platoon, is

equal to $N_i^{(i_0;D_{\rm s}^{(\rm I)})}$. Let $Y_i^{(j)}$ denote the total number of transmissions required for a message to be successfully transmitted across the $j^{\rm th}$ type-i link, where $j = 1...N_i^{(i_0;D_{\rm s}^{(\rm I)})}$. Note that $Y_i^{(j)}$ are independent identically distributed (i.i.d.) geometrically distributed random variables with parameter $P_{\rm s}(i)$. The Cumulative Distribution Function (CDF) of $Y_i^{(j)}$ is written as

$$F_{Y_i^{(j)}}(n) \triangleq \Pr\{Y_i^{(j)} \leq n\} = 1 - (1 - P_{\rm s}(i))^n, \quad n \geq 1, i = 1...N_{\rm V}, j = 1...N_i^{(i_0;D_{\rm s}^{(\rm I)})}. \tag{5.13}$$

The total number of transmissions $N_T^{(i_0;D_{\rm s}^{(\rm I)})}$ required to send a message to all the vehicles within $D_{\rm s}^{(\rm I)}$, starting from V_{i_0}, is equal to $\sum_{i=1}^{N_{\rm V}} \sum_{j=1}^{N_i^{(i_0;D_{\rm s}^{(\rm I)})}} Y_i^{(j)}$. The CDF of $N_T^{(i_0;D_{\rm s}^{(\rm I)})}$ is given as $F_{N_T^{(i_0;D_{\rm s}^{(\rm I)})}}(n) = F_{Y_1}(n) \otimes F_{Y_2}(n) \otimes ... \otimes F_{Y_{N_{\rm V}}}(n)$, where $\otimes$ denotes the convolution sum and $F_{Y_i}(n) \triangleq F_{Y_i^{(1)}}(n) \otimes ... \otimes F_{Y_i^{(N_i^{(i_0;D_{\rm s}^{(\rm I)})})}}(n)$.

The outage probability, when the source is i_0, is thus equal to:

$$\begin{aligned} P_{\rm out}^{(i_0;D_{\rm s}^{(\rm I)})} &= \Pr\left\{\sum_{i=1}^{N_{\rm V}} \sum_{j=1}^{N_i^{(i_0;D_{\rm s}^{(\rm I)})}} [(Y_i^{(j)} - 1)M\sigma + \sigma] > \tau\right\} \\ &= 1 - F_{N_T^{(i_0;D_{\rm s}^{(\rm I)})}}\left(\left\lceil \frac{\tau + \sum_{i=1}^{N_{\rm V}} N_i^{(i_0;D_{\rm s}^{(\rm I)})}(M-1)\sigma}{M\sigma} \right\rceil\right). \end{aligned} \tag{5.14}$$

Assuming each vehicle to be equally likely to become the source vehicle, the average outage probability is equal to

$$P_{\rm out} = \frac{1}{N_{\rm V}} \sum_{i_0=1}^{N_{\rm V}} P_{\rm out}^{(i_0;D_{\rm s}^{(\rm I)})}. \tag{5.15}$$

IV.3 Throughput Capacity Rate for Type II Messages

The end-to-end throughput capacity rate of a Type II message $\eta^{(i_0;D_{\mathrm{s}}^{(\mathrm{II})})}$ is dominated by the capacity of the link with the lowest link throughput rate, in considering all the links nested within the span $D_{\mathrm{s}}^{(\mathrm{II})}$. It is thus calculated as:

$$\eta^{(i_0;D_{\mathrm{s}}^{(\mathrm{II})})} = \frac{1}{M} \min_{\substack{i=1...N_{\mathrm{V}} \\ N_i^{(i_0;D_{\mathrm{s}}^{(\mathrm{II})})} \neq 0}} \frac{P_{\mathrm{s}}(i)}{N_{\mathrm{s}}(i)} R, \tag{5.16}$$

where $N_{\mathrm{s}}(i)$ is the number of source stations whose span covers type-i link. We proceed to divide the link throughput capacity $P_{\mathrm{s}}(i)R$ by $N_{\mathrm{s}}(i)$, as we assume that the link throughput capacity is equally shared among all flows using it. Under a given platoon configuration, $N_{\mathrm{s}}(i)$ is expressed as follows:

$$N_{\mathrm{s}}(i) = \begin{cases} \lfloor \frac{D_{\mathrm{s}}^{(\mathrm{II})}}{D_{\mathrm{V}}} \rfloor & D_{\mathrm{E}}(i) \leq 0 \; i = 1...N_{\mathrm{V}} - 1 \\ i + \lfloor \frac{D_{\mathrm{E}}(i)}{D_{\mathrm{T}}} \rfloor N_{\mathrm{V}} + \max\left\{ -1, \lfloor \frac{D_{\mathrm{E}}(i) - \lfloor \frac{D_{\mathrm{E}}(i)}{D_{\mathrm{T}}} \rfloor D_{\mathrm{T}} - D_{\mathrm{P}}}{D_{\mathrm{V}}} \rfloor \right\} + 1 & D_{\mathrm{E}}(i) > 0 \; i = 1...N_{\mathrm{V}} - 1 \\ 0 & D_{\mathrm{s}}^{(\mathrm{II})} < D_{\mathrm{P}} \;\; i = N_{\mathrm{V}} \\ \lfloor \frac{D_{\mathrm{s}}^{(\mathrm{II})} - D_{\mathrm{P}}}{D_{\mathrm{V}}} + 1 \rfloor & D_{\mathrm{P}} \leq D_{\mathrm{s}}^{(\mathrm{II})} \leq D_{\mathrm{T}} \; i = N_{\mathrm{V}} \\ N_{\mathrm{V}} + \lfloor \frac{D_{\mathrm{E}}(i)}{D_{\mathrm{T}}} \rfloor N_{\mathrm{V}} + \max\left\{ -1, \lfloor \frac{D_{\mathrm{E}}(i) - \lfloor \frac{D_{\mathrm{E}}(i)}{D_{\mathrm{T}}} \rfloor D_{\mathrm{T}} - D_{\mathrm{P}}}{D_{\mathrm{V}}} \rfloor \right\} + 1 & D_{\mathrm{s}}^{(\mathrm{II})} > D_{\mathrm{T}} \; i = N_{\mathrm{V}} \end{cases} \tag{5.17}$$

Note that $D_{\mathrm{T}} = D_{\mathrm{V}}(N_{\mathrm{V}} - 1) + D_{\mathrm{P}}$ and

$$D_{\mathrm{E}}(i) = \begin{cases} D_{\mathrm{s}}^{(\mathrm{II})} - iD_{\mathrm{V}} & i = 1...N_{\mathrm{V}} - 1 \\ D_{\mathrm{s}}^{(\mathrm{II})} - D_{\mathrm{T}} & i = N_{\mathrm{V}} \end{cases}. \tag{5.18}$$

Assuming that each vehicle is equally likely to become the source vehicle, the average

data throughput rate per flow is calculated as follows:

$$\eta = \frac{1}{N_{\mathrm{V}}} \sum_{i_0=1}^{N_{\mathrm{V}}} \eta^{(i_0; D_{\mathrm{s}}^{(\mathrm{II})})}. \tag{5.19}$$

The average aggregated data throughput rate, summing over all N flows, is expressed as $\eta_{\mathrm{T}} = N\eta$:

V Ramp Control Mechanisms

In the previous sections, we have investigated the delay-induced outage performance of Type I message flows and data throughput rate performance of Type II messages under a prescribed platoon configuration (intra-platoon spacings D_{V}, inter-platoon distances D_{P}, maximum number of vehicles per platoon N_{V}, and a targeted vehicular density $\frac{N}{L}$). However, given that vehicles arrive at highway ramps in a stochastic manner, regulating vehicles into desired platoon structures requires additional efforts. Such a traffic regulation mechanism can be implemented either in-road or on-ramp. The former allows vehicles to join the highway at will. However, coordinations among vehicles traveling on the highway are required to adjust inter-vehicle distances and platoon sizes. This in turn generates additional control data traffic requiring transport across the VANET system. On the other hand, with the aid of Ramp Control Units (RCUs), e.g., ramp meters, we can implement a simple admission control process at each ramp to determine when a vehicle should join a platoon. Although such a system can still require communications between platoon leaders and RCUs, it only takes place in the vicinity of ramp locations and imposes relatively limited excess bandwidth requirements.

In the following, we focus on the on-ramp traffic regulation scheme. For a given platoon configuration, we study the distribution of platoon sizes, and the consequent induced data throughput rate, by incorporating the stochastic modelling of vehicles arriving at ramps.

The on-ramp waiting time levels experienced by vehicles as a result of the regulation process used in admitting vehicles into the highway is also derived.

V.1 On-Ramp Admission Control

Consider K ramps equally spaced along a linear highway. The distance between ramp entrances is equal to L. Vehicles intending to enter the highway arrive at the k^{th} ramp in accordance with a Poisson process at rate λ_k (vehicles/minute), where k is the ramp index. Arrival processes at different ramps are assumed to be statistically independent. The ramp queue capacity is R_{cap} (vehicles). A vehicle traveling on the highway will depart the highway at a ramp that it passes by with probability p. Vehicle departure events are assumed to be statistically independent. It is assumed that the distance between the platoon leader and the platoon trailer in the same platoon is less than L. That is, $sN_{\text{V}} + D_{\text{V}}(N_{\text{V}} - 1) < L$.

We consider a ramp control mechanism that aims at regulating platoon configurations, impacting their structures as realized between two ramp entrances of distance L by selecting the following parameters: maximum number of vehicles between two ramps ($N_{\max}$), maximum number of platoons (N_{P}), maximum number of vehicles per platoon (N_{V}), and an intra-platoon spacing (D_{V}). Due to the simplified geo-symmetrical character of the model, we have set the platoons to assume the same N_{V} capacity levels. Yet, we note that the actual number of vehicles included at a time in each platoon would vary in a stochastic manner, induced by the random characteristics of vehicular arrivals to and departures from the highway system.

To describe the on-ramp admission control mechanism, we define the following metrics and parameters:

Definition 2. ***Platoon cycle time*** T_{c} *is the minimum time difference between two platoon leaders passing a ramp access point. It is calculated as:*

$$T_{\mathrm{c}} = \begin{cases} \frac{N_{\mathrm{V}}s + D_{\mathrm{V}}(N_{\mathrm{V}}-1) + D_{\mathrm{P}}}{\sqrt{2D_{\mathrm{V}}u}} & N_{\mathrm{V}} > 1 \\ \frac{N_{\mathrm{V}}s + D_{\mathrm{V}}(N_{\mathrm{V}}-1) + D_{\mathrm{P}}}{\sqrt{2D_{\mathrm{P}}u}} & N_{\mathrm{V}} = 1 \end{cases}, \tag{5.20}$$

where the denominator is the maximum travelling speed allowed, which is calculated by using Eq. (5.2).

Definition 3. *The n^{th}* ***platoon cycle*** *is the time interval $[(n-1)T_{\mathrm{c}}, nT_{\mathrm{c}}]$, $n \geq 1$. Let $T_n^- \triangleq \sup\{t | t < (n-1)T_{\mathrm{c}}\}$ and $T_n^+ \triangleq \inf\{t | t > (n-1)T_{\mathrm{c}}\}$. $T_n^{++} = \inf\{t | t > T_n^+\}$*

Definition 4. *The* ***serving platoon*** *associated with ramp k during the n^{th} cycle is the platoon whose leader arrives at time T_n^- . A serving platoon can be of size 0.*

We consider the following RCU-aided ramp admission control mechanism. RCUs use a control channel to coordinate their understanding of the targeted platoon configuration. During each platoon cycle, events take place in the following order:

- A platoon arrives at a ramp at time T_n^-.
- Some vehicles depart from the platoon and leave the highway at time T_n^+.
- For each ramp, the RCU allows vehicles waiting at the ramp to join the serving platoon at time T_n^{++} on a first-in-first-out basis, including those waiting in the ramp queue and those arriving in the concurrent platoon cycle, as long as the serving platoon is not full. A vehicle that is admitted into the highway while a serving platoon is passing by its access point is allowed to join the platoon at any position; no joining delay is included. In turn, if the trailer of the serving platoon has already passed the ramp access point at its admission time, it is assumed that the vehicle accelerate temporarily to catch up and join the platoon at a trailing position.[2]

[2]Allowing new vehicles to join a serving platoon at any position within the platoon, one may introduce temporal speed/distance fluctuations. Such variations are not incorporated into the models analyzed in this chapter.

- All vehicles not admitted into the highway in the current platoon cycle continue to wait in the ramp queue.

Note that this on-ramp access control algorithm shares the common design philosophy that is customarily employed by many currently used ramp control algorithms. For example, under the ALINEA [62] regulation system, the ramp admission rate is adjusted to limit the number of vehicles admitted into a designated segment of the highway based on the current highway occupancy. In extending such mechanisms, we note that under the access control algorithms employed in this chapter, such an admission scheme has been extended by including the joint setting of platoon configuration parameters. This extended scheme have not been included in currently employed ramp control algorithms as the latter are designed to accommodate traffic flows induced by human drivers.

The total time that a vehicle spends in using the highway is typically dominated by its waiting time on ramp and its travel time along the road. Hence, we do not include a separate delay component representing the time required for a vehicle to join a designated platoon.

V.2 Platoon Size & Ramp Queue Size Distribution

In the following, we derive mathematical expressions for the calculation of the steady state distribution of the platoon size and the ramp queue size sampled at time instant T_n^-, under the ramp control mechanism described above. At no loss of generality, we assume a uniform arrival rate across all ramps, i.e. $\lambda_k = \lambda \quad \forall k$.

The underlying series of on-ramp queues that feed vehicles into the linear highway segment forms a tandem queueing system. The individual queueing processes, however, do not behave in a statistically independent manner. The stochastic dynamics of the queue size process at a ramp queue depend on the incoming platoon size, which in turn depends on the incurred queue sizes at upstream ramp queues. Although a transition probability matrix for the joint platoon and ramp sizes observed at the highway ramps can be formulated, the size

of the matrix grows exponentially fast as the number of ramps increase [63]. To simplify the system's analysis, we adopt a lower complexity iterative algorithm, similar to that proposed in [63]. We use it to obtain an analytical procedure that enables us to evaluate the performance behavior of this tandem queueing system.

Let $\mathbf{r}^{(k)}(n)$ denotes the number of vehicles that are waiting at ramp k when sampled at time instant T_n^-. Let $\pi^{(k)}(n) = \{\pi_m^{(k)}(n) | m = 0...N_{\mathrm{V}}\}$, where $\pi_m^{(k)}(n)$ denotes the probability that there are m vehicles in the platoon serving ramp k when sampled at time instant T_n^-.

The iterative procedure starts by considering the ramp that is located at the upstream end point of the highway. No platoons arrive at this point to pick up waiting vehicles. Vehicles are admitted at this access point in a manner that serves to form platoons whose structures adhere to the targeted platoon configuration layout and the cycle time. The stochastic evolution of the queue size process at ramp 1, sampled at time T_n^-, forms a Discrete Time Markov Chain (DTMC). The DTMC is characterized by the transition probability matrix $\mathbf{R}^{(1)} = \{R_{ij}^{(1)}\}$, where

$$R_{ij}^{(1)} \triangleq \Pr\{r^{(1)}(n+1) = j | r^{(1)}(n) = i\} = \begin{cases} \sum_{m=0}^{N_{\mathrm{V}}-i} a_m & j = 0 \\ a_{j+N_{\mathrm{V}}-i} & j = 1...R_{\mathrm{cap}} - 1 \\ \sum_{m=R_{\mathrm{cap}}+N_{\mathrm{V}}-i}^{\infty} a_m & j = R_{\mathrm{cap}} \end{cases}, \tag{5.21}$$

where a_m is the probability that there are m vehicles arriving at a ramp during a cycle time.

For a Poisson process, a_m is expressed as

$$a_m = \begin{cases} \frac{(\lambda T_{\mathrm{c}})^m e^{-\lambda T_{\mathrm{c}}}}{m!} & m \geq 0 \\ 0 & m < 0 \end{cases}. \tag{5.22}$$

Using Eq. (5.21), we note that this Markov Chain process is aperiodic, irreducible, and positive recurrent. Hence, there exists a unique steady state ramp queue size distribution; it

is denoted as $\mathbf{r}^{(1)} = \{r_m^{(1)} | m = 0...R_{\text{cap}}\}$ and is calculated by solving the following equations:

$$\begin{cases} \mathbf{r}^{(1)}\mathbf{R}^{(1)} = \mathbf{r}^{(1)} \\ \sum_{m=0}^{R_{\text{cap}}} r_m^{(1)} = 1 \end{cases} . \tag{5.23}$$

Given the ramp queue size distribution, we can calculate the steady state platoon size distribution $\pi^{(1)} = \{\pi_m^{(1)} | m = 0...N_{\text{V}}\}$, where $\pi_m^{(1)}$ is calculated as follows:

$$\pi_m^{(1)} = \begin{cases} \sum_{n=0}^{R_{\text{cap}}} r_n^{(1)} a_{m-n} & m = 0...N_{\text{V}} - 1 \\ 1 - \sum_{n=0}^{R_{\text{cap}}} r_n^{(1)} a_{m-n} & m = N_{\text{V}} \end{cases} . \tag{5.24}$$

The procedure then iterates over each ramp by assuming that the serving platoon sizes observed at at T_n^- at the access point of ramp k are independent and identically distributed (i.i.d.) random variables, governed by the distribution $\pi^{(k-1)}$. In iterating, we first compute the platoon size distribution $\tilde{\pi}^{(k-1)} = \{\tilde{\pi}_m^{(k)} | m = 0...N_{\text{V}}\}$, which is measured at T_n^+:

$$\tilde{\pi}_m^{(k-1)} = \sum_{n \geq m}^{N_{\text{V}}} \pi_m^{(k-1)} q_{n-m}^{(n)} \quad m = 0...N_{\text{V}}, \tag{5.25}$$

where $q_l^{(i)}$ is the probability that l vehicles leave a platoon of size i. If each vehicle leaves independently with probability p, we have $q_l^{(i)} = \binom{i}{l} p^l (1-p)^{i-l}$, $l = 0...i$, $i = 0...N_{\text{V}}$.

The steady state queue size distribution $\mathbf{r}^{(k)} = \{r_m^{(k)} | m = 0...R_{\text{cap}}\}$ at ramp k is obtained as the unique solution to the set of stationary equations of the Markov Chain, whose transition probability matrix $\mathbf{R}^{(k)} = \{R_{ij}^{(k)}\}$ is given as:

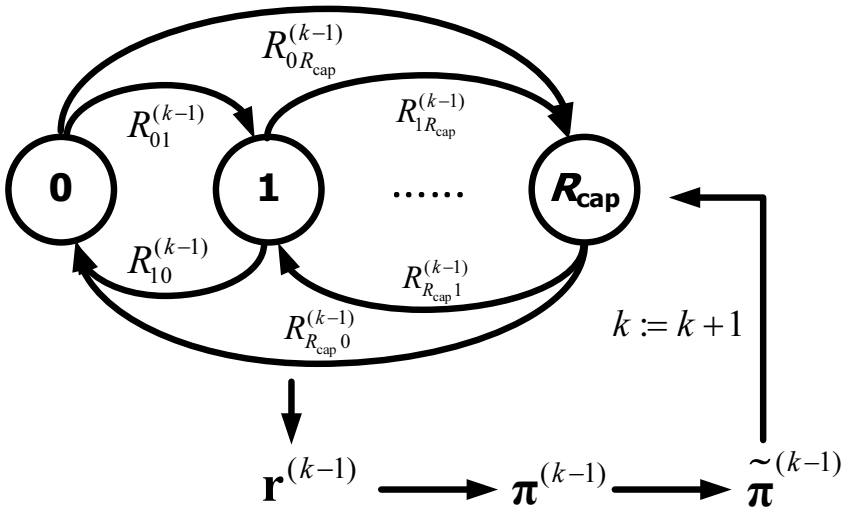

Figure 5.2: Proposed decomposition method to compute ramp size and platoon size distributions

$$R_{ij}^{(k)} \triangleq \Pr\{r^{(k)}(n+1)=j | r^{(k)}(n)=i\} = \begin{cases} \sum_{l=0}^{N_{\text{V}}} \tilde{\pi}_l^{(k-1)} \sum_{m=0}^{N_{\text{V}}-l-i} a_m & j=0 \\ \sum_{l=0}^{N_{\text{V}}} \tilde{\pi}_l^{(k-1)} a_{j+N_{\text{V}}-l-i} & j=1...R_{\text{cap}}-1 \\ \sum_{l=0}^{N_{\text{V}}} \tilde{\pi}_l^{(k-1)} \sum_{m=R_{\text{cap}}+N_{\text{V}}-l-i-1}^{\infty} a_m & j=R_{\text{cap}} \end{cases} . \tag{5.26}$$

The steady state platoon size distribution $\pi^{(k)}$ is subsequently calculated as follows:

$$\pi_m^{(k)} = \begin{cases} \sum_{l=0}^{N_{\text{V}}} \sum_{n=0}^{R_{\text{cap}}} r_n^{(k)} \tilde{\pi}_l^{(k-1)} a_{m-l-n} & m=0...N_{\text{V}}-1 \\ 1 - \sum_{l=0}^{N_{\text{V}}} \sum_{n=0}^{R_{\text{cap}}} r_n^{(k)} \tilde{\pi}_l^{(k-1)} a_{m-l-n} & m=N_{\text{V}} \end{cases} . \tag{5.27}$$

We have summarized the proposed decomposition method used to solve the steady state distribution of platoon sizes and ramp sizes in Fig. 5.2.

V.3 Waiting Time Analysis

In this section, we calculate the average waiting time of a vehicle in the ramp queue. For this purpose, we first derive the following Lemma:

Lemma 3. *The average number of platoon cycles $\mathbb{E}[N_i^{(k)}]$ that the i^{th} vehicle situated in the queue at ramp k has to wait before it is admitted into the highway, excluding the platoon cycle in which the vehicle arrives and the one in which the vehicle joins the highway, is computed by employing the following recursive relation:*

$$\mathbb{E}[N_1^{(k)}] = \frac{v_0^{(k-1)}}{1 - v_0^{(k-1)}}. \tag{5.28}$$

$$\mathbb{E}[N_i^{(k)}] = \frac{\sum_{j=1}^{\min\{i-1, N_{\text{V}}\}} (\mathbb{E}[N_{i-j}^{(k)}] + 1) v_j^{(k-1)} + v_0^{(k-1)}}{1 - v_0^{(k-1)}}, \tag{5.29}$$

where $v_j^{(k-1)} = \tilde{\pi}_{N_{\text{V}}-j}^{(k-1)}$ is the steady state distribution of the number of vacancy positions available in the platoon arriving at ramp k at time T_n^+.

Proof. See Appendix A. □

In computing the average on-ramp waiting time, we make use of the following variables:

Definition 5. *$N_{\text{ad}}^{(k)}(n)$ is the number of vehicles admitted into either highway or the ramp k queue in the n^{th} platoon cycle.*

Definition 6. *$N_{\text{c}}^{(k,m)}(n)$ is the total number of platoon cycles experienced by the m^{th} vehicle admitted into ramp k queue in the n^{th} platoon cycle prior to its admission into the highway, excluding the cycle during which the vehicle arrives at the ramp and the cycle during which the vehicle is admitted in the highway.*

Definition 7. $W_{\mathrm{L}}^{(k,m)}(n)$ *is the frame latency experienced by the* m^{th} *vehicle admitted into the ramp* k *queue in the* n^{th} *platoon cycle. It is the time duration that a vehicle has to wait in a ramp queue before the start of the next platoon cycle. If the serving platoon associated with the ramp is not full when a vehicle arrives at the ramp, the frame latency is equal to 0.*

Definition 8. $N_{\mathrm{e}}^{ij}(n) = R_{\mathrm{cap}} - i + j$ *is the total number of vacancies (including those in the serving platoon and over the ramp) given that there are* i *vehicles waiting in the ramp queue and* j *vacancies in the serving platoon when sampled at time* T_n^+.

Definition 9. $N_{\mathrm{w}}^{ijm}(n) = (m - (j - i)^+)^+$ *is the number of residual vehicles that remain waiting at the ramp, given that there are* m *new arrivals during the cycle time,* i *vehicles were waiting in the ramp queue, and* j *vacancies exist in the serving platoon when sampled at time* T_n^+. *Note that* $x^+ = \max\{x, 0\}$.

For mathematical tractability, for given ramp, we ignore the inter-dependency of platoon occupancy sizes and ramp sizes sampled at time instants T_n^- by assuming that they are i.i.d. random variables, and that the values assumed by each are governed by the steady state distribution derived in Eqs. (5.26)-(5.27), respectively. We therefore drop the time indices n in referring to related variables. Consequently, we note that the sequence of random variables $N_{\mathrm{ad}}^{(k)}$ sampled at time T_n^- form a renewal reward process [64]. Thus, arrivals of successive platoons occur at a ramp in accordance with a renewal point process, which is governed by a sequence of cycle times that are assumed to be modeled as independent and identically distributed random variables. The *reward* variable associated with the associated platoon cycle represents the sum of expected waiting times of those vehicles that have arrived to this ramp during this cycle period. The average waiting time of a vehicle at its ramp is calculated as follows:

Theorem 1. *The average on-ramp waiting time of vehicles arriving at ramp* k*, denoted by*

$\mathbb{E}[W^{(k)}]$, *is calculated as follows:*

$$\mathbb{E}[W^{(k)}] = \frac{\mathbb{E}\left[\sum_{m=1}^{N_{\mathrm{ad}}^{(k)}} N_{\mathrm{c}}^{(k,m)} \middle| N_{\mathrm{ad}}^{(k)} > 0\right] T_{\mathrm{c}} + \mathbb{E}\left[\sum_{m=1}^{N_{\mathrm{ad}}^{(k)}} W_{\mathrm{L}}^{(k,m)} \middle| N_{\mathrm{ad}}^{(k)} > 0\right]}{\mathbb{E}[N_{\mathrm{ad}}^{(k)} | N_{\mathrm{ad}}^{(k)} > 0]}, \tag{5.30}$$

where $\mathbb{E}[N_{\mathrm{ad}}^{(k)} | N_{\mathrm{ad}}^{(k)} > 0]$, $\mathbb{E}\left[\sum_{m=1}^{N_{\mathrm{ad}}^{(k)}} N_{\mathrm{c}}^{(k,m)} \middle| N_{\mathrm{ad}}^{(k)} > 0\right]$, *and* $\mathbb{E}\left[\sum_{m=1}^{N_{\mathrm{ad}}^{(k)}} W_{\mathrm{L}}^{(k,m)} \middle| N_{\mathrm{ad}}^{(k)} > 0\right]$ *are defined in Eqs. (5.31), (5.32), and (5.33), respectively.*

$$\mathbb{E}[N_{\mathrm{ad}}^{(k)} | N_{\mathrm{ad}}^{(k)} > 0] = \sum_{i=0}^{R_{\mathrm{cap}}} \sum_{j=0}^{N_{\mathrm{V}}} r_i^{(k)} \tilde{\pi}_{N_{\mathrm{V}}-j}^{(k-1)} \left[\sum_{m=1}^{N_{\mathrm{e}}^{ij}-1} \frac{m a_m}{p_{\mathrm{ad}}^{(k)}} + (1 - \varpi_{ij}^{(k)}) N_{\mathrm{e}}^{ij} \right] \tag{5.31}$$

$$\begin{aligned} \mathbb{E}\left[\sum_{m=1}^{N_{\mathrm{ad}}^{(k)}} N_{\mathrm{c}}^{(k,m)} \middle| N_{\mathrm{ad}}^{(k)} > 0\right] = \sum_{i=0}^{R_{\mathrm{cap}}} \sum_{j=0}^{N_{\mathrm{V}}} r_i^{(k)} \tilde{\pi}_{N_{\mathrm{V}}-j}^{(k-1)} \Bigg[\sum_{m=1}^{N_{\mathrm{e}}^{ij}-1} \frac{a_m}{p_{\mathrm{ad}}^{(k)}} \sum_{l=(i-j)^+ +1}^{(i-j)^+ + N_{\mathrm{w}}^{ijm}} \mathbb{E}[N_l^{(k)}] \\ + (1 - \varpi_{ij}^{(k)}) \sum_{l=(i-j)^+ +1}^{R_{\mathrm{cap}}} \mathbb{E}[N_l^{(k)}] \Bigg] \end{aligned} \tag{5.32}$$

$$\begin{aligned} \mathbb{E}\left[\sum_{m=1}^{N_{\mathrm{ad}}^{(k)}} W_{\mathrm{L}}^{(k,m)} \middle| N_{\mathrm{ad}}^{(k)} > 0\right] = \sum_{i=0}^{R_{\mathrm{cap}}} \sum_{j=0}^{N_{\mathrm{V}}} \frac{r_i^{(k)} \tilde{\pi}_{N_{\mathrm{V}}-j}^{(k-1)} T_{\mathrm{c}}}{p_{\mathrm{ad}}^{(k)}} \Bigg[\sum_{m=1}^{N_{\mathrm{e}}^{ij}-1} a_m \sum_{l=m-N_{\mathrm{w}}^{ijm}+1}^{m} (1 - \frac{l}{m+1}) \\ + [N_{\mathrm{e}}^{ij} - (j-i)^+] \left(1 - \sum_{m=0}^{N_{\mathrm{e}}^{ij}-1} a_m\right) - \frac{1}{\lambda T_{\mathrm{c}}} \left(1 - \sum_{m=0}^{N_{\mathrm{e}}^{ij}} a_m\right) \sum_{l=(j-i)^+ +1}^{N_{\mathrm{e}}^{ij}} l \Bigg] \end{aligned} \tag{5.33}$$

Table 5.3: Simulation Parameters

Parameter	Notation	Unit	Value
Distance between ramps	L	m	5000
Vehicle length	s	m	3
Deceleration	u	m/s^2	3
Type I span	$D_{\mathrm{s}}^{(\mathrm{I})}$	m	200
Type I delay constraint	τ	ms	50
Type II span	$D_{\mathrm{s}}^{(\mathrm{II})}$	m	300
Prob. vehicle depart	p	N/A	0.4
Data payload	B	bytes	200
Data rate	R	Mbps	3
SNR threshold	γ	dB	5
Transmit power	P_{t}	mW	200
Noise power	P_{N}	dBm	-104

Note that

$$p_{\mathrm{ad}}^{(k)} = (1 - r_{R_{\mathrm{cap}}}^{(k)} \tilde{\pi}_{N_{\mathrm{V}}}^{(k-1)})(1 - a_0), \tag{5.34}$$

and

$$\varpi_{ij}^{(k)} = \sum_{m=1}^{N_{\mathrm{e}}^{ij}-1} \frac{a_m}{p_{\mathrm{ad}}^{(k)}}. \tag{5.35}$$

Proof. The right hand side of Eq. (5.30) is obtained by applying the Renewal Reward Theorem [64]. See Appendix B for the deviations of Eqs. (5.31), (5.32), and (5.33). □

VI Performance Evaluation

In this section, we demonstrate the performance behavior of the system through the evaluation of the attained outage probability metric for Type I flows and and throughput rate metric for Type II flows, under a multitude of platoon configurations. The scenario parameters are summarized in Table 5.3. The data rate and the corresponding SINR threshold values employed in our illustrative performance models have been selected from Modula-

tion/Coding Set levels supported by the IEEE 802.11p physical layer [6]. Values for the message spans and for delay constraints are compatible with those suggested in the US Department of Transportation reports [65].

VI.1 Average Outage Probability Performance of Type I Messages - Saturated Vehicular Loading Condition

The average outage probability performance behavior is illustrated in Fig. 5.3(a)-5.3(b). We deploy 120 vehicles over a span of 5 (km) highway. Two intra-platoon spacing values are investigated: $D_{\mathrm{V}} = 10$ (m) and $D_{\mathrm{V}} = 30$ (m).

We observe in Fig. 5.3(a) that under a short intra-platoon spacing $D_{\mathrm{V}} = 10$ (m), choices of either a too large or a too small platoon size N_{V}, can lead to a significant increase in the outage probability. Under a large platoon size, a high level of intra-platoon signal interference is induced. On the other hand, when setting a small platoon size, the inter-platoon distance decreases. In this case, a message may require to be sent across multiple less reliable inter-platoon links. We find that setting a platoon size in the range $N_{\mathrm{V}} = 6 - 15$ yields the best performance behavior. Such configurations effectively avoid the need to perform inter-platoon message transport, serving to reduce the degrading impact caused by uncoordinated transmissions executed within neighboring platoons.

When we set a longer intra-platoon spacing, $D_{\mathrm{V}} = 30$ (m), we find that to minimize the outage probability level, we need to create platoons that contain a larger number of vehicles, as illustrated in Fig. 5.3(b). In this case, the message dissemination range can be mostly restricted to span a single platoon, and the longer inter-vehicular distances contribute to alleviating the impact of the intra-platoon signal interference. In contrast, when platoons are set to be of smaller size, so that a larger number of platoons is formed, messages may have to traverse multiple unreliable inter-platoon links.

In observing the most effective values to be selected for the TDMA reuse M level, we note that a reuse-2 scheduling scheme is not effective, as high signal interference is induced. It is

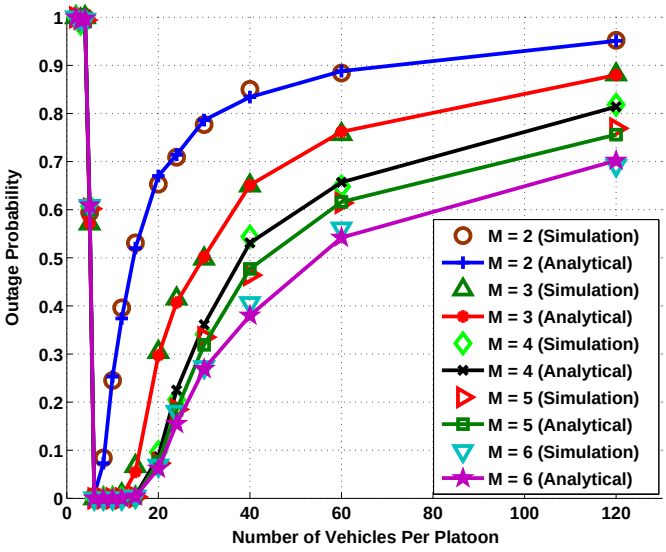

(a) $D_{\mathrm{V}} = 10(\mathrm{m})$

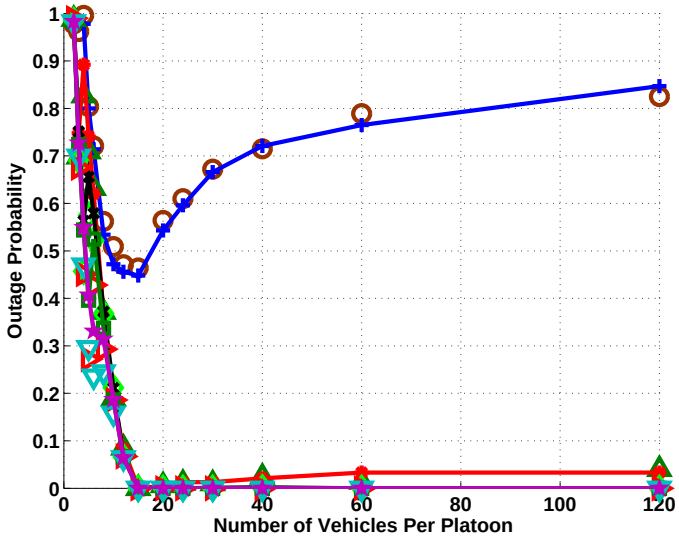

(b) $D_{\mathrm{V}} = 30(\mathrm{m})$

Figure 5.3: Delay induced outage probability of Type I messages v.s. number of vehicles per platoon ($N = 120$).

best to configure a reuse factor in the range $M = 3-6$. When such a setting is coupled with a proper selection of the platoon size, it is possible to achieve a very low outage probability level.

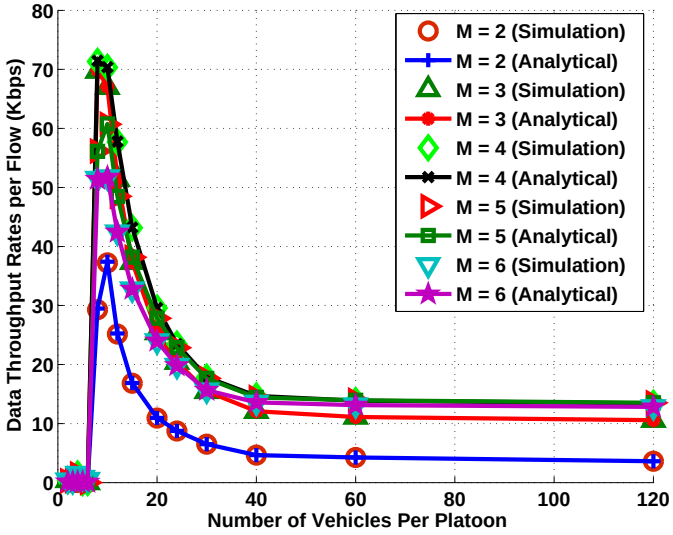

(a) $D_{\mathrm{V}} = 10(\mathrm{m})$

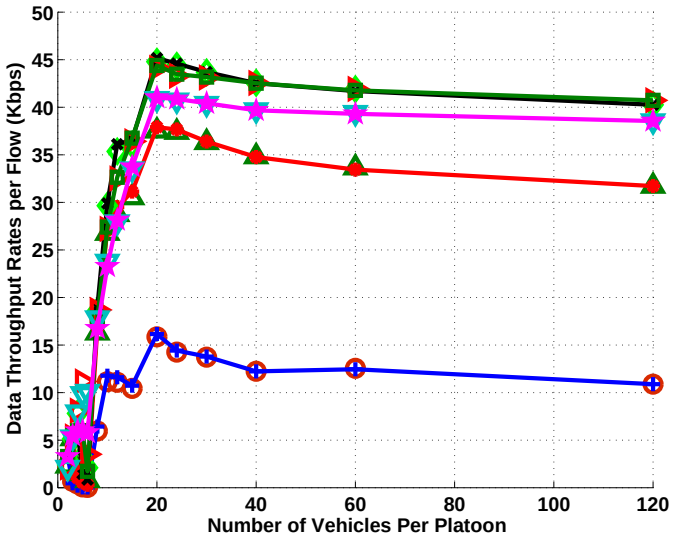

(b) $D_{\mathrm{V}} = 30(\mathrm{m})$

Figure 5.4: Data throughput rates per flow of Type II messages v.s. number of vehicles per platoon ($N = 120$).

VI.2 Average Data Throughput Rate Performances for the Dissemination of Type II Messages - Saturated Vehicular Loading

The performance behavior expressing the data throughput rate attained for the support of Type II message flows is illustrated in Figs. 5.4(a) - 5.4(b). We note that when setting a

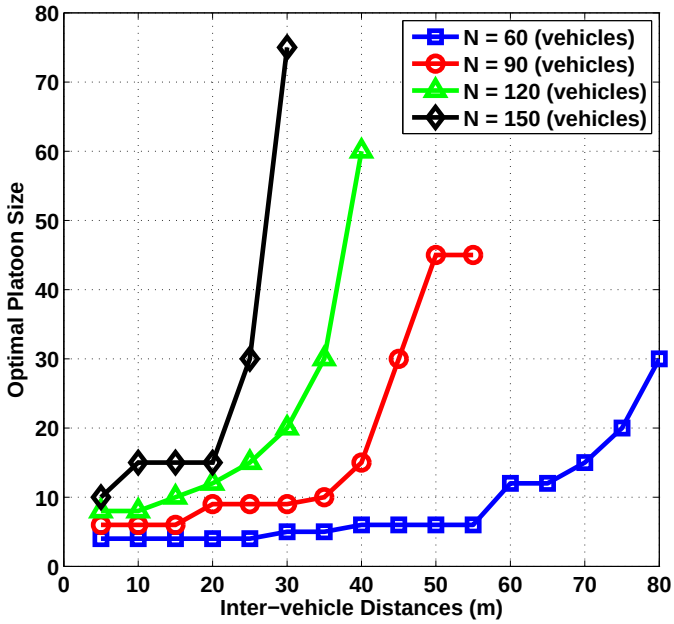

Figure 5.5: Optimal platoon sizes maximizing data throughput rates of Type II messages with 1% outage probability constraint of Type I messages.

shorter intra-platoon spacing $D_{\rm V} = 10$ (m), the optimal choice of a platoon size $N_{\rm V}$ is equal to 10, which achieves a data throughput rate level of 72 (Kbps) per flow under $M = 4$. Under the longer inter-vehicular spacing, $D_{\rm V} = 30$, the optimal choice of $N_{\rm V}$ is noted to be equal to 20, which achieves a data throughput rate level of 45 (Kbps) under a reuse level setting of $M = 4$.

Observing Fig. 5.5, we note that the platoon size $N_{\rm V}$ that attains the maximum data throughput rate level for the dissemination of Type II messages, under a prescribed 1% outage probability for Type I messages, is an increasing function of the intra-platoon spacings. As the latter spacing value decreases, the platoon size must be kept small so that the number of sources sharing each links is reduced. For longer inter-vehicular distances, larger platoon sizes are formed in order to limit the impact of inter-platoon interference signals, as well as to reduce the frequency of transporting messages across platoons. The latter setting, however, leads to an increased number of interfering vehicles that are simultaneously active

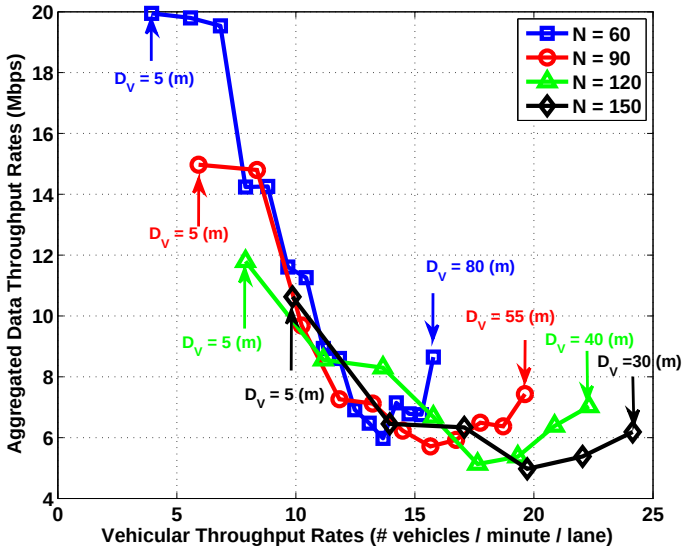

Figure 5.6: Vehicular throughput rates v.s. aggregated optimal data throughput rates of Type II messages under 1% outage constraint of Type I messages.

within a single platoon, reducing the attainable data throughput rate level. We also note that, given a value of the intra-platoon spacing, for a higher highway vehicular traffic density (i.e., a higher N level), a larger platoon size needs to be configured to mitigate the impact of the inter-platoon interference that are caused by the random occurrence of uncoordinated transmissions carried out within distinct platoons.

VI.3 Vehicular and Data Throughput Rate Tradeoffs under Saturated Vehicular Traffic Loading Rate

In Fig. 5.6, we exhibit the aggregated data throughput rate levels attained for the dissemination of Type II messages vs. the realized corresponding levels of the vehicular traffic throughput rates, under different highway traffic density levels. The latter condition is represented by the number of vehicles N admitted into a highway segment of length L. Each operational point on a curve corresponds to a different choice of a $D_{\rm V}$ level. The data throughput rate attained by setting this $D_{\rm V}$ value is equal to the maximum aggregated data

throughput rate of Type II messages attained over all possible spatial reuse factors M and platoon sizes N_{V}, under the 1% outage constraint of Type I messages.

It is interesting to see that under a fixed N value, as D_{V} increases, the data throughput rate first decreases then increases. This behavior is explained as follows: As D_{V} increases, the optimal N_{V} value increases and the data throughput rate decreases, induced by the factors identified in Section VI.2. However, as we further increase the D_{V} level, the throughput degradation due to the ensuing larger N_{V} value diminishes, as the performance is dominated by the impact caused by close interferers. In turn, an incremental increase in D_{V} serves to effectively reduce the number of flows that share a given link, recalling that each flow is required to cover a limited span of the highway. Consequently, setting a value that is higher than a certain D_{V} level, the data throughput rate tends to increase as we increase the configured D_{V} value. We note that when setting lower D_{V} levels, higher data throughput rates can be attained. However, due to the mobility induced safety constraint expressed by Eq. (5.2), a lower spacing D_{V} value requires a corresponding reduction in the allowable vehicular speed. The vehicular throughput capacity of the highway is noted then to generally decrease. It is observed that under a prescribed vehicular traffic density $\frac{N}{L}$ level, a lower speed yields a lower vehicular throughput rate.

We also observe that under a given configured D_{V} value, as the highway load N decreases, a higher data throughput rate is attainable. This behavior stems from the corresponding reduction in the signal interference level prompted by the lower number of simultaneously active vehicles. However, due to the lower number of vehicles traveling along the highway segment, the vehicular throughput rate is also reduced.

We conclude from Fig. 5.6 that for a fixed vehicular density, two optimal platoon formation alternatives are of interest: (1) Selecting the lowest possible D_{V} value coupled with a lower platoon size (N_{V}), used to support a higher data throughput rate at the expense of a lower vehicular throughput rate and a lower vehicular traveling speed; or (2) Configuring platoon structures that sustain high, including the highest possible D_{V} values, coupled with

the formation of large platoon sizes, used to attain a higher vehicular throughput rate at the expense of realizing reduced data throughput rates.

VI.4 Performance Enhancement Through the Use of Traffic Regulation of Platoon Based Formations

In the following, we study the enhancement level that is attributed to the employment of platoon formations. The performance of a system that employs a platoon-based traffic regulation system is compared with those using unregulated access operations. Two unregulated schemes, the Poisson Point Process (PPP) and the Double Displaced Negative Exponential Distribution (DDNED) model [66], are considered. The latter model is validated by fitting with the real headway data from Interstate-5 freeway in Seattle [5]. This model yields accurate prediction even under congested mode. For unregulated operations, we assume employment of an ideal TDMA scheme that is globally synchronized, so that all vehicles traveling over the highway segment under consideration can coordinate their transmissions accordingly in a reuse-M manner. The ensuing performance results thus serve as upper bounds for the outage probability and throughput rate.

In Fig. 5.7(a) and Fig. 5.7(b), we present graphs that exhibit the behavior of the delay-outage probability and aggregated throughput rate performance metrics with respect to the vehicular density level, respectively. Under a system that employs platoon based configurations, the displayed throughput rate represents the maximum throughput rate attained under a targeted 1% outage probability. Under the unregulated mode operation, the performance graphs that exhibit the outage probability and throughput rate levels represent results obtained after optimizing the spatial reuse M level, with no outage probability constraint imposed.

Examining the performance curves, it is observed that through the use of properly configured platoon structures, the system's outage probability and throughput rate performance can be significantly improved when compared to the corresponding attainable level achiev-

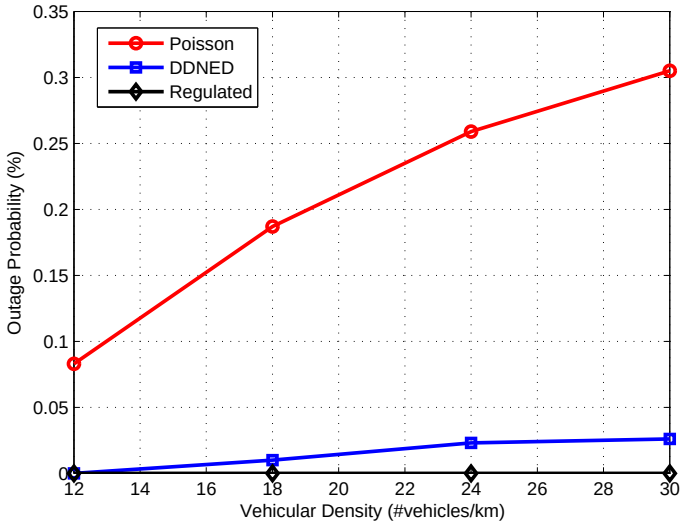

(a)

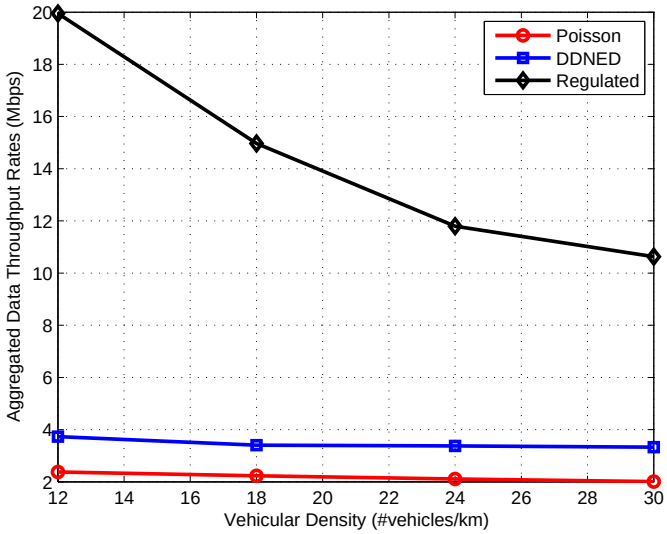

(b)

Figure 5.7: Performance improvement when employing platoon based traffic regulation: (a) Delay-outage probability of Type I messages (2) Aggregated throughput rate of Type II messages.

able under the unregulated mode. The performance of the latter scheme, even under the assumed implementation of a demanding global reuse-M TDMA scheduling scheme, is severely degraded. Under the unregulated operation, one often observes the distance between a trans-

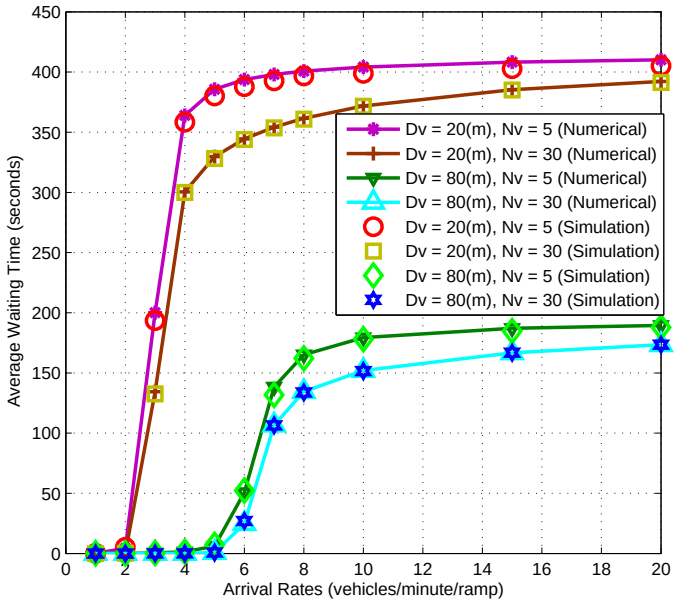

Figure 5.8: Average waiting time v.s. vehicle arrival rates under different N_{V} and D_{V} configurations.

mitting vehicle and its intended receiver to be longer than that between the receiver and signal interferers, leading to severe degradations in the efficiency of the communications networking process. The DDNED model yields performance better than that attained by PPP. It results from the fact that in real traffic, the topology is not completely random and the car-following nature of human drivers may lead to formation of platoons on the highway.

VI.5 Average Waiting Time v.s. Vehicular Loading Rate

In Fig. 5.8, we show the variation of the incurrent vehicular average waiting time at its ramp vs. the vehicular arrival rate level, under different platoon configuration parameters. It is observed that the results obtained through the use of our iterative mathematical model are very close to those obtained through Monte Carlo simulations.

It is noted that the synthesis of platoon formations that employ longer intra-platoon spacings and larger platoon sizes generally provide a better waiting time performance. The

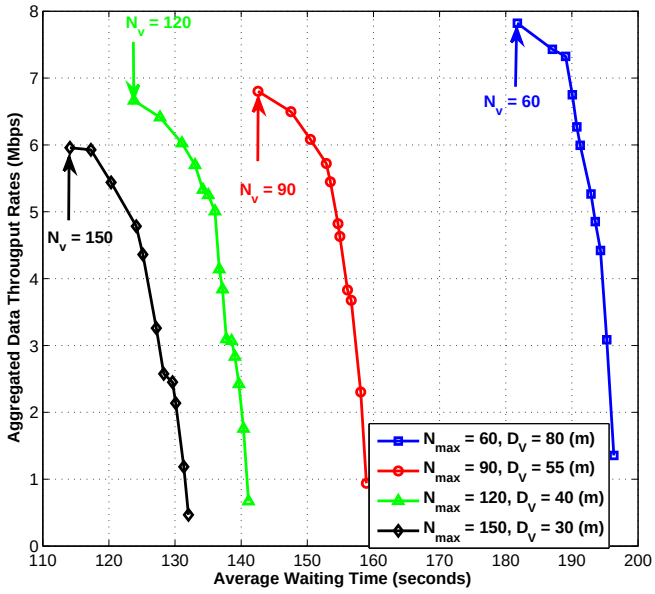

Figure 5.9: Average waiting time v.s. data throughput rates with different $N_{\max}$.

former parameter setting provides for a higher maximum allowable traveling speed and hence reduces the platoon cycle time. The setting of the later parameter serves to associate with a platoon a larger number of vehicles, and thus accommodating the admission of a larger number of vehicles during each platoon cycle. Although the setting of a larger platoon size induces a longer cycle time and hence a longer frame latency, the waiting time performance behavior is improved since the variance of the service time is reduced while the average service time level remains largely unchanged.

VI.6 Waiting Time & Data Throughput Rate Comparison under Different Vehicular Densities

In Fig. 5.9, we illustrate the relation between the average waiting time experienced by an on-ramp queued vehicle and the data throughput rate attained in transporting second priority message flows, under different settings of vehicular density $\frac{N_{\max}}{L}$ levels. We consider the case under which the system is operated in the saturation loading region. For each $N_{\max}$ value,

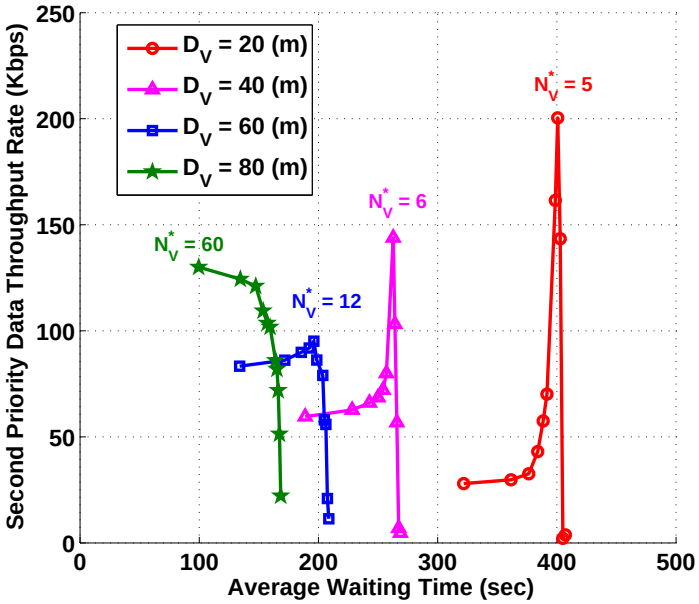

Figure 5.10: Average on-ramp waiting time v.s. data throughput rates under high vehicular arrival rate when $N_{\max}$ =60 and $\lambda = 8$ (vehicles/minute/ramp).

D_{V} is set to a value that is equal to its maximum allowable value so that the vehicular speed is maximized.

It is observed that under a lower vehicular density level, $N_{\max} = 60$, a vehicle will experience a longer average waiting time than that experienced when a higher vehicular density $N_{\max} = 150$ is allowed, even though vehicles are allowed to travel at a higher speed under the lower density scenario. In observing the results exhibited in Fig. 5.6 and Fig. 5.9, we note that the vehicular throughput rate and the average on-ramp waiting time values are inter-related. As one may expect, the setting of the operation to sustain a higher vehicular throughput rate, leads to shorter average waiting time levels.

VI.7 Waiting Time & Data Throughput Rate Performance Tradeoffs under High Vehicular Arrival Rate

The performance results shown in Figs. 5.10 illustrate the relations between the attainable levels of the Type II data throughput rate and the induced average on-ramp waiting time, under a prescribed targeted platoon configuration $D_{\rm V}$, and $N_{\rm V}$. We set the maximum number of vehicles allowed between two ramps equal to $N_{\max} = 60$. The system is highly loaded at a level of 8 (vehicles/minute/ramp).

Each performance curve is associated with a system in which the platoon formations are characterized by a fixed intra-platoon spacing level. Each point on a curve corresponds to a specific setting of the individual platoon capacity $N_{\rm V}$ value. For each curve, we mark the value of $N_{\rm V}^*$, identifying the optimal $N_{\rm V}$ value as the one that maximizes the data throughput rate given an underlying intra-platoon spacing. By using the iterative algorithm presented in Section V, we calculate the average waiting time experienced by a vehicle queued at ramp $k = 100$, which suffices to alleviate the impact of boundary effects.

We observe in Fig. 5.10 that a smaller value of $D_{\rm V} = 20$ (m) attains a higher data throughput rate with a proper choice of $N_{\rm V}^* = 5$. Such a configuration can effectively increase the inter-platoon spacing and hence restrict the message span (300(m)) within a single platoon. However, such a configuration is not a favorable design choice in terms of the induced on-ramp waiting time since the vehicular speed must be reduced for safety reasons. On the other hand, when a longer spacing $D_{\rm V} = 80$ (m) is set, it is desirable to configure the platoons so that they assume a larger size, $N_{\rm V} = 60$, in order to maximize the data throughput rate of Type II message flows. However, since a large number of vehicles are configured as members of a single platoon, a higher interference level is induced and therefore the throughput rate is degraded. We observe that by setting a longer $D_{\rm V}$ value, coupled with the use of the larger size platoons, allows vehicles to travel at higher speeds, and improves the statistics of the service process provided by the platoons as they roam and admit vehicles at ramp access points. Consequently, the waiting time of vehicles in the

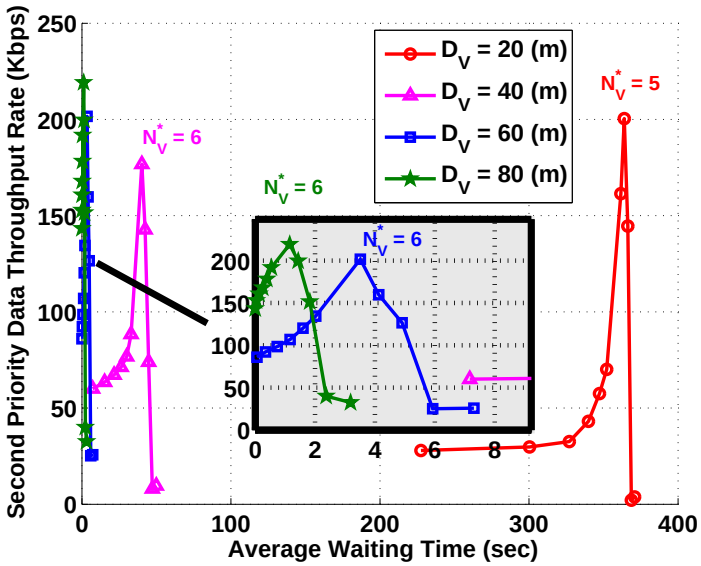

Figure 5.11: Average on-ramp waiting time v.s. data throughput rates under light vehicular arrival rate when $N_{\max} = 60$ and $\lambda = 4$ (vehicles/minute/ramp).

ramps prior to admission into the highway is highly enhanced.

VI.8 Waiting Time & Data Throughput Rate Performance Tradeoffs under Light Vehicular Arrival Rate

In Fig. 5.11, we consider the case where the arrival rate of vehicles on ramp is at a level of only 4 (vehicles/minute/ramp). We can see that configuring long $D_{\rm V}$ values attains both a higher data throughput rate and a lower on-ramp waiting time. This behavior is explained as follows. Under a saturated highway loading scenario, when choosing a longer $D_{\rm V}$ spacing level, we are forced to set a large platoon size ($N_{\rm V}$) aiming to prevent inter-platoon transmissions. Such a design would generally reduce the data throughput rate significantly, due to the increased number of intra-platoon simultaneously active interference sources. However, under a lightly loaded highway condition, the actual number of vehicles that are simultaneously active in each platoon is not high. Therefore, we set a lower $N_{\rm V}$ value without inducing performance degradation. For example, The optimal choice of the

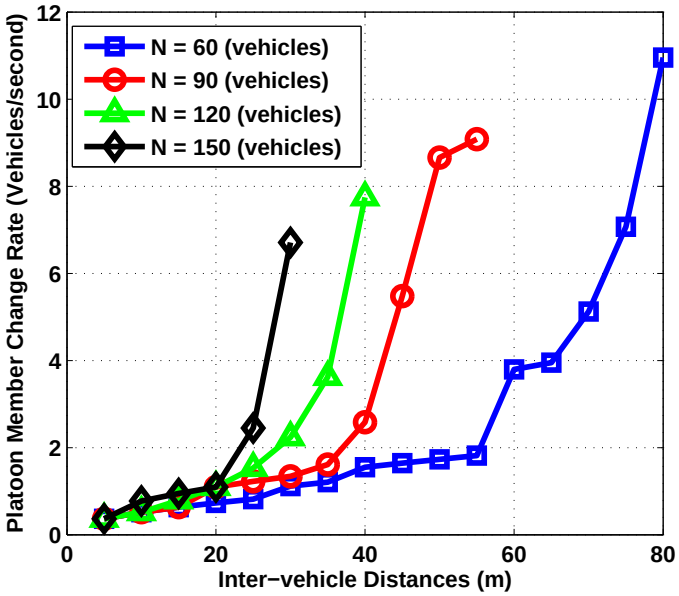

Figure 5.12: Average platoon member change rate under saturated loading.

N_{V} value is equal to 6 when $D_{\mathrm{V}} = 80$ (m), which is lower than that used under the highly loaded scenario.

VI.9 Platoon Scalability

In Fig. 5.12, we study a metric that relates to platoon scalability by evaluating the rate at which members change their association with a platoon. It is calculated as $\frac{N_{\mathrm{V}}p}{L/v}$, which expresses the average number of platoon member departures divided by the time that it takes for a platoon leader to travel from one ramp to the next. The platoon member change rate is indicative of the rate of control data required to reform the platoon and re-synchronize its members. It is noted that setting longer intra-platoon spacings can result in the increase of the vehicular traffic throughput rate as well as in the reduction of the average on-ramp waiting time. However, such an increase can also induce a higher control traffic data rate, as a larger number of platoon vehicles must be coordinated.

VII Concluding Remarks

The development and modeling of vehicular traffic topology regulation and communication networking systems have been treated to-date as independent research disciplines. In contrast to existing communication protocols and traffic regulation mechanisms, which are largely built to accommodate human driver induced traffic flows, an integrated design brings up a new design paradigm by taking advantage of driverless autonomous vehicles. In this chapter, we propose a scalable and implementable platoon based traffic regulation mechanism, coupled with the proper configuration of a spatial TDMA scheduling scheme and on-ramp access control mechanism. Platoon formation configurations are studied and evaluated, aiming to achieve enhanced message delay performance for high priority safety messages while attaining a high data throughput rate for the dissemination of second priority status message flows. The corresponding performance tradeoffs are investigated using metrics that include message delay and throughput rates, vehicular throughput rates, and on-ramp vehicular waiting times. The models and results presented in this chapter serve as guidelines for the design of integrated traffic control mechanisms that combine the configuration of the communications networking and mobility aspects of a next generation autonomous intelligent transportation system. Possible extensions of mechanisms employed in this chapter involve the installation of Road Side Units (RSUs) based core communications networks and making use of vehicles flowing in opposite directions to facilitate message disseminations. Future studies will also involve multi-lane highway structures, non-linear highway topologies, the impact of junction points, and other transportation elements.

5.A Proof of Lemma 1

Eq. (5.28) is derived by noting that $\mathbb{E}[N_1^{(k)}] = (\mathbb{E}[N_1^{(k)}] + 1)v_0^{(k-1)}$. That is, the first vehicle has to wait one additional platoon cycle if the next platoon to arrive is full. For the second vehicle waiting in the ramp, we have $\mathbb{E}[N_2^{(k)}] = (\mathbb{E}[N_2^{(k)}] + 1)v_0^{(k-1)} + (\mathbb{E}[N_1^{(k)}] + 1)v_1^{(k-1)}$. The

first term on the right hand side of the equation accounts for the event under which the next platoon to arrive is full; in this case, the vehicle keeps its second position in the queue. On the other hand, the second vehicle would occupy the head of the line position if the incoming platoon has exactly a single vacancy, as expressed by the second term of the equation. The recursive relation in Eq. (5.29) is derived by iterating through each waiting position in the queue.

5.B Proof of Theorem 1

$$\mathbb{E}\Big[\sum_{m=1}^{N_{\rm ad}^{(k)}} W_{\rm L}^{(k,m)} | N_{\rm ad}^{(k)} > 0\Big] \overset{(a)}{=} \sum_{i=0}^{R_{\rm cap}} \sum_{j=0}^{N_{\rm V}} r_i^{(k)} \tilde{\pi}_{N_{\rm V}-j}^{(k-1)} T_{\rm c} \Bigg[\sum_{m=1}^{N_{\rm e}^{ij}-1} \frac{a_m}{p_{\rm ad}^{(k)}} \sum_{l=m-N_{\rm w}^{ijm}+1}^{m} (1 - \frac{l}{m+1}) + \sum_{m=N_{\rm e}^{ij}}^{\infty} \frac{a_m}{p_{\rm ad}^{(k)}} \sum_{l=(j-i)^+ +1}^{N_{\rm e}^{ij}} \Big(1 - \frac{l}{m+1}\Big) \Bigg] \tag{5.36a}$$

$$\overset{(b)}{=} \sum_{i=0}^{R_{\rm cap}} \sum_{j=0}^{N_{\rm V}} r_i^{(k)} \tilde{\pi}_{N_{\rm V}-j}^{(k-1)} T_{\rm c} \Bigg[\sum_{m=1}^{N_{\rm e}^{ij}-1} \frac{a_m}{p_{\rm ad}^{(k)}} \sum_{l=m-N_{\rm w}^{ijm}+1}^{m} (1 - \frac{l}{m+1}) + \frac{[N_{\rm e}^{ij} - (j-i)^+]}{p_{\rm ad}^{(k)}} \Big(1 - \sum_{m=0}^{N_{\rm e}^{ij}-1} a_m\Big) - \frac{1}{\lambda T_{\rm c}} \sum_{m=N_{\rm e}^{ij}+1}^{\infty} \frac{a_m}{p_{\rm ad}^{(k)}} \sum_{l=(j-i)^+ +1}^{N_{\rm e}^{ij}} l \Bigg] \tag{5.36b}$$

Let $N_{\rm ar}$ denote the number of vehicles arriving at the ramp (not necessarily admitted to the ramp queue) during a platoon cycle time. The term $p_{\rm v}^{(k)} = 1 - r_{R_{\rm cap}}^{(k)} \tilde{\pi}_{N_{\rm V}}^{(k-1)}$ represents the probability that there is at least one vacancy in the ramp queue or in the serving platoon arriving at T_n^+. The term $p_{\rm ad}^{(k)} = p_{\rm v}^{(k)}(1 - a_0)$ represents the probability that at least one vehicle is admitted into the ramp queue or into the serving platoon that arrives during the $n^{\rm th}$ cycle. The probability that there are less than $N_{\rm e}^{ij}$ arrivals in a platoon cycle, given that at least one vehicle is admitted, is calculated as:

$$\varpi_{ij}^{(k)} \triangleq \Pr\{N_{\mathrm{e}}^{ij} > N_{\mathrm{ar}} > 0 | N_{\mathrm{ad}} > 0\} = \sum_{m=1}^{N_{\mathrm{e}}^{ij}-1} \frac{a_m}{p_{\mathrm{ad}}^{(k)}}. \tag{5.37}$$

In Eqs. (5.31) and (5.32), the first (second) term in the bracket is associated with the case when the number of new arrivals is smaller than (greater than or equal to) the total number of vacancies in the serving platoon and the ramp queue.

The results presented in Eq. (5.33) using Eqs. (5.36a) - (5.36b) are based on the following observations. Equality (a) is based on the fact that given a platoon cycle $[0, T_{\mathrm{c}}]$ and that m vehicles are admitted into the ramp, governed by the statistics of a Poisson arrival process, the average time of arrival of the n^{th} admitted vehicle is equal to $\frac{nT_{\mathrm{c}}}{m+1}$. The first (the second and the third) term within the brackets associates with the frame latency incurred when the number of new arrivals is lower than (greater than or equal to) the total number of vacancies in the serving platoon and the ramp queue. In the first term within the brackets, the expression $m - N_{\mathrm{w}}^{ijm} + 1$ represents the index of the first vehicle (among m new arrivals) that is required to wait in the ramp queue.

Equality (b) holds by expanding the second term in the bracket of Eq. (5.36a) and applying the following property satisfied by Poisson random variables:

$$\sum_{m=N_{\mathrm{e}}^{ij}}^{\infty} \frac{a_m}{m+1} = \frac{1}{\lambda T_{\mathrm{c}}} \sum_{m=N_{\mathrm{e}}^{ij}+1}^{\infty} a_m. \tag{5.38}$$

Eq. (5.33) represents an alternative formulation of Eq. (5.36b) obtained by applying the unitarity of a probability measure.

CHAPTER 6

Infrastructure Aided Communication Networking and Traffic Regulation for Autonomous Transportation Systems

I Introduction

The market of autonomous vehicles is expected to experience a drastic growth. The use of such vehicles is foreseen to improve in-road safety and alleviate traffic jams. For this purpose, vehicles are designed to gather information from surrounding areas via built-in sensors and/or relying on information provided by other vehicles. Reliable vehicular ad hoc networks (VANETs) [67] are generally integrated in the design of autonomous transportation system.

The employment of autonomous vehicles has introduced new dimensions that are incorporated in the system's design to achieve prescribed system performance. In contrast with approaches that have been employing statistical models to characterize moving patterns of human-driven cars [68–70], we propose to autonomously regulate vehicular mobility patterns. With the aid of Cooperative Adaptive Cruise Control (CACC) systems [2] and the integration of Vehicle-to-Vehicle (V2V) communication networks, vehicles are able to coordinate and configure their mobility patterns, speeds and distance spacings. For this purpose, in moving across a highway, vehicles are often grouped into platoons [5, 57].

Configuring vehicles to move in groups often serves to effectively alleviate traffic jams and improve fuel efficiency [47]. Such configurations are also advantageous in forming a V2V data communications network. Within a platoon, one can readily employ a centralized and reliable communication protocol, such as Time Division Multiple Access (TDMA), which is maintained and dynamically controlled through an intra-platoon management procedure. We demonstrated in a previous work [43] that by properly selecting platoon configuration parameters, the aggregated interference level that impacts the operation of the V2V wireless communications network can be effectively managed and often significantly reduced, improving the data throughput performance of the system. Additional control signaling is however required to provide for the synchronization and coordination of platoon vehicles. Consequently, one must incorporate limitations in the availability of bandwidth resources affecting control channel capacity, and thus restrict the platoon's spatial data messaging and control coverage span, and limit the number of vehicular members of a platoon. For cases that involve wide dissemination of message flows that must traverse multiple platoons, inter-platoon transmissions often become critical throughput bottleneck factors [43].

To facilitate message dissemination over a VANET system and to bridge the link gaps that may exist in communicating among vehicles across platoons, the deployment of Road Side Units (RSUs) is often considered as a promising solution. RSUs are inter-connected to each other through a high speed, generally wired, backbone core network. In accessing RSUs and in disseminating message flows across the core network, when feasible, one can enhance in a significant manner the capacity of the system to distribute message flows over wide distance ranges. Several research studies [71–73] have been published in investigating cost-effective RSU deployment strategies, used to guarantee delay-throughput performance requirements through the employment of a minimal number of RSUs. Yet, these works either assume statistical traffic models or use real world human-driver based data statistics in modeling the underlying vehicular mobility processes. The potential performance improvements achievable by regulating the vehicular topology are yet to be studied and exploited.

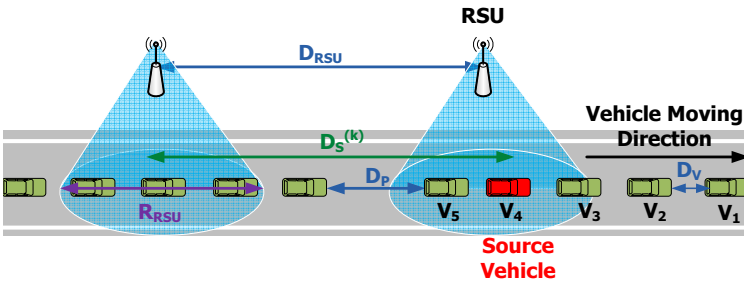

Figure 6.1: RSU-assisted VANET configurations ($N_V = 5$).

In this chapter, we investigate the joint design of vehicular traffic regulation mechanisms and RSU deployment strategies. To attain a cost-effective RSU deployment solution, we aim to maximize the distance between RSUs while configuring vehicles into platoons in a manner that serves to guarantee a minimum level of vehicular throughput rate and to limit the probability of using unreliable inter-platoon V2V links for message disseminations. We consider the dissemination of heterogeneous message types among highway vehicles, as they are differentiated by their targeted message spans. An optimization framework is formulated and a polynomial time algorithm is proposed. It involves the solution of a sequence of linear programming sub-problems. The underlying design tradeoffs in achieving high data networking reliability, low RSU cost, and high vehicular throughput rate, are well demonstrated.

The chapter is organized as follows. In Section II, we introduce our system model, modeling the underlying platoon configurations and RSU deployments. The optimization framework is formulated accordingly. In Section III, we present a computationally efficient algorithm for solving the optimization problem. Numerical results are illustrated in Section IV. The chapter is concluded in Section V.

II System Model

II.1 Platoon Configuration

In an autonomous highway system, the number of vehicles traveling in a segment of a highway can be effectively controlled through an on-ramp access regulation, often identified as *Traffic Density Control* [59]. Accordingly, we assume that a total number of N vehicles are admitted to travel at a constant speed v over a single lane highway segment of length L. Admitted vehicles are regulated to form N_{P} platoons. For simplified analysis, we assume each platoon to consist of an equal number of $N_{\mathrm{V}} = \frac{N}{N_{\mathrm{P}}}$ vehicles and N to be an integral multiple of N_{P}.

The intra-platoon spacing D_{V} is defined as the distance between neighboring vehicles belonging to the same platoon. The value of D_{V} is regulated to be the same for all platoons. Distances between any two neighboring platoons, the inter-platoon distances, are denoted as D_{P}. They are also regulated to assume the same values for all neighboring platoons. An illustrative example of the platoon structure of interest is shown in Fig. 6.1. In this case, D_{P} is calculated as:

$$D_{\mathrm{P}} = \frac{L - N_{\mathrm{P}}[D_{\mathrm{V}}(N_{\mathrm{V}} - 1) + sN_{\mathrm{V}}]}{N_{\mathrm{P}}}, \tag{6.1}$$

where s is the length of each vehicle. In the following, we assume $s = 0$ for formulation simplicity. Nonzero values of s only add a constant term over the derived solutions, which is a straightforward extension. We also assume that $D_{\mathrm{V}} \leq D_{\mathrm{P}}$. In addition, the selection of D_{V} must satisfy a safety constraint. To account for safety spacing margins that are required for a proper reaction to a sudden stop of a vehicle by vehicles hat follow, we set D_{V} to a value that is longer than the stopping distance of the immediate upstream vehicle. That is,

$$\frac{v^2}{2u} \leq D_{\mathrm{V}}, \tag{6.2}$$

where u is the vehicular deceleration level.

In order to manage and coordinate the configuration of vehicles within their platoon, control messages are exchanged among platoon members. As the number of platoon members N_{V} increases, the control data traffic increases accordingly. Also, under longer D_{V} spacing range values, such control message flows may not always be successfully broadcasted across the platoon. Accordingly, we assume that the maximum allowable platoon span $D_{\mathrm{V}}(N_{\mathrm{V}}-1)$ is lower than or equal to R_{c} that limits the range across which coordination among platoon members must be assured.

II.2 Message Categories

The message flow types that are disseminated among highway vehicles are classified into a total of K types, corresponding to distinct application types. Messages of type-k generated by a given source vehicle are required to be disseminated and received by vehicles within a targeted span $D_{\mathrm{s}}^{(k)}$ downstream the source vehicle. A type-k message is randomly generated by a vehicle with probability q_k. Without loss of generality, we assume that $D_{\mathrm{s}}^{(k)} \leq D_{\mathrm{s}}^{(k+1)}$, $k = 1...K-1$. This model is consistent with that described for the intelligent transportation system by the U.S. Department of the Transportation [65]. The latter model identifies message types such as emergency report, lane merging warnings, and traffic condition updates.

II.3 RSU Deployment

Road Side Units (RSUs) are assumed to be deployed uniformly along the highway with an inter-RSU distance equal to D_{RSU}. Each RSU is able to cover vehicles within a range R_{RSU} as illustrated in 6.1. RSU deployment is used to facilitate message transport over

VANET, especially when such messages are required to be sent across multiple platoons. As demonstrated in [43], inter-platoon links form bottleneck factors in the determination of the data throughput capacity available for the dissemination of message flows among vehicles, induced by the occurrence of longer inter-platoon ranges and by the lack of coordination management across platoons. Consequently, we use in this chapter a model that serves to guarantee the reliability of a VANET system by restricting the probability that disseminated message flows need to traverse inter-platoon links. We require the latter probability to be lower than a threshold Ψ value.

The probability that a message needs to be sent from the platoon associated with the source vehicle to the neighboring platoon by using an inter-platoon V2V link is calculated as

$$P_{\text{inter\_}V2V} = P_{\text{iso}} \sum_{k=1}^{K} P_{\text{inter}}^{(k)}, \tag{6.3}$$

where P_{iso} is the platoon isolation probability; i.e. the probability that all the vehicles in a platoon are not covered by any RSU. $P_{\text{inter}}^{(k)}$ is the probability that a type-k message, with span $D_{\text{s}}^{(k)}$, has to be disseminated across multiple platoons. These quantities are calculated as follows:

$$P_{\text{iso}} = 1 - \min\left\{ \frac{D_{\text{V}}(N_{\text{V}} - 1)}{D_{\text{RSU}} - R_{\text{RSU}}}, 1 \right\}. \tag{6.4}$$

$$P_{\text{inter}}^{(k)} = \frac{\max\{\min\{1 + \lfloor \frac{D_{\text{s}}^{(k)} - D_{\text{P}}}{D_{\text{V}}} \rfloor, N_{\text{V}}\}, 0\}}{N_{\text{V}}}. \tag{6.5}$$

II.4 Problem Formulation

To determine a cost efficient RSU deployment strategy while guaranteeing both data network and vehicular network performance rates, we form the following optimization problem **(P-COST-EFF-RSU)**. The objective function aims to maximize the distance between RSUs.

(P-COST-EFF-RSU)

$$\underset{D_{\mathrm{RSU}},D_{\mathrm{V}},D_{\mathrm{P}},v,N_{\mathrm{V}}}{\text{maximize}} \quad D_{\mathrm{RSU}}$$

subject to

$$P_{\mathrm{iso}}\sum_{k=1}^{K}P_{\mathrm{inter}}^{(k)} \leq \Psi \tag{C-1}$$

$$\frac{D_{\mathrm{V}}(N_{\mathrm{V}}-1)}{D_{\mathrm{RSU}}-R_{\mathrm{RSU}}} \leq 1 \tag{C-2}$$

$$D_{\mathrm{P}} = \frac{LN_{\mathrm{V}}}{N} - D_{\mathrm{V}}(N_{\mathrm{V}}-1) \tag{C-3}$$

$$D_{\mathrm{V}} = \frac{v^2}{2u} \tag{C-4}$$

$$D_{\mathrm{V}}(N_{\mathrm{V}}-1) \leq R_{\mathrm{c}} \tag{C-5}$$

$$v \geq v_{\min} \tag{C-6}$$

$$D_{\mathrm{P}} \geq D_{\mathrm{V}} \geq 0 \tag{C-7}$$

$$D_{\mathrm{RSU}} \geq 0 \tag{C-8}$$

The constraint requirements are explained as follows:

- (C-1) Link reliability constraint
- (C-2) The platoon length is not longer than the uncovered region between two neighboring RSUs. If the equality holds, messages can be transported across the network without using inter-platoon links.
- (C-3) The definition of inter-platoon distances

- (C-4) Safety constraint
- (C-5) Platoon coordination range limit
- (C-6) Minimum vehicular speed requirement
- (C-7) Inter-platoon distance is not shorter than the intra-platoon distance.
- (C-8) Nonnegativity of inter-RSU distances

It is observed that the quadratic expression on the left hand side of (C-1) results in non-convexity of **(P-COST-EFF-RSU)**. In the following section, we present a polynomial time algorithm to solve **(P-COST-EFF-RSU)** by solving a sequence of linear programming problems.

III Proposed Algorithm

We first identify two parameters $\underline{K}$ and $\overline{K}$ that group inter-platoon transmission probabilities of different message types into three categories:

$$P_{\text{inter}}^{(k)} = 0 \quad \forall k = 1...\underline{K} \tag{I-1}$$

$$0 < P_{\text{inter}}^{(k)} < 1 \quad \forall k = \underline{K}+1...\overline{K} \tag{I-2}$$

$$P_{\text{inter}}^{(k)} = 1 \quad \forall k = \overline{K}+1...K \tag{I-3}$$

Accordingly, (C-1) in **(P-COST-EFF-RSU)** can be rewritten as

$$[D_{\text{RSU}} - R_{\text{RSU}} - D_{\text{V}}(N_{\text{V}} - 1)] \times \left[\sum_{k=\underline{K}+1}^{\overline{K}} q_k \left(1 + \left\lfloor \frac{D_{\text{s}}^{(k)} - D_{\text{P}}}{D_{\text{V}}} \right\rfloor \right) + \sum_{k=\overline{K}+1}^{K} N_{\text{V}} q_k \right]$$

$$\leq \Psi N_{\text{V}} (D_{\text{RSU}} - R_{\text{RSU}}) \tag{C-1-1}$$

The following observations can also be deduced from **(P-COST-EFF-RSU)**:

- (C-1): The left hand side of the inequality is an increasing function of D_{RSU}.
- (C-2): holds if $D_{\mathrm{RSU}} \geq D_{\mathrm{V}}(N_{\mathrm{V}}-1)+R_{\mathrm{RSU}}$.
- (C-3) - (C-8): Constraints independent from the choices of D_{RSU}

Hence, we can perform a binary search over D_{RSU} to find the largest value of D_{RSU} that satisfies (C-1) - (C-8). We apply a change of variables by setting $g \triangleq \frac{D_{\mathrm{RSU}}-R_{\mathrm{RSU}}}{D_{\mathrm{V}}}$. Then, $D_{\mathrm{RSU}} = R_{\mathrm{RSU}} + gD_{\mathrm{V}}$. We also approximate the floor function by using that $\lfloor x \rfloor \leq x$. As a result, the following constraint is tighter than (C-1):

$$[g-(N_{\mathrm{V}}-1)]\left[\sum_{k=\underline{K}+1}^{\overline{K}} q_k(D_{\mathrm{s}}^{(k)}-D_{\mathrm{P}}+D_{\mathrm{V}})+D_{\mathrm{V}}N_{\mathrm{V}}\sum_{k=\overline{K}+1}^{K} q_k\right] \leq \Psi g N_{\mathrm{V}} D_{\mathrm{V}} \qquad \text{(C-1-2)}$$

For a fixed value of N_{V} and g, the constraint (C-1-2) is a linear constraint in D_{V} and D_{P}.

Hence, for a fixed value of g, N_{V}, $\underline{K}$, and $\overline{K}$. we solve the following linear programming problem:

(P-MAX-DV)

$$\begin{aligned}
&\underset{D_{\mathrm{V}},D_{\mathrm{P}},v}{\text{maximize}} \quad D_{\mathrm{V}} \\
&\text{subject to} \\
&\quad g \geq N_{\mathrm{V}}-1 \\
&\quad D_{\mathrm{s}}^{(k)} \leq D_{\mathrm{P}}-\epsilon,\ k=1...\underline{K} && \text{(I-1')} \\
&\quad D_{\mathrm{P}} \leq D_{\mathrm{s}}^{(k)} \leq (N_{\mathrm{V}}-1)D_{\mathrm{V}}+D_{\mathrm{P}},\ k=\underline{K}+1...\overline{K} && \text{(I-2')} \\
&\quad (N_{\mathrm{V}}-1)D_{\mathrm{V}}+D_{\mathrm{P}}+\epsilon \leq D_{\mathrm{s}}^{(k)},\ k=\overline{K}+1...K && \text{(I-3')} \\
&\quad \text{(C-1-2)} \\
&\quad \text{(C-3)-(C-7) of } \textbf{(P-COST-EFF-RSU)}
\end{aligned}$$

The objective function D_{RSU} is replaced by $R_{\mathrm{RSU}} + gD_{\mathrm{V}}$. For a fixed g value, maximizing D_{RSU} is thus equivalent to maximizing D_{V}. Note that constraints (I-1') - (I-3') are derived from (I-1) - (I-3). The positive scalar ϵ is introduced in (I-1') and (I-3') to handle the strict inequalities in (I-1) and (I-3).

In addition, to incorporate the possibility that all the constraints are met even when no RSU is deployed, we consider the solution of following feasibility problem:

(P-NO-RSU)

$$\begin{aligned}
&\underset{D_{\mathrm{V}}, D_{\mathrm{P}}, v}{\text{maximize}} \quad 1 \\
&\text{subject to} \\
&\left[\sum_{k=\underline{K}+1}^{\overline{K}} q_k (D_{\mathrm{s}}^{(k)} - D_{\mathrm{P}} + D_{\mathrm{V}}) + D_{\mathrm{V}} N_{\mathrm{V}} \sum_{k=\overline{K}+1}^{K} q_k \right] \leq \Psi N_{\mathrm{V}} D_{\mathrm{V}} \\
&\text{(I-1')-(I-3') of } \textbf{(P-MAX-DV)} \\
&\text{(C-3)-(C-7) of } \textbf{(P-COST-EFF-RSU)}
\end{aligned}$$

Similar to **(P-MAX-DV)**, **(P-NO-RSU)** can be solved efficiently using linear programming for a fixed value of g, N_{V}, $\underline{K}$, and $\overline{K}$. Consequently, the following algorithm is proposed for solving **(P-COST-EFF-RSU)**:

The outer-most loop iterates through all possible values of platoon sizes N_{V} (Line 1). The two inner loops (Line 4 and Line 6) iterate through all possible combinations of $\underline{K}$ and $\overline{K}$. In Lines 7-9, we first examine the possibility of the existence of a feasible solution when no RSU is deployed. If a feasible platoon configuration can be obtained by solving **(P-NO-RSU)**, this solution is returned as the optimal solution. Otherwise, we perform in Lines 11-23 a binary search over the values of D_{RSU} through the variable g. The values of $g_{\min}$ and $g_{\max}$ specify the lower and upper bounds for the search region, respectively. Initially, we set $g_{\min} = N_{\mathrm{V}} - 1$ and $g_{\max} = G$, where G is generally chosen to be a large number (e.g.,

Algorithm 1

Require: $D^*_{\mathrm{RSU}} := 0$;
Require: $\mathbf{N}_{\mathrm{V}} \triangleq \{\text{Set of } N_{\mathrm{V}} \text{ values}\} \subseteqq \{1...N\}$;
Require: $n := 1$;
Ensure:

repeat
  $N_{\mathrm{V}} = \mathbf{N}_{\mathrm{V}}[n]$
  $\overline{K} = K$
  repeat
    $\underline{K} = \overline{K} - 1$
    repeat
      Solve **(P-NO-RSU)**
      if feasible **then** $D^*_{\mathrm{RSU}} := \mathrm{Inf}$;
        return
      else
        $g_{\min} := N_{\mathrm{V}} - 1$;
        $g_{\max} := G$;
        repeat
          $g := \frac{g_{\min}+g_{\max}}{2}$;
          Solve **(P-MAX-DV)**
          if feasible **then**

$$D^*_{\mathrm{RSU}} := \max\{R_{\mathrm{RSU}} + gD_{\mathrm{V}}, D^*_{\mathrm{RSU}}\}$$

            $g_{\min} := g$;
          else
            $g_{\max} := g$;
        until $g_{\max} - g_{\min} < \mu$
      $\underline{K} := \underline{K} - 1$
    until $\underline{K} < 0$
    $\overline{K} := \overline{K} - 1$
  until $\overline{K} < 0$
  $n := n + 1$
until $n = \mathrm{length}(\mathbf{N}_{\mathrm{V}}) + 1$

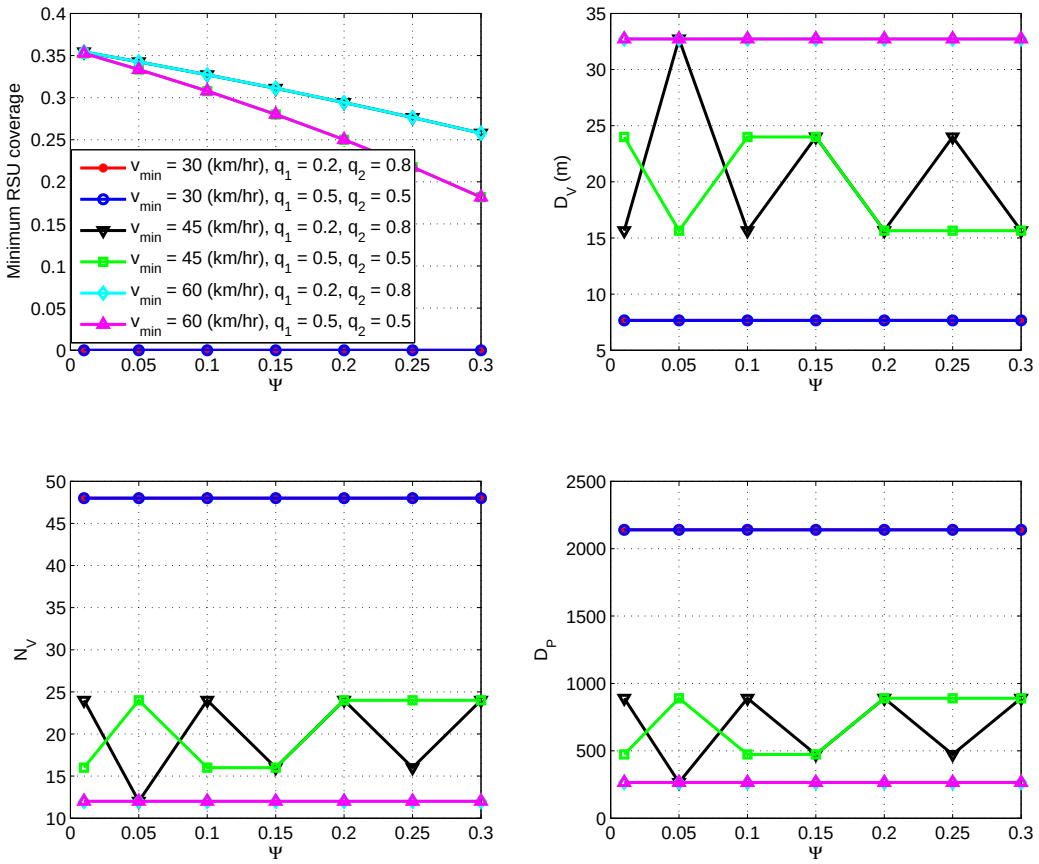

Figure 6.2: Optimal RSU deployment and VANET configurations ($N = 96$, $R_c = 360$ (m)).

a large integer value). If a feasible platoon configuration can be obtained for a given D_{RSU}, we examine a D_{RSU} set with larger values, and vice versa. The search process is terminated when the size of the search region is lower than a tolerance level μ.

IV Performance Evaluation

In this section, we use the proposed algorithm to obtain solutions that illustrate the characteristics of the core network required to support the V2V wireless network associated with the autonomous transportation system. The length of the highway segment of interest is 5 (km). Two different message spans are investigated: $D_{\text{s}}^{(1)} = 250$ (m) and $D_{\text{s}}^{(2)} = 1500$ (m). Two different message-type distributions are studied: (1) $(q_1, q_2) = (0.2, 0.8)$ (2) $(q_1, q_2) = (0.5, 0.5)$.

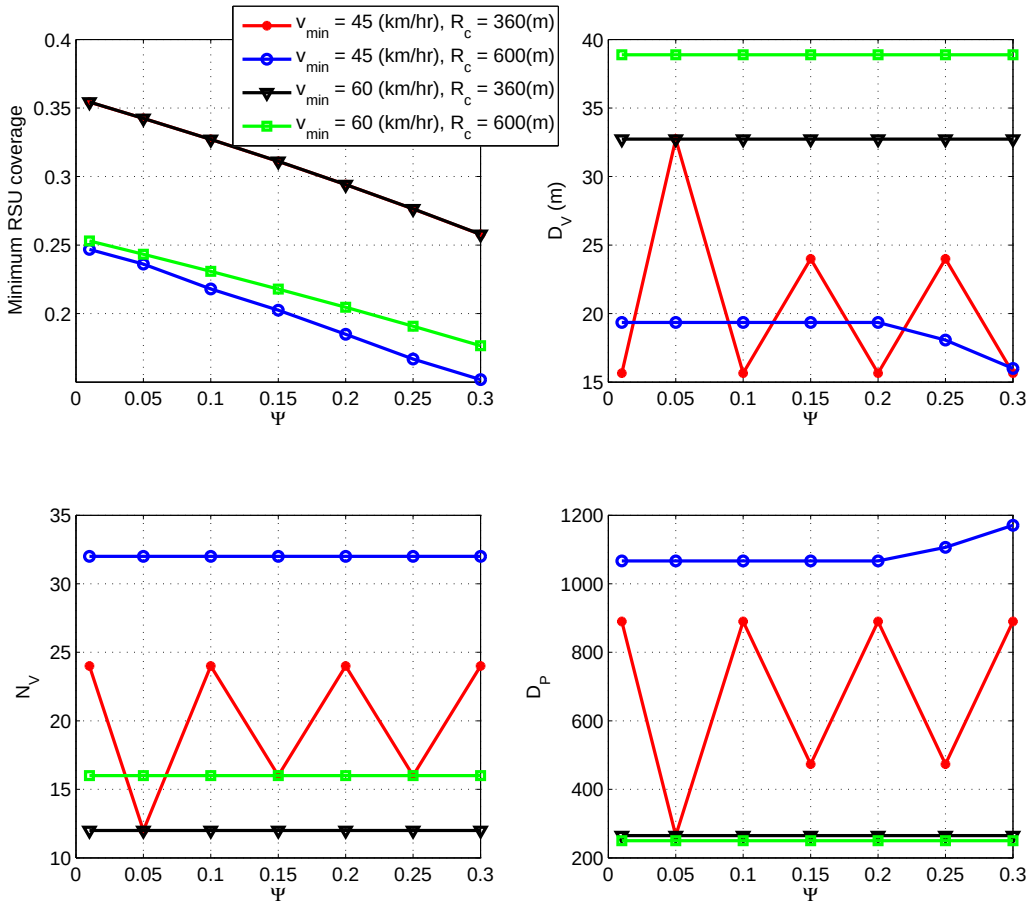

Figure 6.3: Optimal RSU deployment and VANET configurations under different platoon coordination ranges $R_{\rm c}$ ($N = 96$, $q_1 = 0.2$, $q_2 = 0.8$).

The deceleration level is set to 5 (m/s^2). The value of ϵ in (I-1') and (I-3') is set to 10^{-5}. The tolerance level μ for the binary search procedure is equal to 0.01.

IV.1 RSU Coverage vs. Vehicular Throughput

We set the system parameters to $N = 96$ and $R_{\rm c} = 360$ (m). The ensuing system performance behavior is illustrated in Fig. 6.2. The top-left sub-figure shows the minimum RSU coverage required to satisfy the prescribed probability Ψ of using inter-platoon links. The top-right, the bottom left, and the bottom right sub-figures show the corresponding optimal $D_{\rm V}$, $N_{\rm V}$, and $D_{\rm P}$ values, respectively. The RSU coverage is calculated as $\frac{R_{\rm RSU}}{D_{\rm RSU}}$.

It is observed that as the vehicular speed decreases, the required RSU coverage for a fixed value of Ψ, decreases as well. At the lowest speed level $v_{\min} = 30$ (km/hr), no RSU coverage is required. Under lower speeds, the platoon span is reduced, as shorter D_{V} values can be maintained, so that the inter-platoon distance tends to be longer than the required message dissemination range and it is not necessary to be aided by a core network. In turn, to maintain a higher speed, a longer D_{V} value is required. Subsequently, due to the restriction imposed on the platoon coordination range R_{c}, fewer vehicles are assigned as members of a single platoon. As a result, a larger number of platoons (over the highway segment of span L) is synthesized, so that the probability of using inter-platoon links increases. Consequently, a higher RSU density is required. These observations lead to the underlying "RSU coverage vs. vehicular throughput" tradeoffs. Note that the highway vehicular throughput is defined as $\frac{Nv}{L}$. Hence, under fixed values of N and L, the vehicular throughput, representing the capacity rate of the highway in support a flow of vehicles, is proportional to the vehicular speed.

As the speed limit is increased to $v_{\min} = 45, 60$ (km/hr), the minimum RSU coverage level is noted to be insensitive to the speed value $v_{\min}$. It is observed to be dominated by the message type distribution. This can be explained by again noting that for such higher $v_{\min}$ values, a smaller number of vehicles would be grouped into a single platoon, resulting in shorter inter-platoon distances and a higher probability of inter-platoon communications, $P_{\mathrm{inter}}^{(k)}$. Under such conditions, the RSU coverage requirement would be significantly reduced only if we are required to span a relatively shorter average dissemination range, preferring the lower inter-platoon transmission probability $(q_1, q_2) = (0.5, 0.5)$.

IV.2 Platoon Configuration vs. Reliability Constraint Ψ

It is observed that when the vehicular speed is constrained by a low ($v_{\min} = 30$ (km/hr)) level, the use of RSU coverage is often not essential. In turn, under higher speed levels, such as setting($v_{\min} = 60$ (km/hr)), to guarantee the prescribed Ψ level, the use of RSU

coverage would be often needed. For the former,46 vehicles are allowed to group into a single platoon, resulting in a long inter-platoon spanning distance (2140 (m)). In this case, no inter-platoon transmission is required, so that any specified Ψ level is met. For the latter, a larger value of D_{V} and thus a lower value of N_{V} are required, noting that the spanning range of a platoon must be limited due to the coordination range constraint. Therefore, the inter-platoon distance is now reduced. Consequently, to meet the link reliability constraint Ψ, it is now necessary for the design to provide wider RSU coverage.

When setting an intermediate vehicular speed ($v_{\min} = 45$ (km/hr)), the optimal configuration is sensitive to the choice of Ψ. For a low Ψ value, RSU coverage must be high and D_{V} must be kept low to reduce the $P_{\mathrm{inter}}^{(k)}$ value. As the value of Ψ increases, D_{V} can be set to a larger value. However, when we keep increasing the Ψ level, a lower value of D_{V} must again be chosen to restrict the $P_{\mathrm{inter}}^{(k)}$ level. The preferred D_{V} values tend to oscillate for different values of Ψ. However, we note that by searching over a larger solution space of D_{V} when $v_{\min} = 45$ (km/hr), compared with that for $v_{\min} = 60$ (km/hr), we do not reduce the RSU cost significantly. For $v_{\min} = 45$ (km/hr), we can still obtain similar RSU coverage requirement by using the platoon configuration obtained for the $v_{\min} = 60$ (km/hr) case.

IV.3 Impacts of Platoon Coordination Ranges

In Fig. 6.3, we illustrate the optimal RSU and platoon configurations to be synthesized under different coordination range R_{c} levels, assuming $N = 96$. It is noted that under a longer coordination range, the minimum RSU coverage required to achieve a given link reliability constraint Ψ is reduced since the inter-platoon transmission probability is reduced. For $v_{\min} = 45$ (km/hr), we observe that by increasing the coordination range, we achieve a platoon configuration that is more robust to the Ψ values that are selected. Such an observation is explained by noting that for a longer coordination range, such as $R_{\mathrm{c}} = 600$ (m), we are able to configure the system so that we achieve an inter-platoon distance that is longer than 1000 (m) by configuring each platoon to contain a higher number of vehicles.

Consequently, we can significantly reduce the $P_{\text{inter}}^{(k)}$ level for all values Ψ and the optimal platoon configurations become generally much less sensitive to the prescribed Ψ level. The designer must however consider the tradeoffs that exist between RSU deployment costs and intra-platoon signalling overhead rate induced bandwidth resource costs.

V Concluding Remarks

In this chapter, we propose a cost-effective core network that employs Road Side Units to provide access to highway vehicles to/from the core network. We develop and study an algorithm that solves for a RSU deployment strategy that maximizes the inter-RSU distances, under prescribed vehicular throughput and data network reliability levels. Highway vehicles are configured into platoons with properly chosen parameters. The optimization framework demonstrates the fundamental tradeoffs to be considered in designing an autonomous transportation system that provides for the dissemination of data flows through the use of a hybrid wireless network. We show that to attain a higher vehicular throughput rate, while guaranteeing a proper level of communications networking rate, the core network must be designed to provide for a higher level of access coverage to highway vehicles. The proposed framework is readily expandable to accommodate different choices of networking protocols and traffic regulation mechanisms to explore new tradeoffs in jointly design the autonomous transportation system with the hybrid autonomous VANET systems.

CHAPTER 7

Conclusions

The market of autonomous vehicles is expected to experience a drastic growth in the next decades. The use of these vehicles are foreseen to improve in-road safety and alleviate traffic jams. However, the overall system impacts that autonomous vehicles may bring up in the design of the transportation system, especially its interaction with the underlying communication system, remain unclear. This dissertation is the first research work that takes advantage of the flexibility in the moving pattern of autonomous vehicles and presents an integrated view of traffic regulation mechanisms and VANET protocol design.

We first present our study of a platoon based autonomous vehicle highway traffic regulation system. The traffic management system, serving to configure on-board vehicles into platoons and regulating on-ramp vehicular flows into the highway, is jointly designed with a vehicular ad hoc network (VANET) system that supports multi-class and multi-priority message delivery. The fundamental design tradeoffs among vehicular throughput rates, data throughput rates, and the on-ramp waiting time are analyzed and demonstrated through numerical examples.

We further extend our study from pure a VANET to a hybrid network with Road Side Unit (RSU) infrastructure deployment that provides additional data network capacity. To deploy RSUs in a cost effective manner, we take the advantages of the degree of freedoms provided by autonomous vehicles and jointly consider the optimal RSU deployment strategy and the corresponding platoon configuration. We propose an optimization framework and

an efficient algorithm to achieve optimal designs that aim to minimize the RSU costs while guaranteeing the link reliability and vehicular throughput rates.

Our research has exploited multiple degree of freedoms in designing an autonomous transportation system, which integrates performance measures from vehicular traffic regulation and data networking perspectives. This would inspire multi-disciplinary researchers such as those in the public policy and environmental sustainability fields, to involve in developing the next generation transportation system. New design disciplines and tradeoffs will be explored, which may result in a complete revision of the concurrent traffic management and data network systems that are developed mainly to serve human manipulated vehicles.

References

[1] S. Li, Q. Guo, L. Xin, B. Cheng, and K. Li, "Fuel-saving servo-loop control for adaptive cruise control system of road vehicles with step-gear transmission," *IEEE Transactions on Vehicular Technology*, vol. PP, no. 99, pp. 1–1, 2016.

[2] V. Milanes, S. Shladover, J. Spring, C. Nowakowski, H. Kawazoe, and M. Nakamura, "Cooperative adaptive cruise control in real traffic situations," *IEEE Transactions on Intelligent Transportation Systems*, vol. 15, no. 1, pp. 296–305, Feb. 2014.

[3] X. Ma, J. Zhang, X. Yin, and K. S. Trivedi, "Design and analysis of a robust broadcast scheme for VANET safety-related services," *IEEE Transactions on Vehicular Technology*, vol. 61, no. 1, pp. 46–61, Jan. 2012.

[4] H. Omar, W. Zhuang, and L. Li, "VeMAC: A TDMA-based MAC protocol for reliable broadcast in VANETs," *IEEE Transactions on Mobile Computing*, vol. 12, no. 9, pp. 1724–1736, Sept. 2013.

[5] Y. Zhang and G. Cao, "V-PADA: Vehicle-platoon-aware data access in VANETs," *IEEE Transactions on Vehicular Technology*, vol. 60, no. 5, pp. 2326–2339, June 2011.

[6] IEEE, 2011, P802.11p Draft Standard for Information Technology-Telecommunications and Information exchange between systems-Local and Metropolitan area networks-Specific requirements-Part 11: Wireless LAN Medium Access Control (MAC) and Physical Layer (PHY) specifications Amendment 7: Wireless Access in Vehicular Environments.

[7] S.-Y. Ni, Y.-C. Tseng, Y.-S. Chen, and J.-P. Sheu, "The broadcast storm problem in a mobile ad hoc network," in *Proc. the 5th Annual ACM/IEEE Int'l Conference on Mobile Computing and Networking (MobiCom)*, Aug. 1999, pp. 151–162.

[8] G. Korkmaz, E. Ekici, F. Ozguner, and U. Ozguner, "Urban multi-hop broadcast protocol for inter-vehicle communication systems," in *Proc. ACM Intl Workshop on Vehicular Ad Hoc Netowrks. (VANET)*, Sept. 2004.

[9] E. Fasolo, A. Zanella, and M. Zorzi, "An effective broadcast scheme for alert message propagation in vehicular ad hoc networks," in *Proc. IEEE Int'l Conference on Communications (ICC)*, vol. 9, June 2006, pp. 3960–3965.

[10] T. Little and A. Agarwal, "An information propagation scheme for VANETs," in *Proc. IEEE Intelligent Transportation Systems*, Sept. 2005, pp. 155–160.

[11] L. Bononi and M. Di Felice, "DBA-MAC: Dynamic backbone assisted medium access control for efficient broadcast in VANETs," *Journal of Interconnection Networks (JOIN)*, vol. 10, no. 4, pp. 1793–1813, Dec. 2009.

[12] I. Rubin, A. Baiocchi, F. Cuomo, and P. Salvo, "GPS aided inter-vehicular wireless networking," in *Proc. Information Theory and Applications Workshop (ITA)*, Feb. 2013, pp. 1–9.

[13] D. Li, H. Huang, X. Li, M. Li, and F. Tang, "A distance-based directional broadcast protocol for urban vehicular ad hoc network," in *Proc. Int'l Conference on Wireless Communications, Networking and Mobile Computing*, Sept. 2007, pp. 1520–1523.

[14] S. Kuribayashi, Y. Sakumoto, H. Ohsaki, S. Hasegawa, and M. Imase, "Performance evaluation of epidemic broadcast with directional antennas in vehicular ad-hoc networks," in *Proc. IEEE/IPSJ Int'l Symposium on Applications and the Internet*, July 2011, pp. 260–265.

[15] A. Nasipuri, S. Ye, J. You, and R. E. Hiromoto, "A MAC protocol for mobile ad hoc networks using directional antennas," in *Proc. IEEE Wireless Communications and Networking Conference (WCNC)*, vol. 3, Sept. 2000, pp. 1214–1219.

[16] C. A. Balanis, *Antenna Theory: Analysis and Design*. New York: Wiley, 1982.

[17] A. J. Goldsmith, *Wireless Communications*. New York: Cambridge University Press, 2005.

[18] L. Cheng, B. E. Henty, D. D. Stancil, F. Bai, and P. Mudalige, "Mobile vehicle-to-vehicle narrow-band channel measurement and characterization of the 5.9 GHz dedicated short range communication (DSRC) frequency band," *IEEE Journal on Selected Areas in Communications*, vol. 25, no. 8, pp. 1501–1516, Oct. 2007.

[19] P. Salvo, M. D. Felice, A. Baiocchi, F. Cuomo, and I. Rubin, "Timer-based distributed dissemination protocols for vanets and their interaction with MAC layer," in *Proc. IEEE 77th Vehicular Technology Conference (VTC Spring)*, June 2013, pp. 1–6.

[20] W. Zhang, Y. Chen, Y. Yang, X. Wang, Y. Zhang, X. Hong, and G. Mao, "Multi-hop connectivity probability in infrastructure-based vehicular networks," *IEEE Journal on Selected Areas in Communications*, vol. 30, no. 4, pp. 740–747, May 2012.

[21] H. Schrank, "Directivity of omnidirectional antennas," *IEEE Antennas and Propagation Magazine*, vol. 35, no. 5, pp. 50–51, Oct. 1993.

[22] A. Amoroso, G. Marfia, and M. Roccetti, "Going realistic and optimal: A distributed multi-hop broadcast algorithm for vehicular safety," *Computer networks*, vol. 55, no. 10, pp. 2504–2519, July 2011.

[23] G. Marfia, M. Roccetti, A. Amoroso, and G. Pau, "Safe driving in LA: Report from the greatest intervehicular accident detection test ever," *IEEE Transactions on Vehicular Technology*, vol. 62, no. 2, pp. 522–535, July 2013.

[24] K. Stamatiou and M. Haenggi, "Delay characterization of multihop transmission in a Poisson field of interference," *IEEE/ACM Transactions on Networking*, vol. 22, no. 6, pp. 1794–1807, Oct. 2013.

[25] B. Blaszczyszyn, P. Muhlethaler, and Y. Toor, "Maximizing throughput of linear vehicular ad-hoc networks (VANETs) - a stochastic approach," in *Proc. European Wireless Conference*, May 2009, pp. 32–36.

[26] I. Rubin, Y.-Y. Lin, A. Baiocchi, F. Cuomo, and P. Salvo, "Micro base station aided vehicular ad hoc networking," in *Proc. Int'l Conference on Computing, Networking and Communications (ICNC)*, Feb. 2014, pp. 231–235.

[27] A. Paier, D. Faetani, and C. Mecklenbrauker, "Performance evaluation of IEEE 802.11p physical layer infrastructure-to-vehicle real-world measurements," in *Proc. 3rd International Symposium on Applied Sciences in Biomedical and Communication Technologies (ISABEL)*, Nov. 2010, pp. 1–5.

[28] F. Bai and B. Krishnamachari, "Spatio-temporal variations of vehicle traffic in VANETs: facts and implications," in *Proc. ACM Int'l Workshop on VehiculAr Inter-NETworking*, Sept. 2009, pp. 43–52.

[29] H.-J. Ju and I. Rubin, "Mobile backbone synthesis for ad hoc wireless networks," *IEEE Transactions on Wireless Communications*, vol. 6, no. 12, pp. 4285–4298, 2007.

[30] I. Rubin, A. Baiocchi, F. Cuomo, and P. Salvo, "Vehicular backbone network approach to vehicular military ad hoc networks," in *Proc. IEEE Military Communications Conference (MILCOM)*, Nov. 2013, pp. 901–909.

[31] I. Rubin, Y.-Y. Lin, A. Baiocchi, F. Cuomo, and P. Salvo, "Vehicular backbone networking protocol for highway broadcasting using directional antennas," in *Proc. IEEE Global Communications Conference (GLOBECOM)*, Dec. 2013, pp. 4414–4419.

[32] I. Rubin, "Message path delays in packet-switching communication networks," *IEEE Transactions on Communications*, vol. 23, no. 2, pp. 186–192, Feb. 1975.

[33] N. Wisitpongphan, O. K. Tonguz, J. S. Parikh, P. Mudalige, F. Bai, and V. Sadekar, "Broadcast storm mitigation techniques in vehicular ad hoc networks," *IEEE Wireless Communications*, vol. 14, no. 6, pp. 84–94, Dec. 2007.

[34] H. Alshaer and E. Horlait, "An optimized adaptive broadcast scheme for inter-vehicle communication," in *Proc. IEEE Vehicular Technology Conference (VTC)*, May 2005, pp. 2840–2844.

[35] A. Wegener, H. Hellbrück, S. Fischer, C. Schmidt, and S. Fekete, "AutoCast: An adaptive data dissemination protocol for traffic information systems," in *Proc. IEEE Vehicular Technology Conference (VTC)*, Sept. 2007, pp. 1947–1951.

[36] Y. Gunter, B. Wiegel, and H. Grossmann, "Cluster-based medium access scheme for VANETs," in *Proc. IEEE Conference on Intelligent Transportation Systems (ITSC)*, Oct. 2007, pp. 343–348.

[37] H. Su and X. Zhang, "Clustering-based multichannel MAC protocols for QoS provisionings over vehicular ad hoc networks," *IEEE Transactions on Vehicular Techonology*, vol. 56, no. 6, pp. 3309–3323, Nov. 2007.

[38] Y. Yao, L. Rao, and X. Liu, "Performance and reliability analysis of IEEE 802.11p safety communication in a highway environment," *IEEE Transactions on Vehicular Techonology*, vol. 62, no. 9, pp. 4198–4212, Nov. 2013.

[39] F. Borgonovo, A. Capone, M. Cesana, and L. Fratta, "ADHOC MAC: New MAC architecture for ad hoc networks providing efficient and reliable point-to-point and broadcast services," *Wireless Networks*, vol. 10, pp. 359–366, July 2004.

[40] H. A. Omar, W. Zhuang, and L. Li, "VeMAC: A TDMA-based MAC protocol for reliable broadcast in VANETs," *IEEE Transactions on Mobile Computing*, vol. 12, no. 9, pp. 1724–1736, Sept. 2013.

[41] S. E. Shladover, C. A. Desoer, J. K. Hedrick, M. Tomizuka, J. Walrand, W.-B. Zhang, D. H. McMahon, H. Peng, S. Sheikholeslam, and N. McKeown, "Automatic vehicle control developments in the PATH program," *IEEE Transactions on Vehicular Technology*, vol. 40, no. 1, pp. 114–130, Feb. 1991.

[42] F. Cuomo, I. Rubin, A. Baiocchi, and P. Salvo, "Enhanced VANET broadcast throughput capacity via a dynamic backbone architecture," *Ad Hoc Networks*, vol. 21, pp. 42–59, Oct. 2014.

[43] Y. Y. Lin and I. Rubin, "Vehicular and messaging throughput tradeoffs in autonomous highway systems," in *Proc. IEEE Global Communications Conference (GLOBECOM)*, Dec. 2015, pp. 1–6.

[44] A. Kesting, M. Treiber, and D. Helbing, "Connectivity statistics of store-and-forward intervehicle communication," *IEEE Transactions on Intelligent Transportation System*, vol. 11, no. 1, Mar. 2010.

[45] M. Ni, J. Pan, L. Cai, J. Yu, H. Wu, and Z. Zhong, "Interference-based capacity analysis for vehicular ad hoc networks," *IEEE Communications Letters*, vol. 19, no. 4, pp. 621–624, Apr. 2015.

[46] N. Akhtar, S. C. Ergen, and O. Ozkasap, "Vehicle mobility and communication channel models for realistic and efficient highway VANET simulation," *IEEE Transactions on Vehicular Technology*, vol. 64, no. 1, pp. 248–262, Jan. 2015.

[47] T. Robinson, E. Chan, and E. Coelingh, "Operating platoons on public motorways: An introduction to the SARTRE platooning programme," in *Proc. 17th World Congress on Intelligent Transport Systems*, Oct. 2010.

[48] J. Martensson, A. Alam, S. Behere, M. A. A. Khan, J. Kjellberg, K.-Y. Liang, H. Pettersson, and D. Sundman, "The development of a cooperative heavy-duty vehicle for the GCDC 2011: Team scoop," *IEEE Transactions on Intelligent Transportation Systems*, vol. 13, no. 3, pp. 1033–1049, Sept. 2012.

[49] B. van Arem, C. van Driel, and R. Visser, "The impact of cooperative adaptive cruise control on traffic-flow characteristics," *IEEE Transactions on Intelligent Transportation Systems*, vol. 7, no. 4, pp. 429–436, Dec. 2006.

[50] H. Zhang, S. Ritchie, and W. Recker, "Some general results on the optimal ramp metering control problem," *Transportation Research Part C*, vol. 4, no. 2, pp. 51–69, Apr. 1996.

[51] M. Papageorgiou and A. Kotsialos, "Freeway ramp metering: an overview," *IEEE Transactions on Intelligent Transportation Systems*, vol. 3, no. 4, pp. 271–281, Dec. 2002.

[52] L. Baskar, B. De Schutter, J. Hellendoorn, and Z. Papp, "Traffic control and intelligent vehicle highway systems: a survey," *IET Intelligent Transport Systems*, vol. 5, no. 1, pp. 38–52, Mar. 2011.

[53] J. Al-Obaedi and S. Yousif, "Microsimulation model for motorway merges with ramp-metering controls," *IEEE Transactions on Intelligent Transportation Systems*, vol. 13, no. 1, pp. 296–306, Mar. 2012.

[54] H. T. Roh and J. W. Lee, "Communication-aware position control for mobile nodes in vehicular networks," *IEEE Journal on Selected Areas in Communications*, vol. 29, no. 1, pp. 173–186, Jan. 2011.

[55] C. Shao, S. Leng, Y. Zhang, A. Vinel, and M. Jonsson, "Performance analysis of connectivity probability and connectivity-aware MAC protocol design for platoon-based VANETs," *IEEE Transactions on Vehicular Technology*, vol. 64, no. 12, pp. 5596–5609, Dec. 2015.

[56] H. Peng, D. Li, K. Abboud, H. Zhou, H. Zhao, W. Zhuang, and X. Shen, "Performance analysis of IEEE 802.11p DCF for multiplatooning communications with autonomous vehicles," *IEEE Transactions on Vehicular Technology*, vol. PP, no. 99, pp. 1–1, 2016.

[57] D. Jia, K. Lu, and J. Wang, "On the network connectivity of platoon-based vehicular cyber-physical systems," *Transportation Research Part C*, vol. 40, pp. 215–230, Mar. 2014.

[58] M. Nekoui and H. Pishro-Nik, "Analytic design of active safety systems for vehicular ad hoc networks," *IEEE Journal on Selected Areas in Communications*, vol. 31, no. 9, pp. 491–503, Sept. 2013.

[59] C.-C. Chien, Y. Zhang, and P. A. Ioannou, "Traffic density control for automated highway systems," *Automatica*, vol. 33, no. 7, pp. 1273–1285, July 1997.

[60] X. Liu and M. Haenggi, "The impact of the topology on the throughput of interference-limited sensor networks with rayleigh fading," in *Proc. 2nd Annual IEEE Communications Society Conference on Sensor and Ad Hoc Communications and Networks (IEEE SECON)*, Sept. 2005, pp. 317–327.

[61] J. Sahoo, E.-K. Wu, P. Sahu, and M. Gerla, "Congestion-controlled-coordinator-based MAC for safety-critical message transmission in VANETs," *IEEE Transactions on Intelligent Transportation Systems*, vol. 14, no. 3, pp. 1423–1437, Sept. 2013.

[62] M. Papageorgiou, H. Hadj-Salem, and J.-M. Blosseville, "ALINEA: A local feedback control law for on-ramp metering," *Transportation Research Board*, pp. 58–64, Dec. 1991.

[63] L. Le and E. Hossain, "Tandem queue models with applications to QoS routing in multihop wireless networks," *IEEE Transactions on Mobile Computing*, vol. 7, no. 8, pp. 1025–1040, Aug. 2008.

[64] S. Ross, *Applied Probability Models with Optimization Applications*, ser. Dover Books on Advanced Mathematics. Dover Publications, 1970.

[65] U. D. of Transportation, *Identify Intelligent Vehicle Safety Applications Enabled by DSRC*, ser. Vehicle Safety Communications Project Task 3 Final Report, 2005.

[66] J. D. Griffiths and J. G. Hunt, "Vehicle headways in urban areas," *Traffic Engineering Control*, vol. 32, no. 10, pp. 458–462, 1991.

[67] H. Hartenstein and L. P. Laberteaux, "A tutorial survey on vehicular ad hoc networks," *IEEE Communications Magazine*, vol. 46, no. 6, pp. 164–171, June 2008.

[68] H. Qiu, I.-H. Ho, C. Tse, and Y. Xie, "A methodology for studying 802.11p VANET broadcasting performance with practical vehicle distribution," *IEEE Transactions on Vehicular Technology*, vol. 64, no. 10, pp. 4756–4769, Oct. 2015.

[69] H. Wang, R. P. Liu, W. Ni, W. Chen, and I. Collings, "VANET modeling and clustering design under practical traffic, channel and mobility conditions," *IEEE Transactions on Communications*, vol. 63, no. 3, pp. 870–881, Mar. 2015.

[70] Z. Zhang, G. Mao, and B. Anderson, "Stochastic characterization of information propagation process in vehicular ad hoc networks," *IEEE Transactions on Intelligent Transportation Systems*, vol. 15, no. 1, pp. 122–135, Feb. 2014.

[71] T. J. Wu, W. Liao, and C. J. Chang, "A cost-effective strategy for road-side unit placement in vehicular networks," *IEEE Transactions on Communications*, vol. 60, no. 8, pp. 2295–2303, Aug. 2012.

[72] A. Abdrabou and W. Zhuang, "Probabilistic delay control and road side unit placement for vehicular ad hoc networks with disrupted connectivity," *IEEE Journal on Selected Areas in Communications*, vol. 29, no. 1, pp. 129–139, Jan. 2011.

[73] D. Kim, Y. Velasco, W. Wang, R. Uma, R. Hussain, and S. Lee, "A new comprehensive RSU installation strategy for cost-efficient VANET deployment," *IEEE Transactions on Vehicular Technology*, vol. PP, no. 99, pp. 1–1, 2016.